Fractionation of marine algae to its constituents towards valuable chemicals and energy products

Ricardo Miguel Pezoa Conte

Laboratory of Industrial Chemistry and Reaction Engineering
Faculty of Science and Engineering / Chemical Engineering
Åbo Akademi University
Turku / Åbo 2017

Fractionation of marine algae to its constituents towards valuable chemicals and energy products

Doctoral thesis

Ricardo Miguel Pezoa Conte

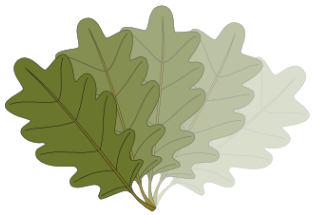

Johan Gadolin
Process Chemistry Centre

Laboratory of Industrial Chemistry and Reaction Engineering
Faculty of Science and Engineering
Åbo Akademi University
Turku / Åbo 2017

Supervised by

Doc. Päivi Mäki Arvela
Laboratory of Industrial Chemistry and Reaction Engineering
Faculty of Science and Engineering / Chemical Engineering
Åbo Akademi University, Turku, Finland

Prof. Jyri-Pekka Mikkola
Laboratory of Industrial Chemistry and Reaction Engineering
Faculty of Science and Engineering / Chemical Engineering
Åbo Akademi University, Turku Finland
Technical Chemistry
Department of Chemistry
Chemical-Biological Centre
Umeå University, Umeå, Sweden

Reviewers

Dr. Rafał Marcin Bogel-Łukasik
Unit of Bioenergy
National Laboratory of Energy and Geology, Lisbon, Portugal

Assoc. Prof. Gonzalo Águila Avilés
Department of Engineering Science
Faculty of Engineering
Universidad Nacional Andrés Bello, Santiago, Chile

Opponent

Dr. Rafał Marcin Bogel-Łukasik
Unit of Bioenergy
National Laboratory of Energy and Geology, Lisbon, Portugal

Cover images credit:
Tracey Saxby (*Ulva* spp.), IAN Image Library.
Jane Thomas (*Macrocystis pyrifera*), IAN Image Library.

ISBN 978-952-12-3599-3 (printed version)
ISBN 978-952-12-3600-6 (electronic version)
Painosalama Oy–Turku, Finland 2017

Para Magdalena y María Teresa

Ricardo Miguel Pezoa Conte
born 1985 in Santiago, Chile

B. Sc. Chemical Engineering, 2008
University of Chile, Chile

M. Sc. Chemical Engineering, 2010
University of Chile, Chile

Mañumfin mapu tañi nien mew
feychi mapu, fewla piwkentukufin.
Apomontegun, leitun, tañi kimal
tañi pewmalenun.

Nütram
Graciela del Carmen Huinao
Alarcón

Preface

The completion of this work has resulted in a very fruitful life experience whose outcome was accomplished with the help of many people.

First, I would like to thank Professor Jyri-Pekka Mikkola for introducing me into the world of biomass, and for all the invaluable advice in the many talks we had together. I also thank the Dean of the Faculty Professor Tapio Salmi for giving me the opportunity to study in the lab and share in such an international atmosphere. I also thank Professor Dmitry Yu. Murzin for all the inspiring lectures he gave during my studies. I am deeply grateful to Docent Päivi Mäki-Arvela for giving daily supervision to my work and for inspiring me with her smart way of sharing work with family. Docent Kari Eränen is also gratefully acknowledged for his assistance with the ins and outs of day-to-day work at the lab. I also thank Docent Henrik Grénman for his help during the last period of my studies. I show my gratitude to the entire personnel of the Laboratory of Wood and Paper Chemistry, under the leadership of Professor Stefan Willför, for allowing me to perform carbohydrate analyses at their premises.

Special thanks go to three of my co-authors: Allison Leyton, Cristina Ravanal, and Andrea Baccini. Thank you so much for your help at the lab and for the time we shared together in Finland. Prof. María Elena Lienqueo is also gratefully acknowledged for all the unselfish and altruistic assistance she provided during the whole period of my studies. I am deeply in debt to my colleagues Nemanja, Erfan, Andrea P., Shuyana, Álvaro, Adriana, María P., Ikenna, Olatunde, Farhan, Vladimir, Cesar, Atte, Passi T., Passi V., Jussi, Lidia, Imane, Karolina, Sari, Anton, Gerson, and Eero. Enormous gratitude goes to the Chilean-Finnish friends we met here in Turku: Mónica, Pato, Dalí, Jorge, Noora, Niko, and Doris. You made us feel like being at home.

I am also deeply grateful to my family in Chile who has been supporting me during my whole life: my mother Patricia, my father Carlos, my sister Natalia, my aunts Paulina and Deyanira and my grandmother Alicia. I also show heartily gratitude to all the love and support provided by my wife's family: Sra. M. Teresa, Don Rodrigo, M. José, M. Jesús, Juan Pablo, Benjamín, and Julián. I would like to show my gratitude and express my everlasting love to María Teresa. You made many sacrifices accompanying me on this adventure, so I owe you a lot. Here we managed to build a beautiful family, and our beloved Magdalena is the proof of that. Her shiny eyes and smile are a sempiternal flame of happiness in our hearts.

Finally, I want to thank the Finnish society. Such a functional society, which welcomed and supported us since we landed in this country, made us have a lifetime experience living here and changed the way we see life

onwards. We hope we can bring this example back to Chile to turn our Chilean society a bit closer to the Nordic spirit.

Abstract

Ricardo Miguel Pezoa Conte

Fractionation of marine algae to its constituents towards valuable chemicals and energy products

Doctoral thesis, Laboratory of Industrial Chemistry and Reaction Engineering, Johan Gadolin Process Chemistry Centre, Faculty of Science and Engineering, Åbo Akademi University, 2017.

Keywords: L-rhamnose, phlorotannins, alginate, biomass, kinetics, fractionation, efficient extraction, ionic liquids.

There is an urgency for finding renewable resources for the replacement of fossil resources aiming at more environmentally friendly processing. The old concept of processing forestry biomass for pulp and paper that dominated the industry for centuries has evolved to the development of biorefineries, which convert most of the biomass into products and energy. One of the most valorized fractions of terrestrial plants is cellulose, which is utilized to produce pulp, paper and recently specialty cellulose. Regarding algae, while the cellulose content is rather low depending on the species, the presence of sulfate and uronic-acid-rich polysaccharides provides a new set of molecules with industrial potential. Consequently, the aim of this work is to demonstrate the efficient processing of seaweeds in line with a biorefinery concept.

In this thesis, brown and green algae were processed for the extraction of their main constituents using water and ionic liquids, following the principle of green chemistry. Subsequently, the work focused on the depolymerization of marine polysaccharides utilizing biotechnological and chemical catalysis. Additionally, the kinetics of these reactions was thoroughly studied using mathematical modeling. Several different analytical techniques were used for characterizing the products, such as high-performance liquid and size-exclusion chromatography, gas chromatography as well as ion chromatography, Fourier transform infrared spectrometry, thermogravimetric analysis, scanning electron microscopy and transmission electron microscopy, among others.

The results showed that it is feasible to extract molecules possessing antioxidant activities, such as phlorotannins, as well as polysaccharides such as the sulfated rhamnoglucuronan ulvan. By means of water processing of the brown alga *Macrocystis pyrifera* (giant kelp), two phlorotannins were identified: phloroeckol and a tetramer of phloroglucinol isomer. The treatment of the green alga *Ulva rigida* (sea lettuce) with the distillable ionic liquid 1,1,3,3-tetramethylguanidine propionate at 120°C allowed for the dissolving of 69 wt.% of the total carbohydrate content, while the extraction

of ulvan with water at temperatures below 130°C resulted in yields of up to 99 wt.%. Further depolymerization of the polysaccharides contained in brown and green algae via enzymatic and chemical catalytic processing allowed for the obtaining of monomer yields up to 86 wt.% of D-mannuronic and L-guluronic acids and 82 wt.% L-rhamnose, respectively. The activation energy for the kinetics of the extraction of ulvan, to be estimated through mathematical modeling of the experimental data, was calculated to be 54 kJ mol^{-1}. Regarding the hydrolysis of ulvan, an activation energy in the range 134–175 kJ mol^{-1} was estimated. These results suggested that the absence of lignin in *U. rigida* facilitated the extraction of sulfated polysaccharides. Admittedly, the presence of uronic acids represented challenges for the efficient processing of the biomass, since the conditions for depolymerization and stability of the molecules are different from those of neutral sugars.

The present work provides evidence that it is possible to obtain a high-yield of products from algal biomass using processing based on the concept of green chemistry. Still, many challenges remain open for research to optimize not only the processing parameters of the biomass, but also to optimize cultivation of the seaweeds and to explore fine chemical or nutraceutical applications for their constituents.

Referat

Ricardo Miguel Pezoa Conte

Fraktionering av komponenter i havsalg för framställning av värdefulla kemikalier och energiprodukter

Doktorsavhandling, Laboratoriet för Teknisk kemi och reaktionsteknik, Johan Gadolin Processkemiska centret, Fakulteten för Naturvetenskaper och Teknik, Åbo Akademi Universitet, 2017.

Nyckelord: L-ramnos, plorotannin, alginat, biomassa, kinetik, fraktionering, effektiv extraktion, joniska vätskor

Det är mycket aktuellt att upptäcka förnybara källor som ersätter fossila råmaterial och att utveckla miljövänliga processer. Den konventionella industriella metoden för förädling av skogens biomassa för massa och papper har lett till utveckling av bioraffinaderier i vilka biomassan omvandlas till produkter och energi. En av det mest utnyttjade fraktionerna är växtcellulosa, som används för framställning av massa, papper och under senaste tider också cellulosa. Alger innehåller ganska låga cellulosahalter beroende på algarten, och å andra sidan närvaro av sulfonerade och uronsyrarika polysackarider utgör en ny typ av industriellt värdefulla molekyler. Målsättningen med detta arbete är att utveckla effektiva processer för sjögräs med hjälp av bioraffinaderikonceptet.

I detta arbete har bruna och gröna alger extraherats med vatten och joniska vätskor för att utvinna algkomponenter i andan av grön kemi. Sålunda arbetet har fokuserats på nedbrytning av polymerer i havets polysackarider med hjälp av bioteknologisk och kemisk katalys. Ytterligare, matematisk modellering har använts som verktyg för att kunna utföra en djupgående undersökning av reaktionskinetik. Många olika analysmetoder har använts vid karakterisering av produkter, ss. vätskekromatografi, storleksuteslutningskromatografi, gaskromatografi, jonkromatografi, Fourier transformering infraröd spektroskopi, termogravimetrisk analys, svepelektronmikroskopi, transmissionselektronmikroskopi, osv.

Resultaten visar att det är möjligt att extrahera molekyler som har antioxidativa aktiviteter, ss. plorotanniner, och polysackarider, samt t.ex. sulfonerade ramnoglukuronan ulvan. Genom vattenbehandling av den bruna algen *Macrocystis pyrifera* (jätte kelp), två olika plorotanniner identifierades: ploroeckol och en tetramer av ploroglucinolisomen. Vid behandling av den gröna algen *Ulva rigida* (havsallat) med den destilerbara joniska vätskan, 1,1,3,3-tetrametylguanidin propionat vid 120°C kunde 69 vikts% av de totala kolhydrater upplösas, medan extraktion av ulvan med vatten vid en temperatur under 130°C gav 99 vikts% utbyte. Nedbrytning av polysackarider bruna och gröna alger utfördes med hjälp av enzymer och

kemiska katalysatorer och resulterade i monomerutbyten för D-mannouronsyra och L-guluronsyra 86 vikts% samt L-ramnos 82 vikts%, Aktiveringsenergin för ulvan extraktion uppskattades med hjälp av matematisk modelling av det experimentella data och den fick ett värde på 54 kJ mol^{-1}. För ulvan hydrolys uppskattades aktiveringsenergi bli 134–175 kJ mol^{-1}. Dessa resultat visade att frånvaron av lignin i *U. rigida* möjliggjorde extraktion av sulfonerade polysackarider. Närvaro av uronsyran förorsakade utmaningar för effektiv behandling av biomassan därför att nedbrytningsförhållandena samt stabiliteten av dessa molekyler är annorlunda jämfört med neutrala sockrar.

Detta arbete visar att det är möjligt att utvinna höga utbyten av algbiomassabaserade produkter enligt gröna kemins koncept. Det finns ytterligare många utmaningar för att lösa, t.ex. att optimera processparametrar för biomassa omvandling, för odling av sjögräs samt för att hitta applikationsområden för dessa sockrar.

Resumen

Ricardo Miguel Pezoa Conte

Fraccionamiento de algas marinas en sus constituyentes para la producción de químicos valiosos y energía

Tesis doctoral, Laboratorio de Química Industrial e Ingeniería de Reacciones, Centro de Química de Procesos Johan Gadolin, Facultad de Ciencias e Ingeniería, Universidad de Åbo Akademi, 2017.

Palabras claves: L-ramnosa, florotaninos, alginato, algas, biomasa, fraccionamiento, extracción eficiente, líquidos iónicos.

Existe urgencia por encontrar recursos renovables que reemplacen a los recursos fósiles, con el propósito de llevar a cabo una producción industrial más amigable con el medio ambiente. El antiguo concepto de procesamiento de la biomasa forestal para la producción de pulpa y papel dominó la industria por décadas. En la actualidad, la industria forestal ha evolucionado al desarrollo de biorefinerías, en donde gran parte de la biomasa es transformada en productos y energía. Una de las fracciones de la biomasa forestal más valorizada es la celulosa, la cual es utilizada para la producción de pulpa, papel y recientemente celulosa especial. Con respecto a las algas, si bien el contenido de celulosa es relativamente bajo dependiendo de la especie, la presencia de polisacáridos ricos en sulfatos y ácidos urónicos provee un nuevo grupo de moléculas para el beneficio de la industria. Por consiguiente, este trabajo tiene por objetivo demostrar el procesamiento eficiente de las algas siguiendo el concepto de biorefinería.

En esta tesis, algas pardas y verdes fueron procesadas para la extracción de sus constituyentes más importantes usando agua o líquidos iónicos, siguiendo el concepto de química verde. En una segunda etapa, el trabajo se enfocó en la despolimerización de polisacáridos marinos utilizando catálisis biotecnológica y química. Adicionalmente, se utilizó modelamiento matemático como una herramienta para realizar un estudio más profundo de la cinética de estas reacciones. Distintas técnicas analíticas fueron utilizadas para caracterizar los productos, tales como cromatografías líquidas de alto rendimiento y de exclusión de tamaño, cromatografía gaseosa, cromatografía de iones, espectrometría de infrarrojos por transformada de Fourier, análisis termo gravimétricos, microscopía de escaneo de electrones, microscopía de transmisión de electrones, entre otros.

Los resultados mostraron una eficiente extracción de moléculas que poseen actividades antioxidantes como los florotaninos, y de polisacáridos como el ramnoglucurano sulfatado ulvano. A través del procesamiento con agua del alga parda *Macrocystis pyrifera* (huiro), dos florotaninos fueron identificados: floroeckol y un isómero de un tetrámero de floroglucinol. El

procesamiento del alga verde *Ulva rigida* (lechuga de mar) con el líquido iónico destilable propionato de 1,1,3,3-tetrametilguanidina a 120°C permitió disolver un 69 wt.% del contenido total de carbohidratos, mientras que el procesamiento con agua a temperaturas inferiores a 130°C resultó en rendimientos de extracción de ulvanos de hasta un 99 wt.%. La despolimerización de los polisacáridos contenidos en algas pardas y verdes, vía procesamiento enzimático y de catálisis química, resultó en rendimientos de monómeros de un 86 wt.% de ácidos D-manurónico y L-gulurónico, y de un 82 wt.% de L-ramnosa, respectivamente. La energía de activación para la cinética de extracción de ulvanos, calculada mediante el modelamiento matemático de los datos experimentales, fue estimada en 54 kJ mol^{-1}. Respecto a la hidrólisis de ulvanos, se estimó una energía de activación dentro del rango entre 134 y 175 kJ mol^{-1}. Estos resultados evidenciaron que la ausencia de lignina en *U. rigida* facilitó la extracción de polisacáridos sulfatados. Es importante destacar que la presencia de ácidos urónicos representó desafíos para el procesamiento eficiente de la biomasa, debido a que las condiciones para llevar a cabo la despolimerización de estos polisacáridos, y la estabilidad de los ácidos hexurónicos difieren de las condiciones requeridas para polisacáridos constituidos exclusivamente por azúcares neutros.

El presente trabajo provee evidencia de que es posible obtener rendimientos elevados de productos a partir de biomasa de algas, a través de procesamiento basados en el concepto de química verde. No obstante, muchos desafíos están aún abiertos para optimizar no sólo el procesamiento de la biomasa, sino que también para la optimización de los cultivos de algas y encontrar aplicaciones valiosas para cada uno de sus constituyentes.

List of publications

[I]. Leyton, A., **Pezoa-Conte, R.**, Barriga, A., Buschmann, A. H., Mäki-Arvela, P., Mikkola, J.-P., and Lienqueo, M. E., 2016. Identification and efficient extraction method of phlorotannins from the brown seaweed *Macrocystis pyrifera* using an orthogonal experimental design. Algal Research, 16, pp. 201-208.

Contribution Realized part of the experiments and chemical analyses and had a major participation in the edition of the article.

[II]. **Pezoa-Conte, R.**, Leyton, A., Anugwom, I., von Schoultz, S., Paranko, J., Mäki-Arvela, P., Willför, S., Muszyński, M., Nowicki, J., Lienqueo, M.E. and Mikkola, J.-P., 2015. Deconstruction of the green alga *Ulva rigida* in ionic liquids: Closing the mass balance. Algal Research, 12, pp.262-273.

Contribution Designed and realized all the experiments and wrote the article.

[III]. **Pezoa-Conte, R.**, Leyton, A., Baccini, A., Mäki-Arvela, P., Grénman, Xu, C., Willför, S., Lienqueo, M.E. and Mikkola, J.-P. Aqueous extraction of the sulfated polysaccharide ulvan from the green alga *Ulva rigida* – Kinetics and modeling. BioEnergy Research, 10(3), pp.915-928.

Contribution Designed and realized all the experiments and wrote the article.

[IV]. Ravanal, M.C., **Pezoa-Conte, R.**, von Schoultz, S., Hemming, J., Salazar, O., Anugwom, I., Jogunola, O., Mäki-Arvela, P., Willför, S., Mikkola, J.-P. and Lienqueo, M.E., 2016. Comparison of different types of pretreatment and enzymatic saccharification of *Macrocystis pyrifera* for the production of biofuel. Algal Research, 13, pp.141-147.

Contribution Realized part of the experiments and chemical analyses and had a major participation in the edition of the article.

[V]. **Pezoa-Conte, R.**, Baccini, A., Leyton, A., Mäki-Arvela, P., Grénman, H., Hemming, J., Willför, S., Lienqueo, M.E., Canu, P. and Mikkola, J.-P. Production of L-rhamnose via acid hydrolysis of the algal polysaccharide ulvan using homogeneous and heterogeneous catalysts: kinetics and modeling. (Submitted for publication)

Contribution Designed all the experiments, realized part of the experiments and wrote the article.

Other publications related to the topic

Scientific publications

Gavilà, L., Constantí, M., Medina, F., **Pezoa-Conte, R.**, Anugwom, I., Mikkola, J.-P. An integrated biomass-to-lactic acid process. (Submitted for publication)

Leyton, A., **Pezoa-Conte, R.**, Mäki-Arvela, P., Mikkola, J.-P. and Lienqueo, M.E., 2017. Improvement in carbohydrate and phlorotannin extraction from *Macrocystis pyrifera* using carbohydrate active enzyme from marine *Alternaria sp*. as pretreatment. Journal of Applied Phycology, 29, 2039-2048.

Lienqueo, M.E., Ravanal, M.C., **Pezoa-Conte, R.**, Cortínez, V., Martínez, L., Niklitschek, T., Salazar, O., Carmona, R., García, A., Hyvärinen, S., Mäki-Arvela, P. and Mikkola, J.-P. 2016. Second generation bioethanol from *Eucalyptus globulus Labill* and *Nothofagus pumilio*: Ionic liquid pretreatment boosts the yields. Industrial Crops and Products, 80, pp.148-155.

Pezoa, R., Cortínez, V., Hyvärinen, S., Reunanen, M., Hemming, J., Lienqueo, M.E., Salazar, O., Carmona, R., García, A., Murzin, D.Yu. and Mikkola, J.-P., 2010. The use of ionic liquids in the pretreatment of forest and agricultural residues for the production of bioethanol. Cellulose Chemistry & Technology, 44(4), p.165.

Oral presentations

Pezoa-Conte, R., Leyton, A., Baccini, A., Mäki-Arvela, P., Grénman, Xu, C., Willför, S., Lienqueo, M.E. and Mikkola, J.-P. Kinetics and mathematical modeling of the extraction of algal polysaccharides. 10th World Congress of Chemical Engineering, Barcelona, Spain, October 1st–5th, 2017.

Pezoa-Conte, R., Baccini, A., Leyton, A., Mäki-Arvela, P., Grénman, H., Willför, S., Lienqueo, M.E. and Mikkola, J.-P. Production of L-rhamnose using solid acid catalysts. EuropaCat 2017, Florence, Italy, August 27th–31st, 2017.

Pezoa-Conte, R., Leyton, A., Mäki-Arvela, P., Willför, S., Lienqueo, M.E. and Mikkola, J.-P. Hydrolysis of the green alga *Ulva rigida* using solid acid catalysts. 17th Nordic Symposium on Catalysis, Lund, Sweden, June 14th–16th, 2016.

Pezoa-Conte, R., Leyton, A., Anugwom, I., von Schoultz, S., Paranko, J., Mäki-Arvela, P., Willför, S., Muszyński, M., Nowicki, J., Lienqueo, M.E. and Mikkola, J.-P. Dissolution of the green alga *Ulva rigida* using ionic liquid systems. Green and Sustainable Chemistry Conference, Berlin, Germany, April 3rd–6th, 2016.

Pezoa-Conte, R., Pham, T.N., Mäki-Arvela, P., Willför, S. and Mikkola, J.-P. Hydrolysis of carbohydrates in green algae using solid acid catalysts. EuropaCat 2015 Catalysis: Balancing the use of fossil and renewable resources, Kazan, Russian Federation. ISBN 978-5-906376-10-7, Boreskov Institute of Catalysis SB RAS, 274-275.

Pezoa, R., Hyvärinen, S., Mäki-Arvela, P., von Schoultz, S., Hemming, J., Willför, S. and Mikkola, J.-P. Ionic liquid treatment for algal biomass. Ionic Liquids: Melting Temperature, other Properties, and Applications, La Serena, Chile, March 20th–21st, 2014.

Pezoa, R., Hyvärinen, S., Mäki-Arvela, P., von Schoultz, S., Hemming, J., Willför, S. and Mikkola, J.-P. Ionic liquid treatment for algal biomass. International Workshop in Algal Biorefinery, Santiago, Chile, March 17th–18th, 2014.

Poster presentations

Pezoa-Conte, R., Baccini, A., Mäki-Arvela, P., Grénman, H., Smeds, A., Hemming, J., Willför, S., Canu, P. and Mikkola, J.-P. Production of L-rhamnose using solid acid catalysts. Wallenberg Wood Workshop 2017, Djurö, Sweden, June 12th–14th, 2017.

Pezoa-Conte, R., Ravanal, M.C., Mäki-Arvela, P., Willför, S., Lienqueo, M.E. and Mikkola, J.-P. Bioethanol production from the green alga *Ulva rigida* and the brown alga *Macrocystis pyrifera*. The 6th Nordic Wood Biorefinery Conference 2015, Helsinki, Finland. ISBN 978-951-38-8353-9, VTT Technology, 319-325. October 20th–22nd, 2015.

Pezoa-Conte, R., Leyton, A., Anugwom, I., Mäki-Arvela, P., Willför, S., Lienqueo, M.E. and Mikkola, J.-P. Algae – an old but unexplored bioresource. SWE-FIN Workshop on New Materials from Trees, Stockholm, Sweden, June 15th–17th, 2015.

Pezoa-Conte, R., Leyton, A., Anugwom, I., von Schoultz, S., Paranko, J., Mäki-Arvela, P., Willför, S., Lienqueo, M.E. and Mikkola, J.-P. Dissolution of green algae in ionic liquids. Sao Paulo Advanced School on the Present and Future of Bioenergy, Campinas, Brazil, October 10th–17th, 2014.

Pezoa, R., Hyvärinen, S., Mäki-Arvela, P., von Schoultz, S., Hemming, J., Willför, S., Leyton, A., Ravanal, M.C., Lienqueo, M.E. and Mikkola, J.-P. Dissolution of algae biomass in ionic liquids. EUCHEM 2014 Molten Salts and Ionic Liquids, Tallinn, Estonia, July 6th–11th, 2014.

Contents

List of figures

List of tables

General Background

Our economy is heavily carbon-based. The exploiting of fossil resources triggered industrialization around the world, bringing benefits and drawbacks to society. Unfortunately, the environment has mostly seen the disadvantages. In the 18th century, several new manufacturing processes were invented and eventually commercialized to introduce manufactured goods, supplies, and energy for society. The chemical industry had a major change when the processes for sulfuric acid, sodium carbonate, and hydrochloric acid among others were established. Additionally, the invention of the paper machine to make continuous sheet paper on a loop of wire fabric was revolutionary in increasing production. By the end of the 18th century, the extraction of oil started in Ukhta, Russia, becoming the first oil refinery delivering oil products to Moscow and St. Petersburg.[1]

In the 19th century, paraffin was refined from crude oil, symbolizing the beginning of the modern history of oil. By 1846, Baku, in today's Azerbaijan, saw the birth of the first well on Earth to be intensively drilled and exploited. Several refinery operations were established until an almost complete depletion and devastation of the surroundings. Unfortunately, Baku became one of the first examples of unsustainable production.[2]

Due to this lack of sustainability, entire civilizations have collapsed. One relatively well-documented example is the *Rapa Nui* people from Easter Island in the Pacific Ocean. Significant deforestation of the island took place somewhere in the 18th century due to overharvesting of trees, overhunting of animal species and climate change. These events dramatically altered the ecosystem, producing a drop in the population from 15,000 down to 2,000–3,000 in a period of 100 years.[3]

The scientific community is responsible for making society aware of the importance of sustainable production. The accumulation of carbon dioxide in our atmosphere is aligned with the increase in the temperature and acidity of the oceans, which theoretically will trigger a change in the climate. Nowadays, the continuous melting of the Arctic and the Antarctic are a few examples of these alterations in the climate. The increase in the level of the seas threatens several small islands in the Pacific Ocean which may eventually disappear by the next century.[4,5] Heatwaves hit different corners of the planet, and torrential rains occur even in the driest places of the world such as the Atacama Desert. It may be very likely that our civilization will overcome this challenge in the future, but the price to pay may be very high, and unfortunately, the most vulnerable inhabitants are most likely to pay that price at the expense of people from more 'developed' societies.

In this regard, the scientific community not only has the moral duty to communicate these problems to society, but also to work to find solutions.

Chemical engineering has a great responsibility in these terms since the conversion of resources into valuable chemicals, materials, and energy is at the very core of our discipline. During the last few years, some valuable initiatives towards addressing climate change effects have been launched. The European Parliament adopted the Directive 2009/28/EC and its following amendments, to create a common set of rules for the use of renewable energy inside the European Union (EU), aiming for the limitation of the greenhouse gas (GHG) emissions and the promotion of cleaner means of transportation. The directive set national binding targets for each country to accomplish an overall share of renewable energy equal to 20% of the total energy consumption of the EU, and specifically 10% for the transport sector.[6] In 2016, the EU adopted new regulations to achieve an overall share of renewable energy of at least 27% in the EU by 2030.[7] In 2010, Finland issued the national action plan for promoting energy from renewable resources. The proposal estimated that by 2020, a share of 38% of the gross energy consumption should come from renewable resources.[8] Globally, the signatory countries of the United Nations agreed in the COP21 Conference held in Paris in 2015 to take actions to limit the rising of the global temperature above 2°C compared to the average temperature of the pre-industrial era, as an effort to reduce the impact of climate change.[9] The agreement entered into force in December 2015 after the approval of the countries accounting for 55% of the global GHG emissions,[10] resulting in a significant commitment of the signatory countries to substantially reduce their GHG emissions in the next decades.

1 Introduction

The prefix bio- does not mean sustainability *per se*. For instance, the palm oil industry extracts chemical compounds from palm trees which are grown in soil that used to be host to Indonesia's rainforest, the third major rainforest in the world just after the Amazon and Congo basins. In this regard, the bioproduction of palm oil is far from being sustainable. Another example are the first-generation biofuels, which are produced from crops that also serve the food market, thus raising ethical concerns whether to use crops for energy purposes instead of food.[11] Many countries still face famine among large populations. Consequently, the choice of renewable raw materials for their conversion into chemicals, materials, and energy in the industry might be one of the requirements to claim sustainability, but it is not sufficient. Still, technological aspects and impact evaluation on society and the environment must be properly assessed before claiming sustainability for a certain process.

Biorefineries represent a novel concept where most of the biomass is converted into products minimizing the generation of waste.[11] Borregard in Norway, the Metsä Group's Äänekoski bioproduct mill in Finland and the RISE processum biorefinery cluster in Örnsköldvik, Sweden are good examples where most of the biomass is converted into paper, cellulose pulp, specialty cellulose, ethanol, lignosulfonates and some different chemicals.[12–14] The currently commercialized biorefineries are based on processes that evolved from the pulp and paper industry, as an effort to add value to the raw materials and provide differentiation from the technologies based on fast-growing tree species in developing countries. In fact, the production of pulp and paper based on eucalyptus and acacia trees in South America and Southeastern Asia is less expensive than the conventional technologies based on the conversion of spruce in the Nordic countries.[15]

Nevertheless, forestry biomass accounts for just a fraction of the worldwide existing biomass. Algae comprise around 50 wt.% of the total growing biomass. Algae are a large group of species that grow mainly in aquatic environments. However, it is also true that only a fraction of this biomass would be readily available for industrial use. Nonetheless, algae grow at a rate of 30–90 metric ton ha^{-1} $year^{-1}$,[16] while eucalyptus has a yield of around 5–25 metric ton ha^{-1} $year^{-1}$.[17] Algae consist of many different carbohydrates, proteins, lipids and ashes, and their composition varies according to the season and the environmental conditions. Most algae do not contain much glucose, which might be a disadvantage for already established processes, but also an advantage when considering the vast spectrum of possibilities that its constituents bring. In this regard, extraction is an important process in biorefineries, since industrially speaking, the aim is to

fractionate biomass in such a way that each fraction is obtained with maximum possible purity. The processing of woody biomass requires delignification steps to utilize the carbohydrate fraction. Processes such as Kraft or sulfite pulping are intensive in the use of energy and chemicals, while the valorization of the lignin has yet very few commercial applications. As a result, the presence of lignin in terrestrial plants is challenging when aiming fractionation of biomass, and even bioengineered plants have been designed to decrease its content. Conversely, algae do not contain much lignin. Only a few species have been reported to contain lignin to some extent, such as *Calliarthron cheilosporioides*.[18] Consequently, the fractionation of algae may be carried out under milder conditions before transforming its constituents into valuable products.

The world production of life stock harvest of algae in 2014 reached 1.2 million t, with Chile remaining as the largest algal harvester with 0.4 million t. The harvesting rate has remained relatively flat during the period 2006–2014. On the other hand, algae produced by aquaculture reached 27 million t in 2014, being 2-fold higher compared to the production achieved in 2006. The market of algae was worth MM US$ 5,637 in 2014, representing an increment of 45% compared to 2006. China and Indonesia remain the main algae producers accounting for 49 and 37% of the world production, respectively. Consequently, the aquaculture market is continuously growing, making evident the need to add value to the different fractions of the biomass.[19]

The main uses of algae are in food products for human consumption, accounting for a substantial share of the worldwide production of algae. Most of the remaining proportion of algae is used for producing chemicals, of which those with the most significant commercial value are agar, alginate, and carrageenan, with sales of MUS$ 173, 318 and 527, respectively, for 2009. These marine polysaccharides belong to the group of algal hydrocolloids, which are valuable for the food and pharmaceutical industries.[16,20] However, besides the extraction of these types of hydrocolloids, algae have no additional commercial use to date.

The importance of selective fractionation of carbohydrates is that their monomer constituents are intermediate molecules from which several additional chemicals can be produced. The selective conversion of sugars via biological or chemical processes results in the production of building blocks which possess different functional groups that provide the starting point for producing many useful chemicals and materials that can eventually replace those currently derived from fossil resources. The US Department of Energy has identified a group of 12 building blocks as key molecules in the transformation of sugars in biorefineries; these are depicted in Figure 1-1.[21] These sugar-based building blocks are different from the conventional commodities derived from oil refineries. Therefore, a huge challenge is

foreseen in developing the process technology capable of transforming these molecules into products that serve the same applications as those derived from fossil resources.

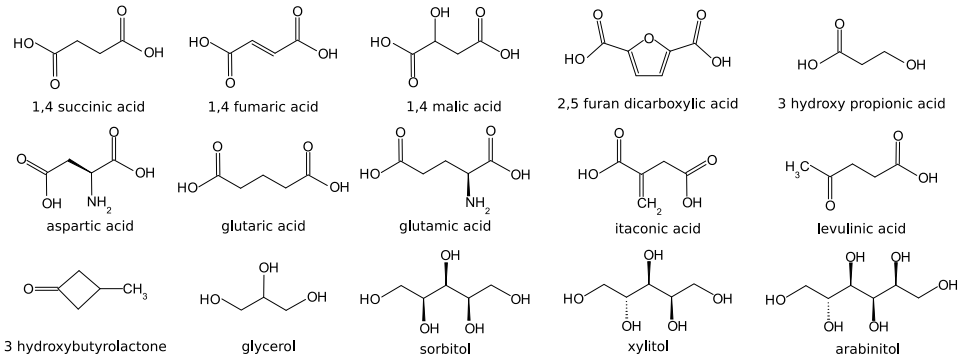

Figure 1-1. Selected building blocks derived from sugars;
Adapted from Werpy *et al.*, 2004.[21]

The aim of this work was to evaluate the feasibility of algal biorefinery for the valorization of its main constituents. The literature regarding the biorefinery of wood biomass is abundant, but their algal counterparts have been scarcely investigated. In this regard, the extraction of algal constituents was studied using water, organic solvents and ionic liquid extraction. Additionally, the hydrolysis of polysaccharides using biochemical and chemical processes was examined, and subsequently, a mathematical modeling for these reactions was proposed.

In order to place the present work in context, background literature of algal biomass as a bioresource is reviewed. Thus, the description of the major constituents of terrestrial plants is provided as a comparison. The main focus of the research was placed on the carbohydrates of algal biomass. Accordingly, basic information on the biochemistry of polysaccharides are also included. Additionally, a brief description of the conventional biomass fractionation processes for terrestrial plants and algae is given. The focus was particularly directed towards the hydrolysis of polysaccharides for the production of monomers.

2 Biomass as a bioresource

Terrestrial plants comprise mainly cellulose, hemicelluloses, starch, lignin, and extractives. Woody biomass as well as corn stover and wheat straw are typical examples of lignocellulosic material. In the case of woody biomass, cellulose accounts for ~ 40 wt.% of the biomass, while hemicelluloses and pectins make up 25–30 wt.% and lignin 25–30 wt.% in softwood. Hardwoods have similar cellulose content, but the hemicelluloses account for 30–35 wt.%, while the lignin content is in the range of 20–25 wt.%. These three groups comprise the structural polymers present in lignocellulosic materials. In the case of lignocellulosic material from crop plantations, the cellulose content is in the range of 35–40 wt.%, while hemicelluloses comprise around 40 wt.% of the dry weight, with the consequent decrease in the lignin content.[22] The extractives comprise single molecules, which account for about 5 wt.% of the dry weight of the biomass.[23] The most common extractive molecules occurring in terrestrial plants include phenolic compounds as well as hydrocarbons and ash. Even though the carbohydrate content of lignocellulosic material from plants is higher than that in woody biomass, the presence of ash in plants is usually higher than the content reported for forestry biomass.

In the case of marine biomass, algae belong to a major group of photosynthetic species that grow in aquatic environments. Among this group, there are multicellular species referred to as macroalgae, and unicellular species called microalgae. Another type of classification responds to the color of the tissue, which corresponds to the kind of chlorophyll in the cells. Consequently, three groups of algae can be found: brown (*Phaeophyceae*), red (*Rhodophyceae*) and green (*Chlorophyceae*). Interestingly, not all algal species belong to the same kingdom under the eukaryotic domain, which is an indication that notable differences in the conformation of the cells can be found. In this regard, green and red algae belong to the *Plantae* kingdom, while brown algae belong to the *Chromista* kingdom. Because of these differences, several different carbohydrates occur among algae species. Cellulose takes place in various compositions among most of the algal species, but they usually occur in association with sulfated polysaccharides which are absent in terrestrial plants. Examples of these polysaccharides are carrageenan, agar, ulvan and fucoidan.[24–30] Additionally, algae show high amounts of anionic polysaccharides such as alginate, the content of which is in the range 15–60 wt.% in brown algae.[25,31,32]

2.1 Basic information concerning the structural biochemistry of carbohydrates

Carbohydrates are widely distributed in different types of biomasses, covering terrestrial plants, algal biomass, bacteria, and so forth. Polysaccharides comprise sugar and uronic acid as their monomeric units. The following sections provide a brief description of the monomeric units of polysaccharides.

2.1.1 Monosaccharides

Monosaccharides are the main constituents of carbohydrates, but they also occur as extractives in the form of single sugars and disaccharides. Sugars can be either D-sugars (R-) or L-sugars (S-), which stands for the configuration of the secondary alcohol with respect to the chiral center of the molecule. Another distinction between these molecules is the α or β configuration that they adopt. This configuration is related to the stereochemistry at the anomeric position of the molecule, where the hydroxyl group adopts either an axial position, in which case it is called α configuration, or an equatorial arrangement, in which case it is referred to as β configuration. Concerning L-sugars, the definition of α and β is exactly the opposite. This anomeric orientation is particularly important in chemical reactions, since there is an equilibrium between α and β configurations for each monomer and the shift from one configuration to another is commonly termed as "mutarotation". Usually, the molecules adopting the α configuration are thermodynamically more stable compared to molecules adopting the β configuration, both in the pyranose form (ring of 6 carbons).[23] For instance, L-rhamnose is adopting α configuration in 66%, while 34% adopt the β configuration after reaching equilibrium in aqueous solution at room temperature (RT). However, D-glucose is an exception, where in equilibrium 38% of the molecules adopt the α configuration, while 62% adopt the β configuration in aqueous solution at 20°C.[23,33] A selection of the most common sugars in their pyranose form is displayed in Figure 2-1.

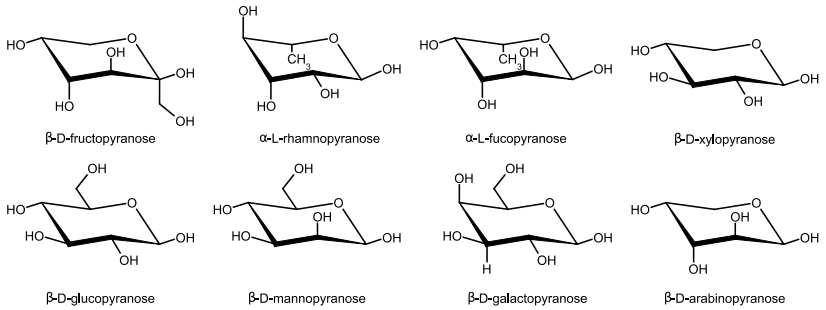

Figure 2-1. The pyranose form of the most common monosaccharides.

Sugar molecules can also exist in furanose form (ring of 5 carbons), but for most of the monosaccharides the proportion of the molecules that adopt this structure is below 1% at 30°C.[33,34] However, D-galactose, D-fructose and D-ribose are exceptions that show 6, 32 and 20% of furanose configuration, respectively. Ultimately, sugar molecules can also show an acyclic form in solution, but this arrangement is below 1% in aqueous solution at RT in most cases.[33]

2.1.2 Uronic acids

Uronic acids are molecules derived from sugars, where the terminal CH_2OH group is replaced with one carboxylic group.[33] Uronic acids derived from C6 sugars are called hexuronic acids, whereas those derived from C5 sugars are referred to as penturonic acids. Uronic acids are an important constituent of hemicelluloses, pectins, and glycoproteins in nature,[35] as will be described later. Since they are derived from sugars, they have the same configuration and stereochemical properties as their predecessors. In this regard, sugar acids are called after the name of the sugar followed by the suffix "uronic acid", as shown in Figure 2-2.

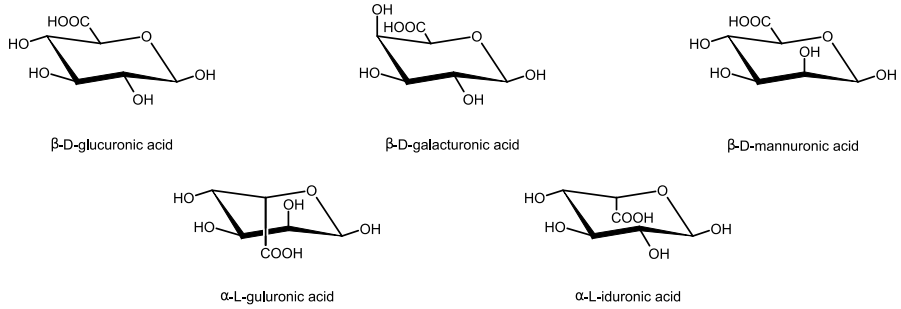

Figure 2-2. The most common uronic acids found in nature.

2.2 Terrestrial plant constituents

The cell wall of woody biomass comprises cellulose which is embedded into a hemicellulose–lignin matrix. This hierarchical conformation is very complex, and yet not completely understood by the scientific community.

The cell wall of terrestrial plants consists of a primary and secondary cell wall. Between the cells, the surrounding area is called middle lamella, which comprises mainly pectins and hemicelluloses. The primary cell wall consists of randomly oriented cellulose, accounting for the highest proportion of lignin. Consequently, the secondary cell wall is divided into three sections referred to as S1, S2, and S3. The S1 layer comprises about 10% of the cell wall, and cellulose microfibrils are wound circumferentially around the cell wall, while the S3 layer comprises about 4% of the cell wall and contains

unresolved cellulose microfibrils. The S2 layer comprises around the 80% of the cell wall, accounting for the highest fraction of cellulose of about 10–30%. In the S2 layer, the cellulose microfibrils are parallel oriented with respect to the vertical axis, providing most of the strength to the whole structure.[36,37]

The chemical interactions between cellulose, hemicelluloses, and lignin inside the cell wall are still a matter of debate in the scientific community. Since lignin is an amorphous polymer, its structure is very complex. Scientists suggest that amorphous hemicellulose interconnects cellulose and lignin, as depicted in Figure 2-4. Hence, arabinofuranoses are responsible for being covalently bonded to phenylpropane units of lignin. Therefore, interactions between arabinogalactans or xyloglucans with cellulose microfibrils are resolved via hydrogen bonds.[38] The extractives do not play any structural role in terrestrial plants, but are capable of protecting the tree against pathogens. Furthermore, the extractives serve as a source of energy and nutrients for the cells.[39]

2.2.1 Cellulose

Cellulose is a linear homopolymer consisting of glucose units linked by β-1,4 bonds. Essentially, the repeating unit in the cellulose backbone is cellobiose. This disaccharide comprises two glucose units, in which one unit is rotated by 180°C with respect to the other unit, as shown in Figure 2-3. The cellulose chain possesses two types of ends: non-reducing and reducing ends,[23] which are relevant to the hydrolysis mechanisms of the polymer.

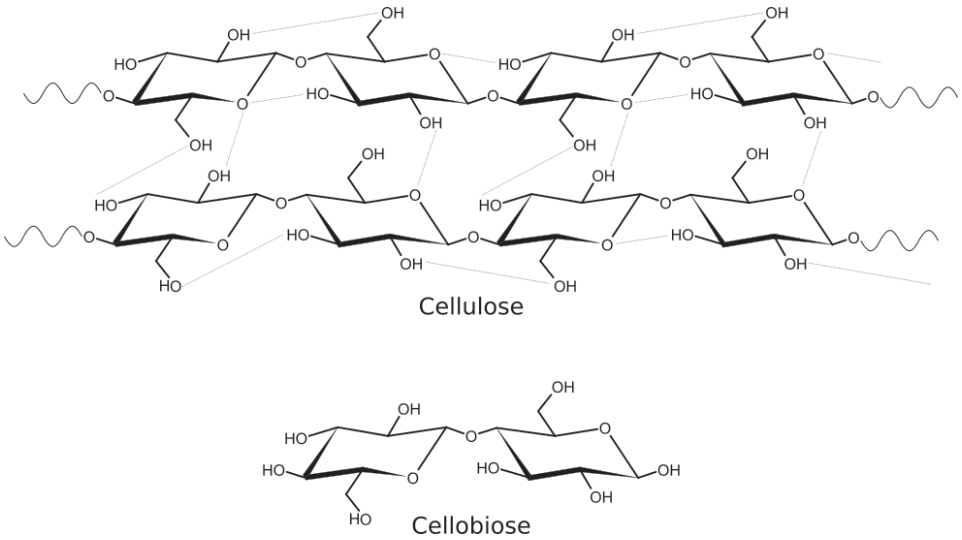

Figure 2-3. The structures of cellulose and cellobiose;
Cellulose structure was adapted from Baptista *et al.*, 2013.[40]

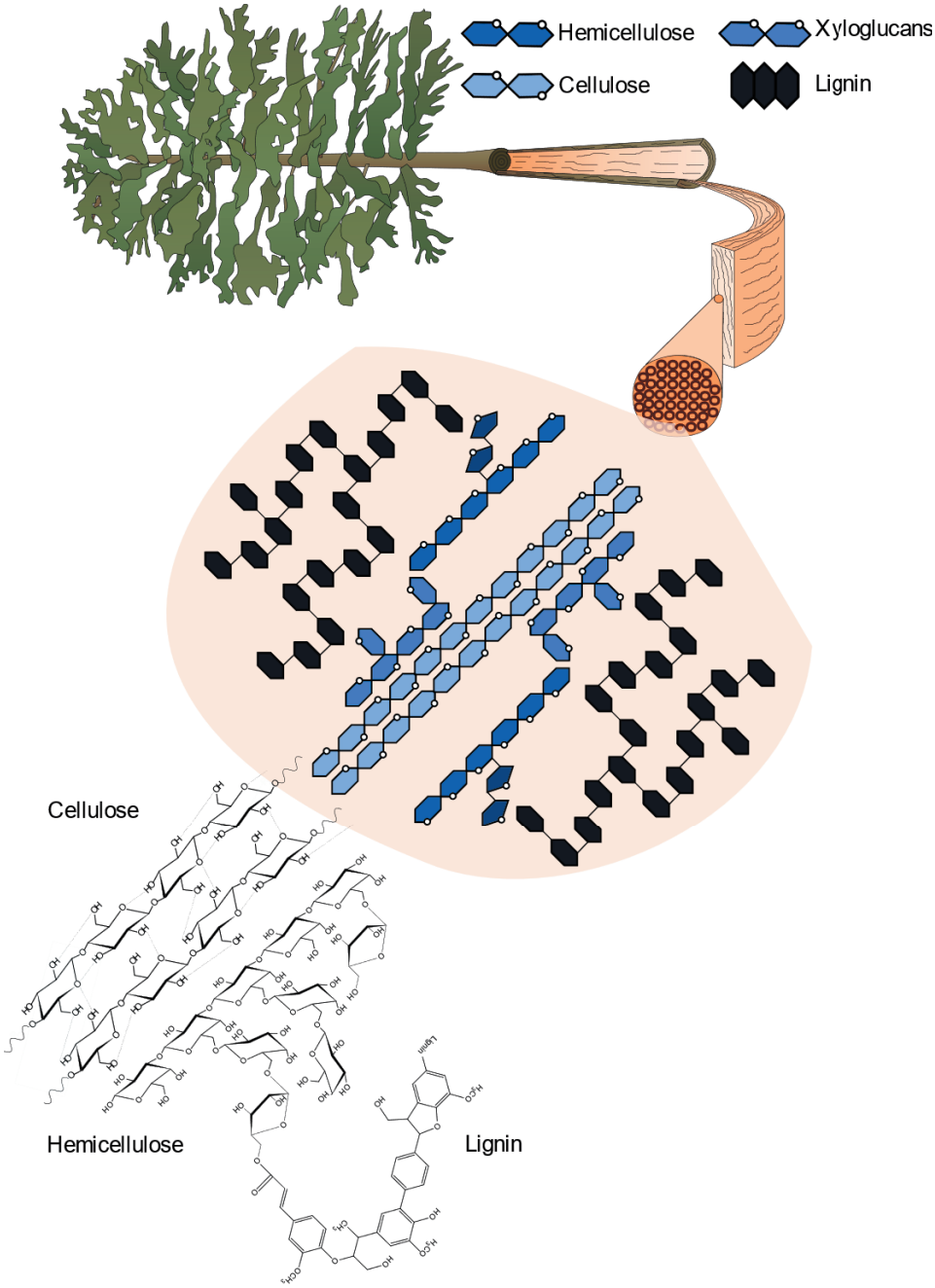

Figure 2-4. The hierarchical structure of the wood cell wall;
Adapted from Bidlack *et al.*, 1992 and Hoffman and Jones, 1990.[37,41]
Image of the tree *(Pinus virginiana)* was designed by Tracey Saxby, IAN Image Library.

Cellulose microfibrils are linked to each other by hydrogen bonds, giving intermolecular stability to the whole polymer. The degree of polymerization for cellulose varies between the species in the range of 900–5,000 units, however, softwood and hardwood have typically a polymerization degree in the range of 4,500–5,500 units, but can reach up to 10,000 units.[42,43] There exist four types of polyforms of cellulose: type I, II, III and IV, as well as, six allomorphs: Iα, Iβ, III_1, III_2, IV_1, and IV_2. Allomorph Iα corresponds to the structure found in primitive organisms such as bacteria, whereas wood has typically type Iβ which is thermodynamically more stable. Polyform II corresponds to regenerated cellulose, which is also thermodynamically more stable than polyform I. Consequently, changes from Iα to Iβ and both types I to cellulose II are irreversible processes. Transformation of cellulose I into cellulose III and IV follows different physicochemical procedures.[23,43]

2.2.2 Hemicellulose

Hemicelluloses are a group of polysaccharides that interconnect cellulose and lignin inside the cell-wall. These polysaccharides are essentially non-crystalline and have lower molar mass than cellulose (usually in the range of 20–100 kDa). Hemicelluloses consist of different units, principally xylose, arabinose, galactose, mannose and galacturonic acid. There are major differences in the type of hemicelluloses that occur in softwood and hardwood. The main hemicelluloses in softwood are galactoglucomannans, glucomannan, and arabinoglucuroxylan, whereas hardwood contains mainly xylan.[44]

2.2.2.1 Glucomannan

Glucomannans are one of the major hemicellulose constituents in softwood. The backbone consists of D-mannopyranose and g-glucopyranose linked by β-1,4 bonds, as shown in Figure 2-5. Glucomannans can be branched by D-galactopyranose linked by α-1,6 bonds to the backbone, in which case they are called galactoglucomannans. These galactoglucomannans occur mainly in softwood, while the non-substituted glucomannans predominate mostly in hardwood.[44]

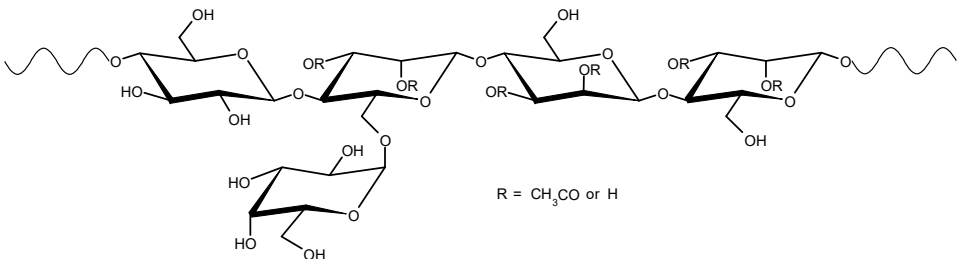

Figure 2-5. The structure of galactoglucomannan;
Adapted from Laine, 2005.[44]

2.2.2.2 Xylan

Xylans are one of the main constituents of hardwood hemicelluloses. The backbone comprises D-xylopyranose linked by β-1,4 bonds, as shown in Figure 2-6. Xylans can be substituted by acetyl groups in positions O2 and O3 of each xylose unit, and by 4-O-methylglucoropyranose units linked by α-1,2 bonds. This configuration is the most common type of xylan found in hardwood and softwood, referred to as O-acetyl-4-O-methylglucurono-β-D-xylan. Additionally, xylans in softwood exhibit a structure containing an L-arabinofuranose unit linked to the backbone by α-1,3 bonds.[44] This last substitution is believed to play a major role in the linkages to lignin.[45]

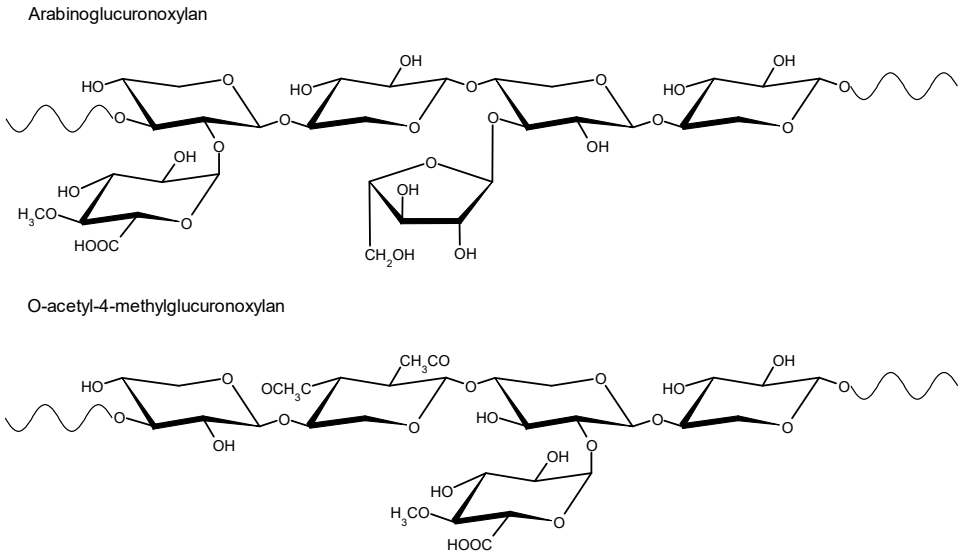

Figure 2-6. The chemical structure of xylan;
Adapted from Laine, 2005.[44]

2.2.2.3 Xyloglucan

Xyloglucan is one of the major types of hemicelluloses occurring in the primary cell wall of plants. The backbone is similar to cellulose comprising D-glucopyranose units linked by β-1,4 bonds. Conversely to cellulose, xyloglucans are extensively substituted by D-xylopyranose units linked by α-1,6 bonds, as shown in Figure 2-7. Additionally, further substitution can occur to the D-xylopyranose units by linkage to D-galactopyranose and L-fucopyranose units.[36,44]

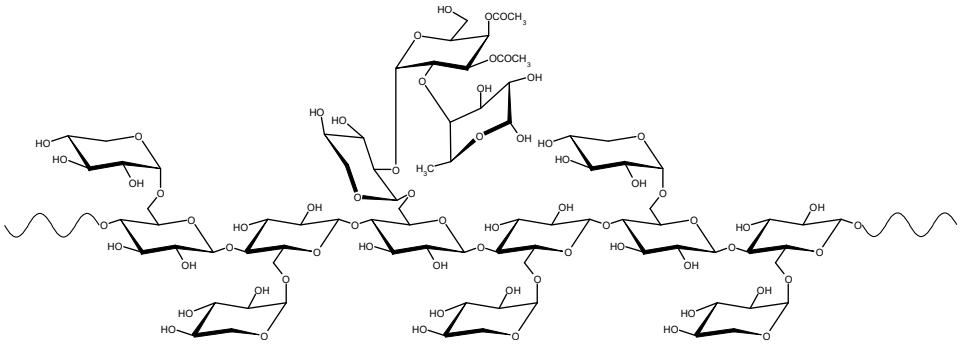

Figure 2-7. The chemical structure of xyloglucan;
Adapted from Ochoa-Villareal *et al.*, 2012.[36]

2.2.3 Starch

Starch is the second most abundant polysaccharide in plants after cellulose.[23] However, unlike cellulose and hemicellulose, starch does not play a structural role in the cell wall.[44] The repeating unit of starch is D-glucopyranose, which is linked by α-1,4 glycosidic bonds. The linear structure of starch is called amylose, which comprises between 200 and 2000 anhydroglucose units. Amylose can also be branched via α-1,6 linkages, which is referred to as amylopectin. This polysaccharide comprises 100–200 linear chains, each of them consisting of 20–30 anhydroglucose units. Amylopectin is the most abundant type of starch in nature. Figure 2-8 shows the structure of both types of starch.[23,44]

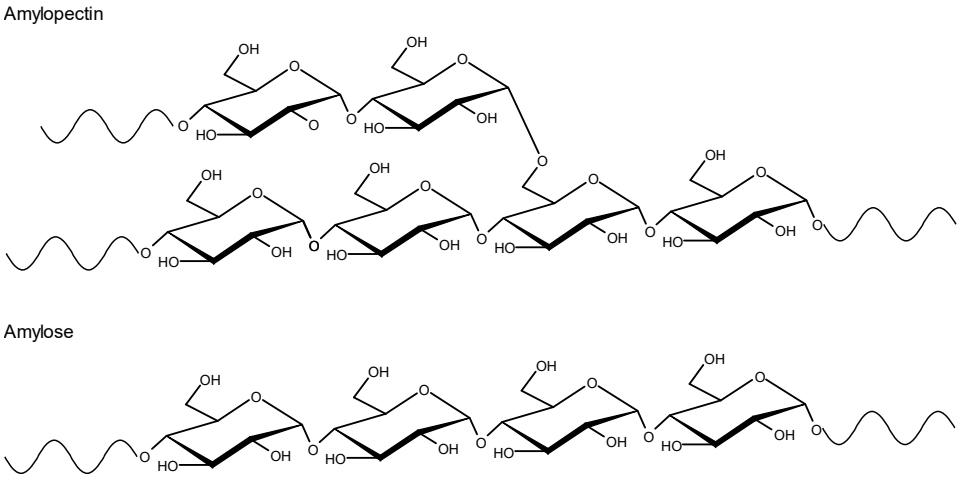

Figure 2-8. The chemical structure of starch.
Adapted from Riitonen *et al.*, 2013.[23]

2.2.4 Pectins

Pectins are polysaccharides comprising mainly D-galacturonic acid and L-rhamnose units.[36] They are water-soluble molecules located principally in the middle lamella between the plant cell walls.[23] Due to the presence of carboxylic acid groups, these types of polysaccharides are anionic and capable of forming gels in association with different ions such as borate and calcium.[46,47] Consequently, these types of polysaccharides are used in the food industry as thickeners.[23,47]

2.2.4.1 Rhamnogalacturonan

One of the most common types of pectins is rhamnogalacturonan, which comprises mainly repeating units of α-1,2-D-galacturonopyranose-α-1,4-rhamnopyranose.[47] Rhamnogalacturonans (RG) are classified into RG(I) and RG(II) depending on their degree of subsititution.[46] Pectins are essentially the only source of L-rhamnose in higher plants. Rhamnogalacturonans are usually linked to galactans and arabinans, where up to 80 wt.% of the L-rhamnose units are substituted, as shown in Figure 2-9.[36,47] One of the major sources of rhamnogalacturonan is potato, where this polysaccharide accounts for up to 56% of the cell wall.[47]

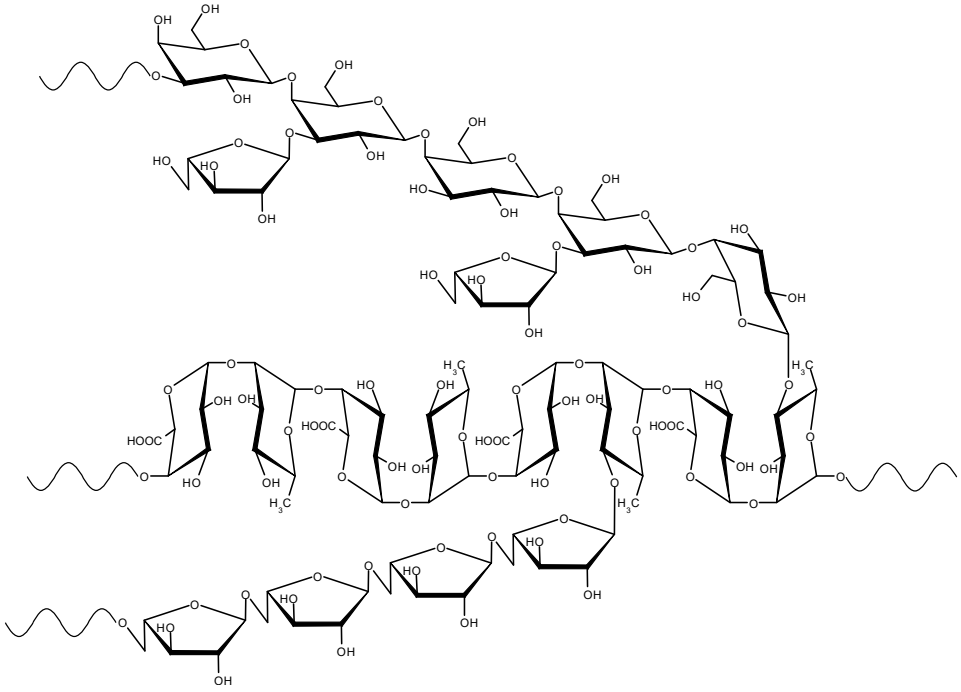

Figure 2-9. The chemical structure of rhamnogalacturonan II;
Adapted from Ochoa-Villareal *et al.*, 2012.[36]

2.2.5 Lignin

Lignin is an amorphous polymer comprising phenyl propane units, as shown in Figure 2-10. In softwoods, coniferyl alcohol is the most common repeating unit, while in hardwood sinapyl and coumaryl alcohols are the predominant precursors. The most common linkage between these units is the β-O-4' carbon-carbon bond.[44,48]

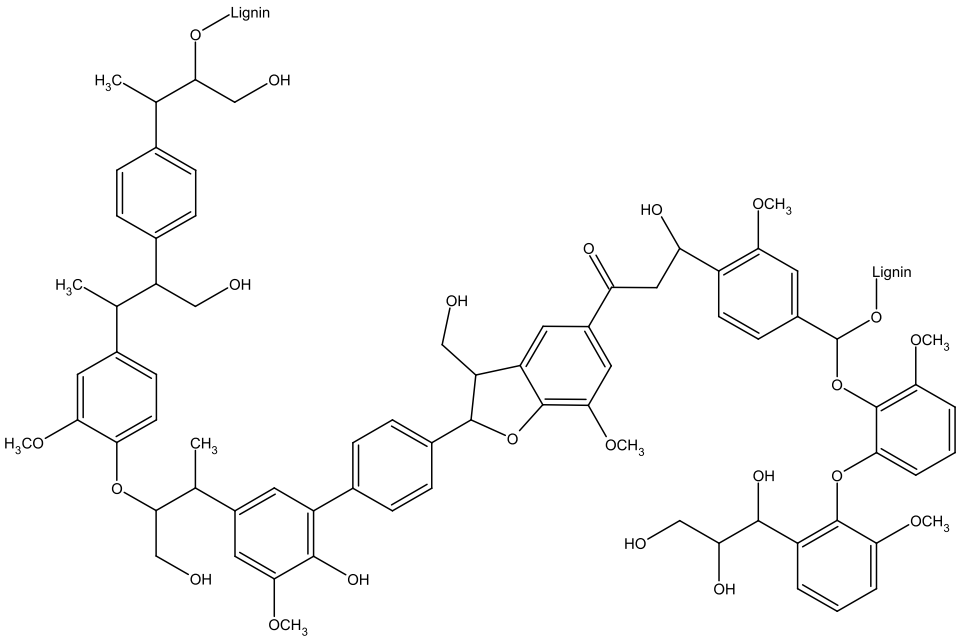

Figure 2-10. The chemical structure of lignin;
Adapted from Anugwom, 2014.[48]

2.2.6 Extractives

Unlike cellulose, hemicellulose, and lignin, the extractives are not structural constituents of the plant cell wall.[48] The extractives can be classified by their affinity towards polar and nonpolar solvents, referred to as lipophilic and hydrophilic extractives. These molecules protect the wood against microbial attack and provide some mechanical protection to the biomass due to the sticky characteristic of some molecules.

2.2.6.1 Ash

Ashes such as salts are also considered to be extractives, since they are usually soluble in polar solvents. Ash content is typically low in trees, but higher in crops.

2.2.6.2 Hydrophilic extractives

The most common hydrophilic extractives are sugars, phenols, and polyphenols. In this regard, polyphenols are the most interesting molecules which are found in the bark and knots of woods. Among this group different lignans, stilbenes and flavonoids are of importance for the chemical industry. Lignans comprise two phenyl propane units linked by β-β' bonds, as shown in Figure 2-11. Stilbenes are molecules derived from 1,2-diphenylethylene or exhibit a C6-C2-C6 skeleton. Flavonoids are similar to stilbenes, but feature a C6-C3-C6 skeleton.

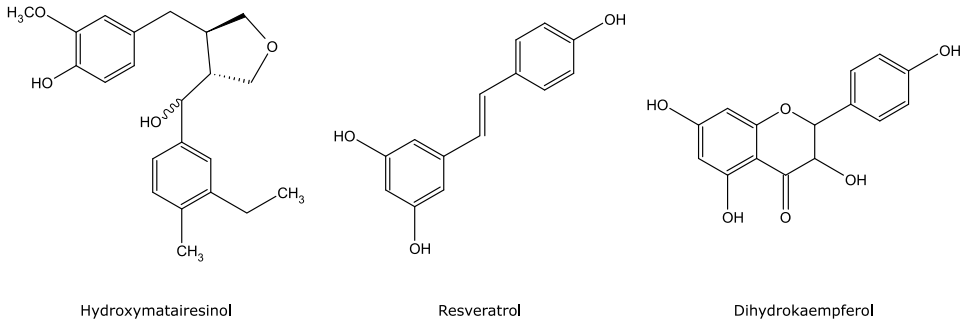

Hydroxymatairesinol Resveratrol Dihydrokaempferol

Figure 2-11. Examples of hydrophilic extractives.

2.2.6.3 Lipophilic extractives

Lipophilic extractives are mainly present in the resin canals (oleoresin) and parenchyma cells (parenchyma resin) of the biomass. Oleoresins are terpenoids derived from isopropene units, classified as monoterpenes (two isoprene units) and diterpenes (four isoprene units). Parenchyma resins are different types of fats, waxes and free fatty acids. Examples of lipophilic extractives of high importance for the chemical industry are shown in Figure 2-12.

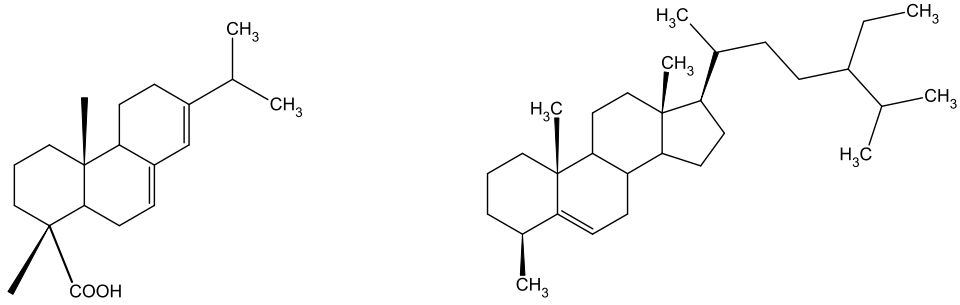

abietic acid sitosterol

Figure 2-12. Examples of lipophilic extractives.

2.3 Algal constituents

Algae comprise a group of many different species. Among the *Archaeplastida* phylum terrestrial plants, green algae and red algae evolved like plant species.[29] Alternatively, brown algae evolved independently from the *Archaeplastida* phylum species.[29,49] Consequently, the structure of the cell wall developed differently regarding its type of constituents in the cell wall.

The arrangement of terrestrial plant cell walls comprises a matrix comprising cellulose, hemicellulose, and lignin, as described in section 2.2. With respect to algal biomass, there is evidence that the almost complete absence of lignin, especially in green and brown algae, results in a different conformation of the algal cell wall compared to the cell wall of terrestrial plants.[49–51] The occurrence of anionic polysaccharides such as fucoidan and alginate in brown algae and ulvan in green algae, together with the occurrence of proteins and cellulose as a microfibrillar structure, results in a different hierarchical formation of the algal cell wall. Such differences will be described in the following section particularly for brown and green algae, with a focus on *Fucales* and *Ulva* species.

2.3.1 Brown algae

The most important constituents of brown algae are cellulose, laminarin, fucoidan, alginate, proteins, and phlorotannins. Cellulose occurs as microfibrils which are embedded into a matrix of fucose containing sulfated polysaccharides (FCSPs), which act as major cross-linkers of the cell wall, as depicted in Figure 2-13. However, it remains undetermined which kinds of linkages are bonding both cellulose and FCSPs. Hypothetically, hemicelluloses act as joints between cellulose microfibrils and FCSPs. Alternatively, proteins are very likely to be associated with FCSPs and play a role in building the structure into the brown algae cell wall.[49]

Alginates are the main constituents of the brown algae cell wall. This polymer is believed to provide rigidity to the cell wall due to its ability to form gels when associated with divalent ions. Consequently, the ratio of guluronic and mannuronic residues provides different rigidity to seaweed. Subsequent extraction of brown algae polysaccharides has shown that alginate act as a network in which the cellulose–FCSPs are embedded. The same experiments have shown that many polyphenols were co-extracted with alginate, suggesting that there are covalent linkages between alginate and phlorotannins, consequently having a structural role in the cell wall.[49]

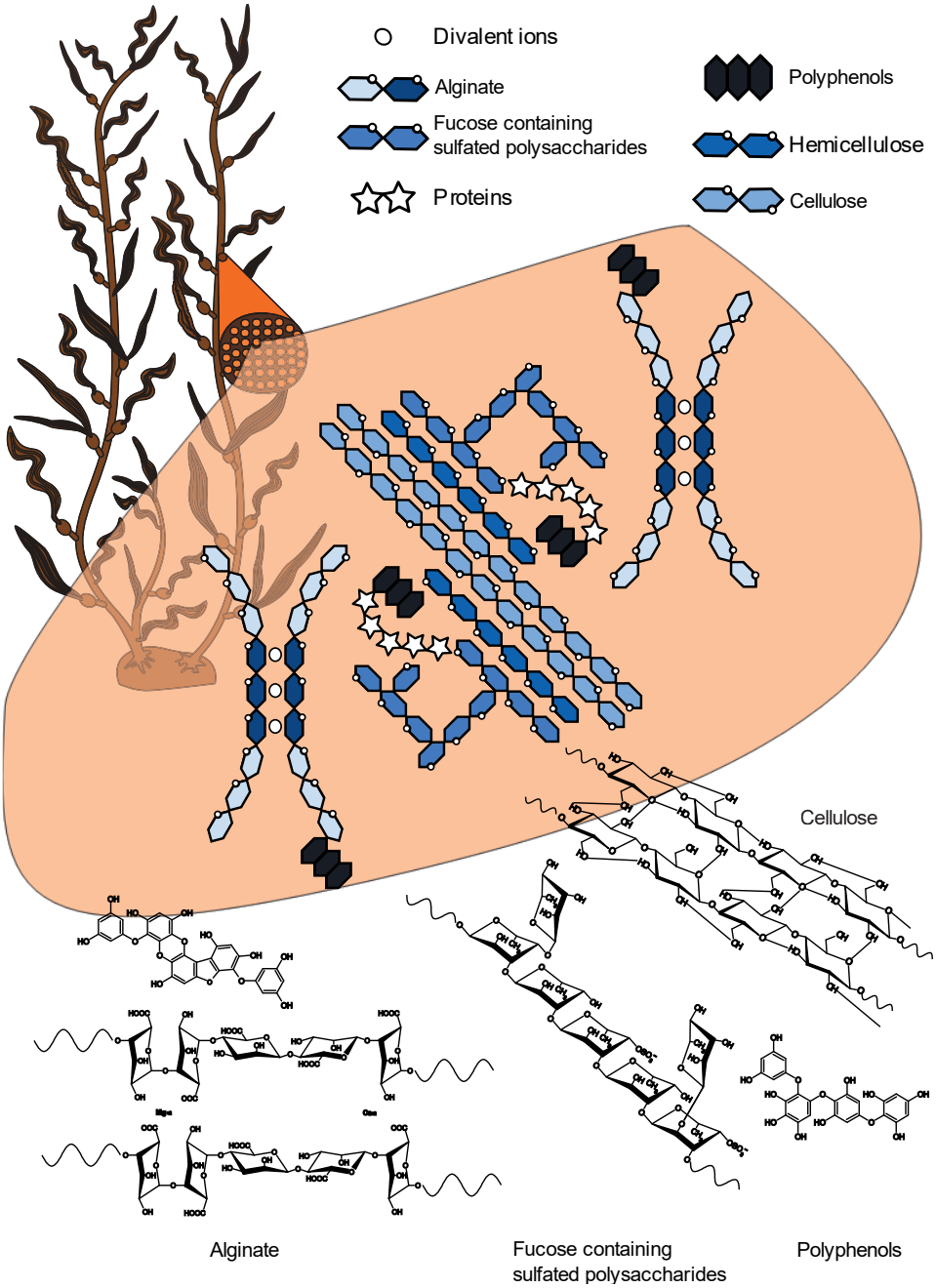

Figure 2-13. Cell wall model for brown algae containing fucans;
Adapted from Deniaud–Bouët *et al.*, 2014 and Stiger–Pouvreau *et al.*, 2016.[30,49]
Image of the brown algae specie was designed by Jane Thomas, IAN Image Library.

2.3.2 Green algae

Green algae have evolutionary roots such as those of red algae and terrestrial plants. Consequently, the composition and conformation of the cell wall are closely related to that of terrestrial plants. Still, in the case of *Ulva* species, the main difference from terrestrial plants is the absence of lignin. *Ulva* species contain cellulose fibers that are linked to xyloglucans in the cell wall. Additionally, the rhamnoglucuronan ulvan might act as a cross-linker of the polysaccharides, analogous to alginate in brown algae, as shown in Figure 2-14. Different extraction approaches and staining of the extracts have demonstrated that the ulvan (rhamnoglucuronan) content is relatively low in the cell wall, whereas higher contents have been found in the intercellular spaces.[51] Interestingly, these intercellular spaces are analogous to the middle lamella section of terrestrial plants, where pectins such as rhamnogalacturonan have been reported to be located.[52] However, there is also evidence that rhamnogalacturonans have taken place in the primary cell wall of plants.[46] In turn, β-1,4-D-glucuronan might be mainly distributed in the cell wall, associated with microfibrillar cellulose and xyloglucans. Glucuronans are polysaccharides that are closely related to proteins,[50] providing a structural role in the cell wall, such as FCSPs in brown algae species.

2.3.3 Skeletal polysaccharides

The skeletal polysaccharides occur in fibrous form in the cell wall. The most common polysaccharide of this type is cellulose, but some xylans and mannans are also produced by certain types of algae.[25,26]

2.3.3.1 Cellulose

Cellulose is the most abundant polysaccharide in terrestrial plants, but not in algal biomass. Brown algae, for instance, are richer in alginate, as it will be described later. The structure of the cellulose occurring in algae is similar to the one occurring in terrestrial plants, but with some differences. For instance, *Valonia* is a type of unicellular green algae that contains cellulose Iα, different in conformation from the cellulose Iβ found in terrestrial plants, as described in section 2.2.1. Cellulose I occurs mainly in green algae, indicating that long fibers are formed providing more rigidity to the structure.[26]

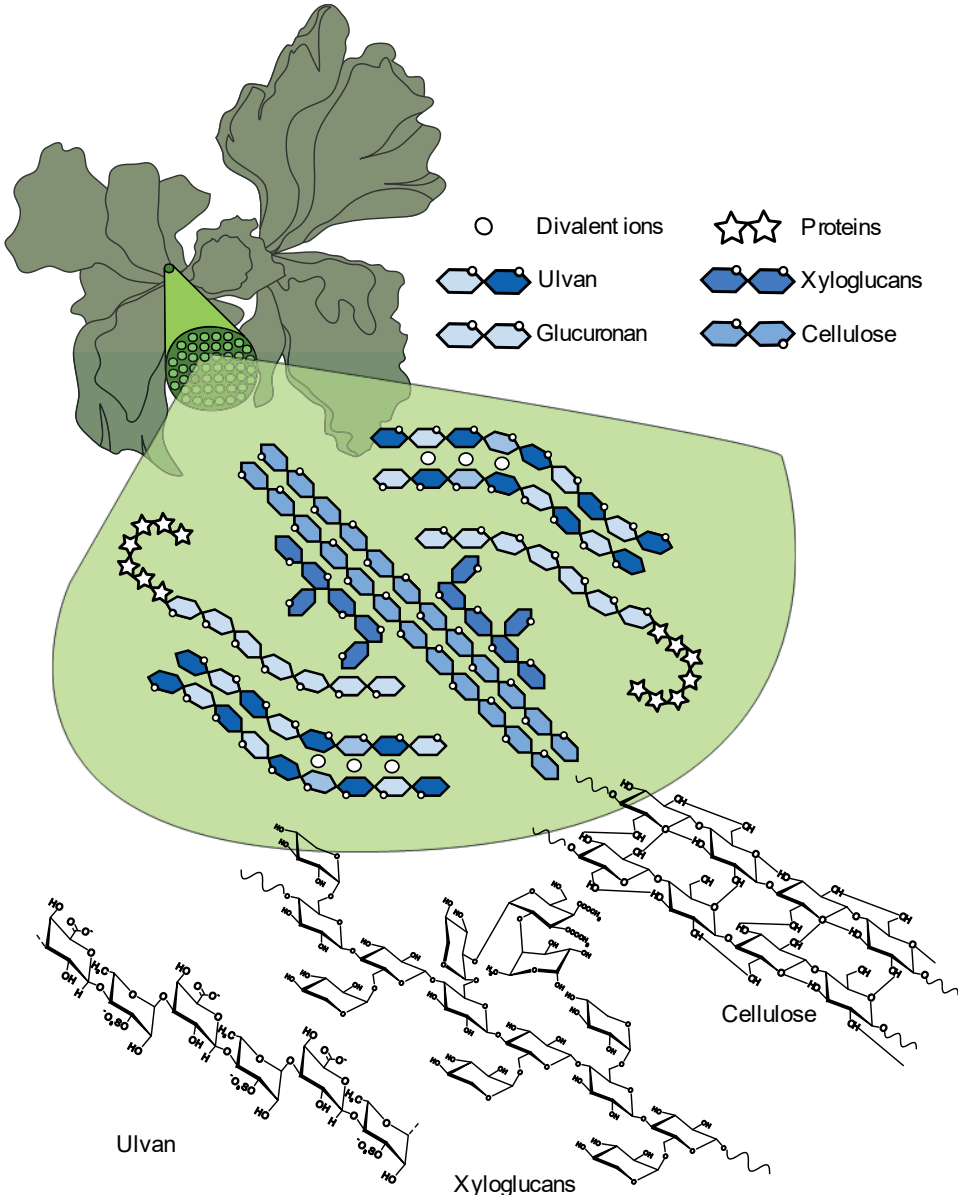

Figure 2-14. Cell wall model for green algae Ulva *species;*
Adapted from Bobin–Dubigeon *et al.*, 1997 and Lahaye and Robic, 2007.[50,51]
Image of the *Ulva* sp. was designed by Tracey Saxby, IAN Image Library.

2.3.3.2 Mannans

Mannans are not abundant in algal biomass, but some species, such as *Porphyra umbilical* and *Codium fragile* contain, mannans to some extent. Unlike the GGM backbone where mannose is linked to glucose by β-1,4, linkages under the presence of branched galactose, algal mannans contain a backbone that comprises mainly β-1,4 mannobiose and is unbranched, as displayed in Figure 2-15. The extraction of this fraction from the green alga *C. fragile* suggests that this type of mannan replaces cellulose as a structural polysaccharide in the cell wall.[26]

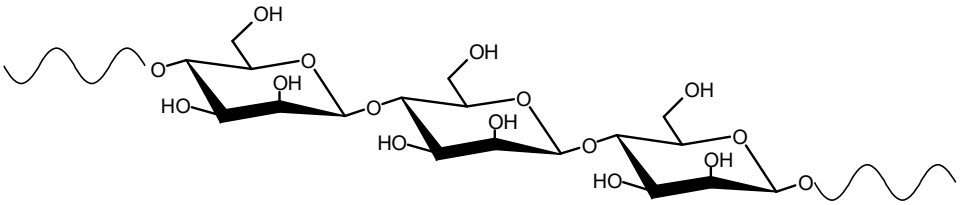

Figure 2-15. The chemical structure of algal mannan.

2.3.3.3 Xylans

Xylose is a common monomer found in the hydrolysate of algae, but a few species contain xylose in the backbone as the main unit. The green alga *Caulerpa filiformis* is one exception presenting D-xylopyranose units linked by β-1,3 linkages, mainly unbranched.[26] This xylan occurs in the cell wall as a fiber made of three helices providing a fibrous structure to the tissue.[31] This kind of xylan displays a major difference compared to terrestrial plant xylans, where the β-1,4 linkage predominates in the backbone. Xylans are one of the main constituents of the cell wall of some red algae species such as *Rhodymenia palmata* and *Palmaria palmata*. In these species, xylans present two types of linkages: β-1,3 and β-1,4, as shown in Figure 2-16.

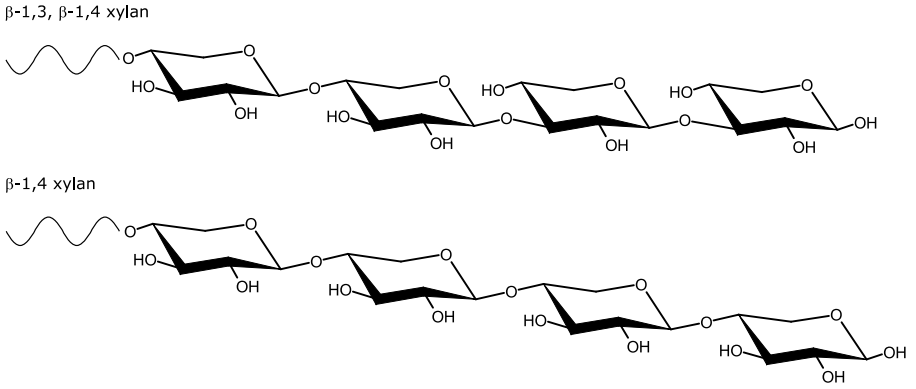

Figure 2-16. The chemical structure of algal xylan;
Adapted from Peat and Turvey, 1965.[26]

2.3.3.4 Alginate

Alginate is a type of polyuronic acid that occurs almost exclusively in brown algae. This polysaccharide comprise α–L–guluronic and β–D–mannuronic acids linked by 1,4 bond, as depicted in Figure 2-17.[25,28] The ratio of α–L–guluronic and β–D–mannuronic acids vary depending on the species, which consequently affect the gelation properties of the molecule.[28] The backbone comprises carboxylic groups that give alginate the possibility to be associated with divalent metallic ions. However, only guluronic acid residues can form a gel in the presence of divalent ions, while mannuronic acid residues do not.[49] Consequently, alginate takes place in the cell wall mainly in the form of salts such as calcium ir sodium alginate. In this regard, when protonated, alginate is referred to as alginic acid. Due to these gelation properties associated with the ionic nature of the backbone, alginate has wide uses in the food industry, also recently in several medical applications. Still, sodium alginate is the most commercialized preparation of this brown seaweed extract.[25]

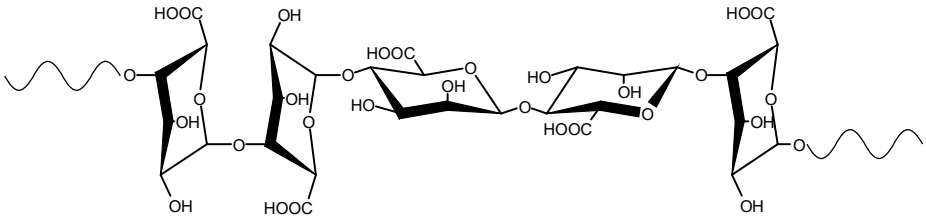

Figure 2-17. The chemical structure of alginic acid;
Adapted from Draget *et al.,* 2005.[28]

2.3.4 Food reserve polysaccharides

Typically, the main source of food in algal species is starch, particularly in green algae. However, red and brown algae show some differences in the type of food reserve polysaccharides, which are described below.

2.3.4.1 Starch

Algal starch is very similar to terrestrial plant starch, especially concerning green algae starch. However, green algae starch granules are smaller than those from terrestrial plant starch, due to a lower molecular weight.[31] Still, both green algae and terrestrial plant starch are produced in the chloroplasts of the cells. In the case of red algae, it synthesizes a different type of starch, which is produced directly in the cytosol of the cells, referred to as Floridian starch. Red algae starch comprise α-1,4, and α-1,6 linkages,[53,54] and the backbone is more branched and contains shorter molecules than the starch from green plants, resembling the structure of glycogen in mammals.[53]

2.3.4.2 Laminarin

Laminarin comprises D-glucopyranose units linked by β-1,3 and β-1,6 bonds. The β-1,3 bond predominates in the backbone, whereas there are some β-1,6 linkages inside the backbone and in side-chain positions. Depending on the last unit located at the reducing end of the backbone, laminarin can contain G or M chains. G chains have a glucose unit at the reducing end of the chain, while M chains feature a mannitol unit at the reducing end of the chain, as shown in Figure 2-18. Mannitol is an important constituent of brown algae species, and its content shows major variations within the harvesting season.

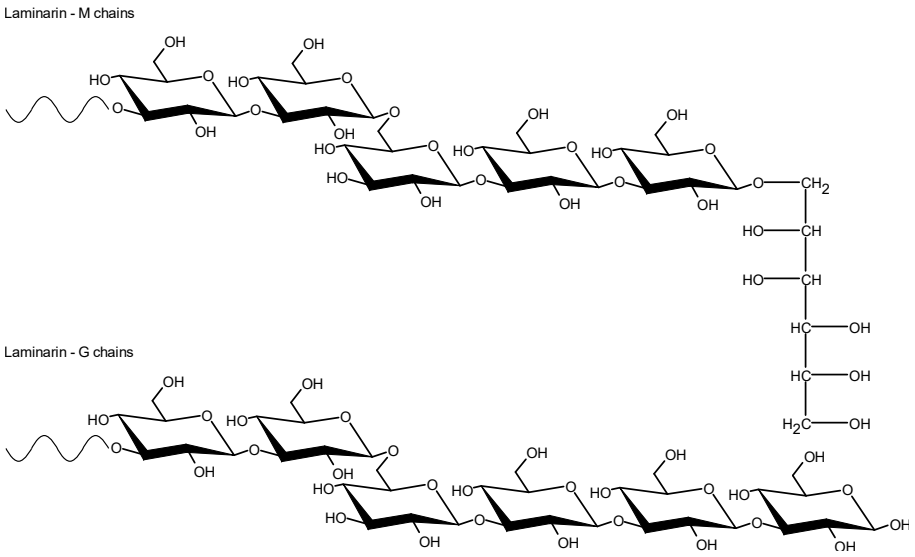

Figure 2-18. The chemical structure of laminarin;
Adapted from Percival, 1979.[31]

2.3.5 Sulfated polysaccharides

One of the most prominent differences between algal and terrestrial plant polysaccharides is the occurrence of sulfated polysaccharides in the algal cell wall. Most of the algal species contain to some extent a fraction of polysaccharides with sulfate groups in certain units, whereas sulfate substituents remain mainly absent in terrestrial plants polysaccharides. The most important sulfated polysaccharides of brown, red and green algae are described below.

2.3.5.1 Fucoidan

Fucoidan comprises α-L-fucopyranose (6-deoxy-α-L-galactopyranose) units linked by α-1,3 bonds. The backbone is branched with additional fucose units at position O4 or O2 in one of every 2-3 fucose units. Galactose and aminoglycoside residues have been found in fucoidan of some species.

Additionally, fucose units can contain a sulfate group located at position 4, as displayed in Figure 2-19. Fucoidan occurs mainly in brown seaweed species. The occurrence of fucose in algae is particularly interesting since L-sugars are relatively rare in nature. Fucoidan has been attributed to possess anti-coagulant, anti-thrombotic, anti-virus, anti-tumor and anti-oxidant activities.[24]

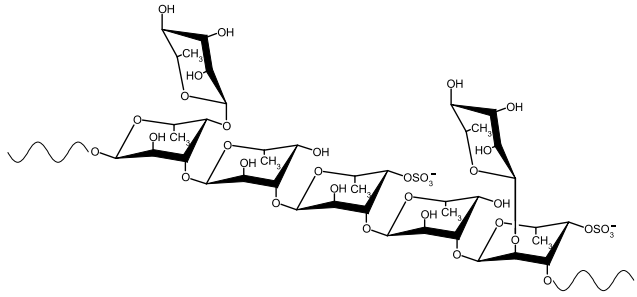

Figure 2-19. The chemical structure of fucoidan;
Adapted from Li *et al.*, 2008.[24]

2.3.5.2 Agarose

Agarose is a type of unbranched polysaccharide present mainly in red algae. The backbone consists principally of repeating units of agarobiose [→3)-β-D-galactopyranose- (1→4)-α-L-galactopyranose-3,6-anhydrous-(-1→].[26,55,56] Agarose has a relatively low sulfate content compared to other sulfated polysaccharides. When sulfated, agarose presents different configurations, as shown in Figure 2-20.[56] Generally speaking, agarose is used mainly by the food industry as a jellifying agent, but some medical applications related to its anti-tumor activity have been attributed to this polysaccharide.[25]

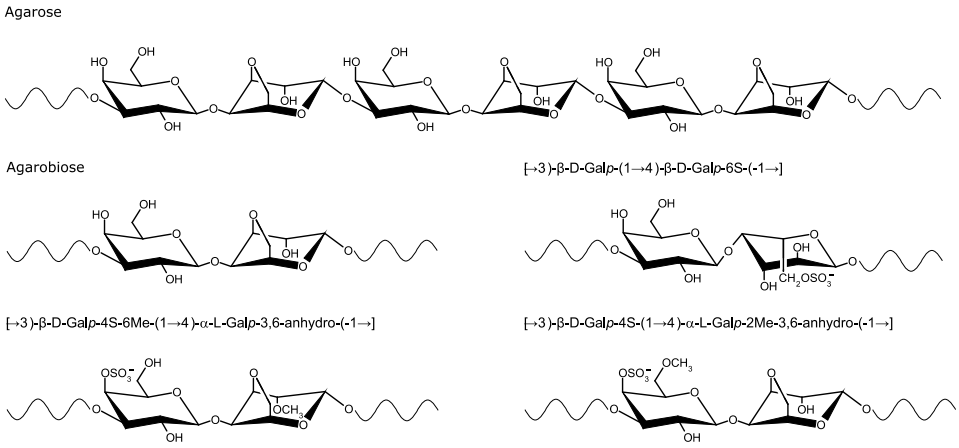

Figure 2-20. The chemical structure of agarose;
Adapted from Armisén and Galatas, 2000.[56]

2.3.5.3 Carrageenan

Carrageenan is another sulfated polysaccharide consisting of galactans, though the major difference compared to agarose is that carrageenan comprises exclusively of D-sugars.[26] Conversely to agarose, carrageenan has much higher sulfate content with most of the galactose units substituted with sulfate groups. The structure of the backbone is relatively similar to the structure of agarose, where D-galactopyranose and 3,6-anhydro-D-galactopyranose are linked via β-1,4 and α-1,3 bonds. In the selective extraction of this polysaccharide, three types of carrageenans can be obtained, and their structure depends on the degree of sulfate substitution of the galactose monomers. The different types of carrageenans are referred to as kappa, iota, and theta carrageenan, respectively, and their structures are shown in Figure 2-21. Mu, nu and lambda carrageenans are postulated to be the precursors of kappa, iota and theta carrageenans, obtained via alkali extraction.[27] Carrageenans are widely used in the food industry because of their rheological properties, varying from viscous thickeners to thermally reversible gels.[27,55] Furthermore, the research has recently focused on medical applications based on the anti-tumor and anti-viral properties that have been attributed to the structure of carrageenans.[57]

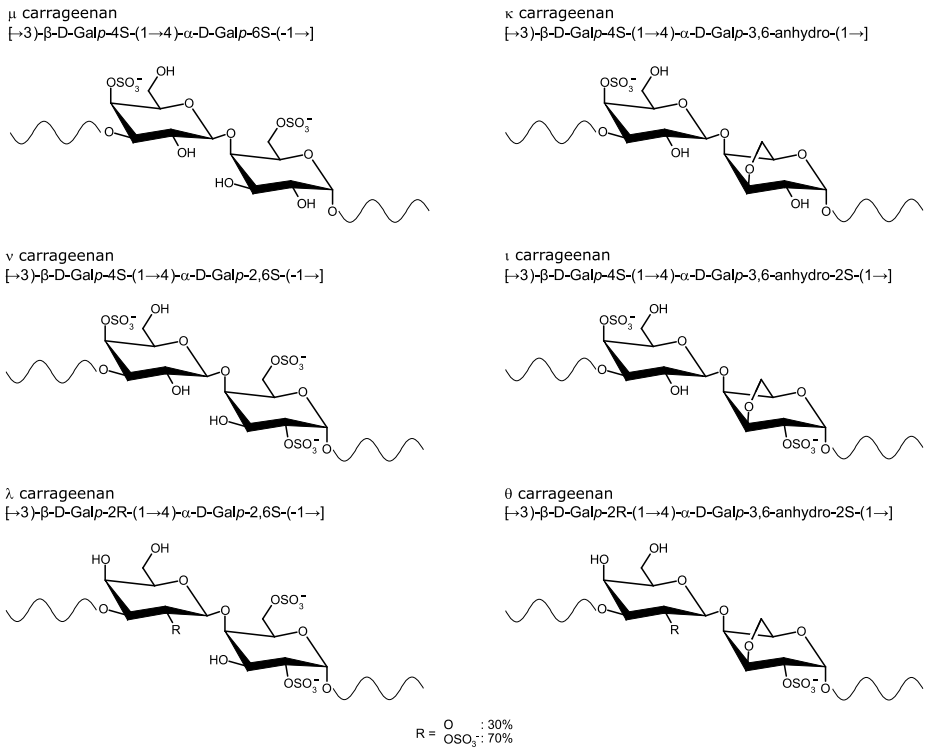

Figure 2-21. The chemical structure of carrageenan;
Adapted from Imeson, 2000.[27]

2.3.5.4 Ulvan

Essentially, ulvan is a polysaccharide that comprises mainly L-rhamnose, D -glucuronic acid, D-xylose and L-iduronic acid. Ulvan occurs primarily in the cell walls of green algae, in association with xyloglucans, glucuronan, and cellulose. The chemical structure of ulvan recognizes two main disaccharides: ulvanobiuronic type A [4→β-D-GlcA*p* (1→4) α-L-Rha*p*-3S] and ulvanobiuronic type B [4→α-L-IduA*p* (1→4) α-L-Rha*p*-3S]. Additionally, disaccharides containing D-xylose have been reported to be part of ulvan, as depicted in Figure 2-22. Similar to agarose and carrageenan, ulvan contains sulfate groups which are linked in a high proportion to L-rhamnosein position O-3 and in a minor extent to D-xylose. In this regard, the sulfate groups and the carboxylic groups from glucuronic and iduronic acids make ulvan an anionic polysaccharide.[50,55,58] These functional groups allow for the formation of weak ulvan gels in association with metallic cations such as borate. Still, the role of ulvan in the green algae cell wall is not completely clear. The jellifying properties of ulvan may be important in allowing the algal tissue to float in tides. Additionally, it has been demonstrated that ulvan inhibits the growth of certain bacteria, probably by blocking the biodegradation of structural cellulose. Indeed, ulvan was attributed to inhibit the action of cellulases and, therefore, to prevent the degradation of cellulose.[51,59]

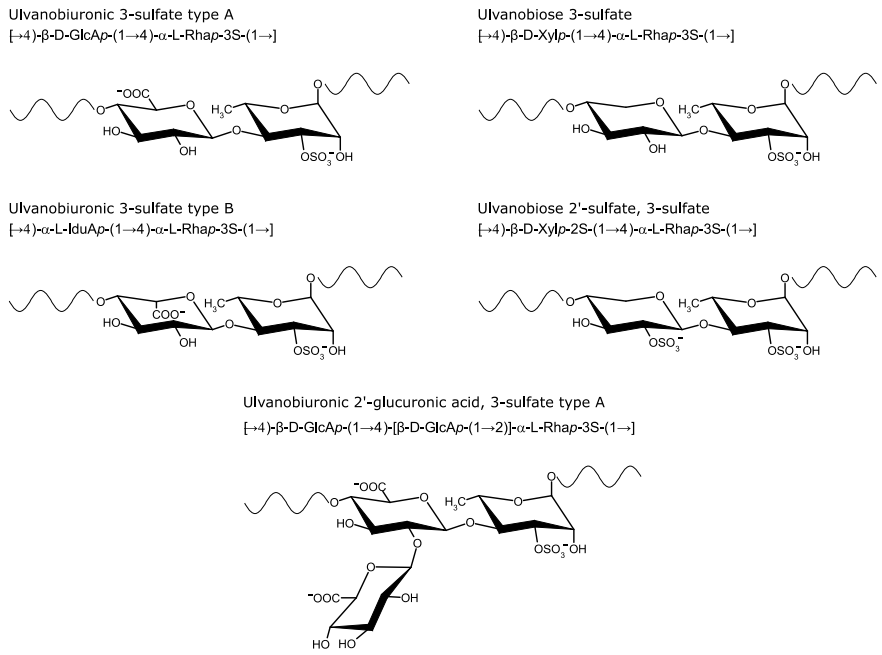

Figure 2-22. The chemical structure of ulvan;

Adapted from Lahaye and Robic, 2007, Jiao *et al.*, 2011 and Cunha and Grenha, 2016.[50,55,58]

From a processing point of view, ulvan attracts interest because of its resemblance to hyaluronic acid and heparin. Hyaluronic acid is an anionic polysaccharide which comprise D-glucuronic acid and D-glucosamine, which is attributed to possess many different physiological properties. Heparin is a polysaccharide belonging to the group of glycosaminoglycan, comprising glucose, glucuronic and iduronic acid residues partially substituted by sulfate and aminosulfate groups. Heparin possesses anti-coagulant properties, and it is used for curing several diseases. However, the available heparin extraction process is coupled to the slaughtering of cattle, which is a highly polluting process. In this regard, ulvan may be a naturally occurring polysaccharide that can substitute the use of heparin industrially. Additionally, since ulvan resembles glycosaminoglycans such as chondroitin, it can also serve in skin health applications.[60]

The high content of L-rhamnose in ulvan is also attractive to the cosmetic industry since it has a role in the health of human skin by preventing severe drying. There are also medical applications of L-rhamnose derivatives such as 5-deoxy-L-ribose. Moreover, since L-sugars are L-nucleotide analogs, L-rhamnose can serve as a starting molecule in the design of vaccines for the cure of certain diseases.[61]

2.3.6 Extractives

Following the same classification as for terrestrial plants, algae contain different types of molecules that can be considered as extractives, since they do not play a major role in the structure of the cell wall.

2.3.6.1 Ash

Algae also contain significant amounts of salts, much higher than what is found as ash in terrestrial plants. Brown and red algae contain around 20-50 wt.% ash on a dry basis,[16,62] while green algae possess around 20-30 wt.% ash on a dry basis.[16,63] The ash content is closely related to the salty nature of marine environments, which promoted the association of anionic polysaccharides with divalent cations.

2.3.6.2 Phlorotannins

Phlorotannins are polyphenolic secondary metabolites mostly found in brown algae, consisting of tannins built from phloroglucinol units and terpenes, as shown in Figure 2-23.[29,64] Some tannins can also be found in green algae. Phlorotannin compounds possess anti-oxidant activities and constitute up to 15 wt.% of the dry weight of the alga, and have molecular weights of around 10–100 kDa.[62,64] These types of molecules are found in cell vacuoles, and they are believed to have a protective function against radiation damage. Other properties are related to the accumulation of heavy

metals.[29] There is also evidence that phlorotannins may help strengthen the cell wall in brown algae by interactions with proteins and alginate.[29,49,65]

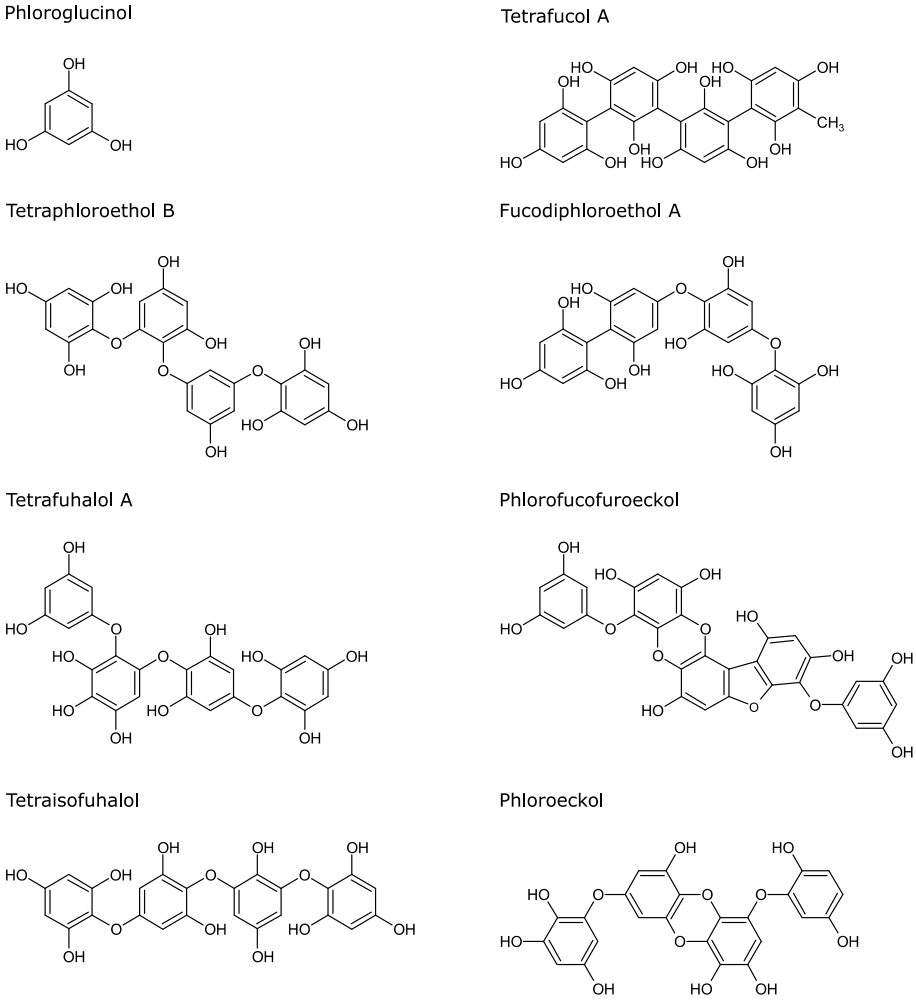

Figure 2-23. The chemical structure of the most common phlorotannins; Adapted from Koivikko, 2008.[64]

2.3.6.3 Sugar alcohols

One of the most important extractives in brown algae is mannitol, which is a sugar alcohol classified as a photosynthetic reserve material. Mannitol is found in the plastids of cells and in the reducing end of laminarin, and it may account for around 20–30 wt.% of the dry alga. Additionally, some units of sucrose and glycerol can be found as extractives in algae. Because of the low molecular weight of these molecules, they can serve to lower the freezing point of the cytoplasm or to balance the osmotic pressure of the cells.[29]

2.3.7 Proteins

Proteins are important constituents of algae, accounting for around 20 wt.% of the dry algae,[16] but in microalgae, the protein content can reach values up to 60 wt.%.[66] Proteins may play a major role in the cell wall, forming mucilage gel also containing fucoidan and laminarins in brown algae.[49] However, brown algae have fewer proteins compared to red and green algae.[66] Particularly in green algae *Ulva* species, proteins associate with glucuronans, which is a carbohydrate which comprise only D-glucuronic acid units. In the case of *Ulva* species, the most prominent aminoacids occurring in the cell wall are aspartic and glutamic acids and alanine, as shown in Figure 2-24.[67,68]

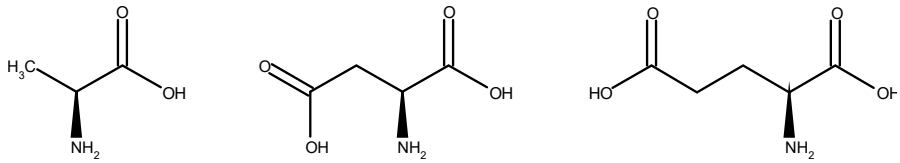

Figure 2-24. The most common aminoacids occurring in Ulva *species.*

3 Biomass fractionation

The exact quantification and determination of the chemical arrangement of the different constituents of biomass are the keys to assess the feasibility of a biorefinery. Accordingly, the valorization of the various fractions of the raw material should aim for more revenues obtained from the biorefinery, and for minimizing the generation of residues. In this regard, the sustainability concept is a key to ensure high efficiency and environmentally-friendly processes.

From the viewpoint of a biorefinery, the transformation of the different fractions into valuable chemicals, materials and energy brings along greatest challenges for process engineers. Biorefineries require different unit operations for transforming platform chemicals into various value-added products, compared to the technology employed by the conventional refineries based on fossil resources. Additionally, the complexity of the biomass cell wall also brings an enormous technological challenge, since the fractionation of the biomass into its constituents not only demands high efficiency, but also keeping the properties of the constituents as similar as they are in raw status. The fractionation processes for biomass usually require harsh conditions such as high temperature, pressure and chemicals to acquire reasonable efficiencies.[69–71] Unfortunately, some constituents, such as extractives or hemicelluloses, are rather unstable under the conditions of conventional fractionation processes, resulting in chemical modification or simply degradation.

There already exist several well-documented fractionation techniques for biomass such as acid hydrolysis, steam explosion, ionic liquid processing, and hydrothermal processing among others, which are summarized below.

3.1 Lignocellulose fractionation

The hierarchical arrangement of the wood cell wall shows the occurrence of hemicelluloses and cellulose microfibrils embedded in a lignin matrix, which results in a high recalcitrance that hinders its fractionation, as described in section 2.2. The roots of biorefineries are connected to the pulp and paper industries back to the 18th century. The pulp processes aimed in principle for the solubilization of lignin and hemicellulose fractions and the recovery of the pulp fibers.[72]

The pulp fibers are obtained mainly using chemical and mechanical processes. The most common chemical process is the Kraft process, which uses a white liquor comprising sodium hydroxide and sodium sulfide under high temperatures (170–180°C) to solubilize lignin and hemicelluloses. Consequently, the cooking chemicals are recovered, and the black liquor

consisting of solubilized lignin and hemicellulose is burnt for the generation of energy and to facilitate the recovery of the cooking chemicals in the reductive conditions of the recovery boiler. The insolubilized cellulose fibers are subsequently further processed to produce pulp.[44,45,72,73]

In turn, the sulfite process uses sulfite and bisulfite salts for the generation of pulp. In this process, lignin is depolymerized and functionalized with sulfonate groups in the cooking process, while hemicelluloses are hydrolyzed. The biorefinery of Borregaard in Norway uses the sulfite process for producing specialty cellulose. The lignin sulfonates are processed to obtain agglomeration agents and food additives as side products. Accordingly, hemicelluloses consisting of C5 and C6 sugars are fermented to produce bioethanol.[23,72,73]

Beyond these two processes in the pulp industry, the research has focused on various pretreatment protocols aiming for producing bioethanol and finding alternative processes for the pulp industry. In this regard, most of the pretreatment processes have been designed to remove lignin and hemicellulose fractions to improve the hydrolysis of cellulose via enzymatic processes. In these types of pretreatments, hemicelluloses usually undergo depolymerization to produce oligomers and monomers. When the acidity and the temperature conditions are too harsh, further degradation of the monosaccharides causes furfural and 5-hydroxymethyl furfural (HMF) occurs.[70] However, in certain applications where the degree of polymerization of hemicelluloses is relevant, an extensive degradation of the hemicellulose fraction may not be desired, and more sophisticated means of processing may be required.

In the following sections, the different fractionation methods will be described, with a focus on the processes that aim for the fractionation of the biomass preventing an extensive depolymerization of the main lignocellulosic constituents.

3.1.1 Physical processes

3.1.1.1 Mechanical comminution

The mechanical comminution of lignocelluloses is required for lowering the crystallinity of cellulose. The comminution is usually applied in biorefineries to achieve a particle-size in the range of 10–30 mm after chipping, or sawdust- size in the range of 0.2–2 mm after milling. This process is strongly energy- demanding, which depends on the nature of the lignocellulose resource as well as the technology applied.[74]

3.1.1.2 Thermoconversion of lignocelluloses

There are four main routes through which biomass is fractionated using processes based on thermal conversion: torrefaction, pyrolysis, gasification, and combustion. The common denominator in all these processes is the action of heat and the limited presence of water for the conversion of biomass into desired products. Due to the heterogeneous nature of the constituents of biomass, several different and consecutive reactions take place in the thermochemical conversion of biomass. As a result, these processes are very complex and challenging to be controlled.

Torrefaction is a process that aims for the improvement of the biomass properties by upgrading the lignocellulosic material into a more attractive biofuel. The process aims for increasing the C/O ratio by the removal of oxygen, resulting in a product with a higher heating value. The torrefaction process is usually carried out under temperatures in the range of 200–300°C with residence time ranging between 10 and 45 min. The volatiles obtained in the process consists of, among others, water, carbon dioxide, acetic acid, tars, carbon monoxide, hydrogen, and methane, which are recirculated to the main chamber. The final product is a bio-coal that retains 90% of the energy and reduces 30% of the initial mass. Subsequent uses of this bio-coal cover gasification or combustion processes.[75,76]

Pyrolysis is carried out under more elevated temperatures in the range of 400–600°C resulting in different simultaneous and consecutive reactions that degrade lignocelluloses. The product consists of a mixture of char, bio-oil and non-condensable gases such as carbon monoxide, carbon dioxide, hydrogen or methane. The process aims for the maximization of the bio-oil production, which comprise a very heterogeneous mixture of chemicals including, among others, aldehydes, acids, alcohols, ketones, phenols, and water. The process requires a rapid heating of the particles, along with a short contact between the vapors and the char, a short residence time (<2 s) and a rapid quenching of the pyrolysis vapors. Subsequently, this bio-oil can be upgraded to produce biofuels.[75,77] The commercial applications of pyrolysis-based processes for the valorization of biomass are scarce. However, different pilot plants with capacities in the range of 50–200 t/h produce bio-oil, most of them located in Finland (Metso Power), Canada (Dynamotive and Ensyn) and The Netherlands (Biomass Technology Group).[75]

The exposure of biomass to higher temperatures (above 600°C) leads to the gasification or even the combustion of the biomass. The mixture of gases produced may be catalytically upgraded for obtaining methanol, dimethyl ether or utilized as an input for the Fischer-Tropsch process. A particular care should be taken in the ash content of the biomass since the impact of alkali

metals can hinder the yields[75] particularly in the case of high ash content biomasses such as agricultural residues and algae, as it will be discussed later.

3.1.2 Physicochemical processes

3.1.2.1 Steam explosion

Steam explosion is a process in which chipped biomass is treated under high-pressure saturated steam for a given period of time, after which the pressure is swiftly released resulting in a blast that fibrillates the lignocellulosic cell wall, due to the vaporization of water inside the pores of the material. The temperature applied is usually in the range of 160–260°C, while the pressure is in the range of 0.69–4.83 MPa for periods of time from several seconds to a few minutes.[74] The steam explosion process can be enhanced by using sulfur or carbon dioxide acting as catalysts for the disintegration of the biomass. Without the use of acidic catalysts, steam explosion is known as autohydrolysis because water is acting as an acidic molecule at elevated temperatures. After the process, most of the hemicellulose fraction is solubilized and even hydrolyzed to oligomers and monomers. Depending on the conditions of the treatment, a degradation of the monomers may occur.[74,78] Still, the steam explosion method is more energy-efficient compared to the mechanical comminution of biomass.[74]

3.1.2.2 Ammonia fiber explosion (AFEX)

Similar to steam explosion, the ammonia fiber explosion is a process, in which the biomass is loaded into a pressurized reactor, and where subsequently, the pressure is swiftly released producing the explosion and fibrillation of the biomass. The typical temperature range of 90–100°C, ammonia dosage of 1–2 kg ammonia kg^{-1} dry biomass and residence time between 5 and 30 min are applied.[74,79] The AFEX process efficiently cleaves various ester linkages between lignin and hemicelluloses, producing oligomers that are soluble in the reaction medium.[79] This solubilization may be caused due to the deacetylation of the backbone of certain types of hemicelluloses, lowering the pH of the mixture and facilitating the hydrolysis of this fraction.[48] However, a complete solubilization of the hemicelluloses is not attained. Due to the mild temperatures utilized in this process, dehydration products from monosaccharides are seldom obtained.[74]

3.1.2.3 Carbon dioxide explosion

The use of carbon dioxide is similar to the steam explosion and the AFEX treatments. Two variations of the process are available: supercritical carbon dioxide explosion and sub/supercritical water hydrolysis with carbon dioxide.[80] The formation of the carbonic acid increases the disruption of the cell wall of the biomass, and even enhances the hydrolysis of hemicelluloses

and cellulose. The presence of this acid is particularly favorable for the production of monomers, lowering the requirement of enzymes in processes where the production of sugars is desired.[74,80] Typically no degradation products are observed.[74] The carbon dioxide explosion is preferred for the high lignin content types of biomass, where the enhancing effect of the disruption of the cell wall and the enzyme digestibility of the biomass are more noticeable compared to the processing of more flexible lignocellulosic material (lower lignin content).[80]

3.1.3 Chemical processes

3.1.3.1 Acid hydrolysis

The processing of lignocelluloses with acids is a fundamental process in the conversion of the constituents of biomass into bio-based products. This type of process is required for lowering the recalcitrance of biomass, which is caused by the complexity of the LCC matrix, where cellulose is entrapped into the lignin matrix, interconnected by hemicellulose chains. Additionally, cellulose shows a high crystallinity and a high degree of polymerization, which results in a low surface area that hinders the depolymerization action of enzymes. The use of acid for the processing of lignocelluloses is one of the most used technolgies for the disruption of the cell wall of biomass due to its high effectiveness.[70] Different types of acids can be used for the processing of biomass, including mineral acids, such as sulfuric, phosphoric, hydrochloric, hydrofluoric, nitric and formic acids[70,74], and organic acids, such as maleic, oxalic, acetic and fumaric acids.[70] However, the main drawbacks are linked to the environmental impacts of the use of acids in the process and the requirement of downstream neutralization.[70,74]

In the acid hydrolysis of biomass, the acid acts as a catalyst in the cleavage of the intra and intermolecular bonds linking the LCC matrix, hydrolyzing hetero- and homopolysaccharides into oligosaccharides and eventually into single monomers depending on the severity of the process. Consequently, the use of acids accelerates importantly the kinetics of the hydrolysis. The mechanism through which the glycosidic bonds are cleaved in the presence of acids is represented in Figure 3-1.

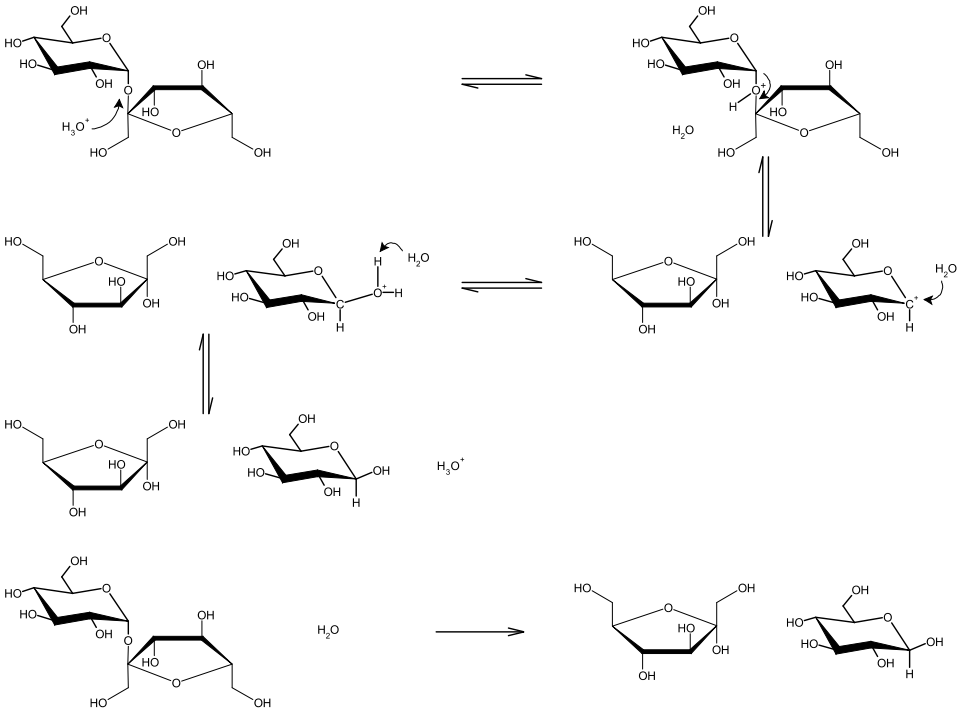

Figure 3-1. The mechanism of the acid hydrolysis of glycosidic bonds;
Adapted from Mäki-Arvela et al., 2011.[61]

3.1.3.1.1 Homogeneous hydrolysis

Whenever the polysaccharide and the catalyst are solubilized into the same medium, the reaction is called homogeneous hydrolysis. There are two types of acid hydrolysis processes, which vary according to the concentration of the acids. The first one is the dilute acid hydrolysis, which is usually carried out under acid concentrations below 5% w/v, temperatures in the range of 120–210°C and pressures until 10 atm. Under these conditions, a major fraction of hemicelluloses is broken down during the pretreatment, while low yields of glucose from cellulose are attained.[70,74] The second type of processing is the concentrated acid hydrolysis, where an acid concentration of above 30% w/v, temperatures below 100°C, and atmospheric pressures are used. Under these conditions, most of the hemicellulose and cellulose are hydrolyzed providing high sugar yields. However, several conditions affect the yield of sugars, namely the concentration of the acid, the solid loading, the reaction temperature and the time of processing. Under severe conditions, decomposition products from the dehydration of the sugar molecules can occur, resulting in elevated concentrations of furfural and 5-hydroxymethyl furfural as well as formic and levulinic acids.[61,70,81,82] The use of mineral acids requires the recovery of the catalysts to make the process economically feasible, which is a relatively expensive operation in industrial scale.[70]

3.1.3.1.2 Heterogeneous hydrolysis

Heterogeneous catalysis has been proposed as a novel and environmentally-friendly approach for the hydrolysis of polysaccharides by using different types of solid materials bearing acidity. Heterogeneous catalysts have been widely employed in the industry, particularly in oil refining processes. However, the same is not true for biorefineries, where the use of homogeneous catalysis is still dominating most of the processes.[83] The advantage of this method is that the solid catalysts can be recovered, separated from the liquid medium and eventually reused for subsequent hydrolysis steps.[61,84] The main types of solid catalysts used in the hydrolysis of polysaccharides are zeolites, resin polymers, carbon materials, functionalized silica, metal oxides and heteropolyacids.[84]

Zeolites are crystalline aluminosilicate particles with complex structures, which result in particles possessing both macro- and micropores. Depending on the preparation method, the acidity of zeolites can be tuned for a particular process. In the case of carbohydrates, zeolites have been used for the hydrolysis of disaccharides such as sucrose, cellobiose, and maltose, as well as inulin.[61,84] In this regard, the Si/Al ratio is essential, since a higher ratio decreases the level of Brønsted acid sites, but increases the acidity strength, thus enhancing the hydrolysis. However, the stability of zeolites in aqueous medium is rather questionable, thus hindering their application for this type of reactions.[84]

Carbon materials are especially interesting, since they are based on biomass or waste materials as precursors, providing a versatile support for the preparation of inexpensive catalysts.[83] The use of these materials results in particles with a high porosity, consisting mainly of macropores, which can be treated with acids to provide sulfonic group functionality.[83,84] Even though carbon materials are known to be stable in aqueous medium, the eventual leaching of sulfonic groups is one of the main challenges in the design of these catalysts.[84] Konwar *et al*. demonstrated in his doctoral thesis the preparation of sulfonated carbon materials prepared from plant residues obtained after oil extraction processing. In this study, cellulose was successfully hydrolyzed in presence of sulfonated carbon materials, achieving conversions up to 60 wt.% for the hydrolysis of cellulose and up to 90 wt.% upon hydrolysis of ionic liquid treated cellulose.[83]

Ion-exchange resins are polymers synthesized as beads or fibers, which ion exchange capacity is used for substituting cations or anions. The acidity of the resins is usually provided by sulfonic group functionality that has been added to the matrix, normally exhibiting a high and relatively uniform concentration of acid sites.[84,85] Since the acidity is readily available on the surface of the resin, there are fewer corrosion problems compared to the use of mineral acids.[86] The main disadvantages of these resins are that they have

low thermal stability and low acid strength.[84,85] Most of the commercialized resins are based on a polystyrene matrix, and their catalytic activity mostly depends on the accessibility of the acid sites via diffusion through this polymer matrix. At the same time, such accessibility to the acid sites depends on the ability of the resin to solvate and swell in the reaction medium as well as on the porosity of the material.[85] *Amberlyst™* which is a macroporous resin and *Smopex®* which is a fibrous non-porous resin-based on polystyrene matrix, and both bearing sulfonic acid groups have been used for the hydrolysis of cellulose, hemicellulose, and algae, though thermal stability and reusability of the catalysts remain questionable.[61,81,84,87–93]

Polyoxometalate (POM) clusters also known as heteropolyacids are high molecular weight clusters having a metal-oxygen octahedral structure as a basic unit.[84,94] These heteropolyacids are barely soluble in polar solvents, but they can be supported on silica, carbons or acid ion-exchange resins.[84] Micellar heteropolyacids have been successfully applied in the hydrolysis of sucrose, starch, crystalline cellulose and green algae.[84,94]

3.1.3.2 Alkali hydrolysis

The use of alkali for the fractionation of biomass aims in principle for the solubilization of lignin similar to the Kraft process for pulping. The conditions at which the alkali treatment is carried out usually comprises low temperature and pressure, and even ambient conditions can be applied.[95] It is believed that lignin is solubilized by saponification of the ester bonds via cross-linking lignin and hemicelluloses, which increases at the same time the porosity of the material.[74] Alkali also removes the acetyl groups of hemicelluloses, thus lowering the steric hindrance of hydrolytic enzymes and increasing the digestibility of cellulose.[95]

3.1.3.3 Organosolv

The organosolv process was initially proposed for the pulping industry for the delignification of wood.[71] The method comprises the use of organic solvents, such as methanol, ethanol, acetone, ethylene glycol, triethylene glycol, and tetrahydrofurfuryl alcohol coupled with organic acid catalysts, such as oxalic, acetylsalicylic or salicylic acids, to break the linkages between hemicelluloses and lignin.[74] The organosolv process affects to some extent the structure of cellulose, which hinders its application in the pulping industry. Still, when the saccharification of cellulose is aimed at, the use of the organosolv process aids the enzymatic hydrolysis due to the partial degradation of the fibers during the process. The Lignol Co. adopted this technology in its biorefinery unit using temperatures in the range of 180–195°C, reaction times in the range of 30–90 min, ethanol concentration of 30–70 wt.% and liquid to solid ratio of 4:1 to 10:1 in weight. After the process,

the so-called organosolv lignin and hemicelluloses are recovered from the solvent as well as water.[71]

3.1.3.4 Hydrothermal liquid fractionation of lignocelluloses

The use of pressurized hot water process is an up-and-coming alternative for the processing of biomass in biorefineries aiming for the extraction of hemicelluloses, using water as an inexpensive and environmentally-friendly solvent. Additionally, most of the technology is currently well-established by the industry. The process is usually carried out under the absence of additional chemicals such as mineral acids or enzymes. Consequently, the extraction and partial hydrolysis of hemicelluloses are catalyzed by hydronium ions, which in a first stage are generated via water dissociation. As the extraction proceeds, the deacetylation of hemicelluloses leads to the generation of acetic acid, which further dissociates and produces more hydronium ions improving the reaction kinetics. In the presence of protons and elevated temperatures, monomers can relatively easily undergo degradation to form dehydration products such as furfural, 5-hydroxymethylfurfural, formic acid and levulinic acid.[96,97]

The process is usually carried out at temperatures above the saturation point of water, between 150 and 230°C, while the reaction times can vary from a few seconds up to hours. The most frequent values of solid loading are around 10 wt.%, while continuous reactors tolerate higher solid loadings. During the hydrothermal processing of biomass, the linkages of the LCC matrix are broken down, though mostly hemicelluloses are solubilized while cellulose and lignin remain mainly undissolved.[97] This feature is important in efficient and selective biomass fractionation, which should also minimize the requirement of downstream purification processes.

3.1.3.5 Ionic liquid fractionation of lignocelluloses

Ionic liquids are salts that remain in the liquid state in a vast range of temperatures and can be liquid even below 100°C. The structure comprises a large cation normally based on hydrocarbons and an anion, as shown in Figure 3-2. These molecules exhibit excellent solvation properties and very low vapor pressures.[98] Chemical processes dealing with ionic liquids are usually attributed to the topic of green chemistry, claiming less impact to the environment compared to conventional chemical processes. Still, such environmental benefits cannot be completely assured, since the preparation of ionic liquids often involves the utilization of poisonous or hazardous chemicals.

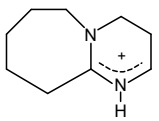

1,8-Diazabicyclo[5.4.0]undec-7-ene protonated thiocyanide
[DBUH$^+$][SCN$^-$]

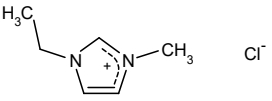

1-ethyl-3-methyl imidazolium chloride
[EMIM$^+$][Cl$^-$]

Figure 3-2. Examples of ionic liquids.

The processing of biomass in applications involving ionic liquids exploded in the last decade, when Varanasi and co-workers patented the use of ionic liquids for the pretreatment of biomass prior enzymatic hydrolysis of lignocelluloses aiming to produce bioethanol. The patent described the use of imidazole-based ionic liquids for the disruption of the cell wall, enhancing the subsequent enzymatic hydrolysis of the cellulose fraction.[99] Accordingly, different works evaluating various types of biomasses processed in ionic liquids for enzymatic saccharification and fermentation were published.[22,100–106]

3.1.3.5.1 Dissolution of cellulose in ionic liquids

Various parameters play a role when dissolving biomass in ionic liquids; the particle size of the biomass, the solid loading ratio, the temperature of the process and the viscosity of the ionic liquid are very important. Additionally, in the case of the dissolution of cellulose in ionic liquids, one should consider the size and the functional groups of the cation, the size of the anion, and also the hydrogen bond basicity of the molecule. The use of relatively small cations usually enhances the dissolution of cellulose in contrast to large alkyl chains. In this regard, the presence of hydroxyl end-groups in the cation have been observed to be detrimental in the dissolution of cellulose. Regarding the anion, usually small anions enhance the dissolution of cellulose compared to large ones. However, chloride anions are better for the dissolution of cellulose compared to bromide and fluoride anions.[73] Chloride effectively disrupts the hydrogen bonds interconnecting cellulose fibrils, by generating new hydrogens bonds with the anion. These fibrils are prevented from regenerating cellulose due to the dipole-type interactions between the cation and the anion, which stabilizes the fibrils.[107] Cellulose dissolving ionic liquids also show a high hydrogen bond basicity, which means that the ionic liquid is capable of acting as a hydrogen bond acceptor.[108] Consequently, the basicity of the ionic liquids becomes one of the most important properties for the dissolution of biopolymers in these types of systems.[109]

D'andola and co-workers patented various ionic liquids derived from polycyclic amidine bases aiming at the solubilization of polymers, particularly of cellulose.[110] Ionic liquids that combine alkylimidazolium cations with anions, such as chloride and acetate, also show significant solubility of cellulose, particularly 1-ethyl-3-methylimidazolium chloride

([EMIM$^+$][Cl$^-$], 1-ethyl-3-methylimidazolium acetate ([EMIM$^+$][OAc$^-$]), 1-butyl-3-methylimidazolium chloride ([BMIM$^+$][Cl$^-$]), and 1-butyl-3-methylimidazolium acetate ([BMIM$^+$][OAc$^-$]).[73,107,111,112] Other anions that show a great ability for dissolving cellulose include formates, amides, imides, thiocyanates, phosphates, sulfates, sulfonates, and dichloroaluminates. Cations such as imidazolium-, pyridium-, triethylammonium and 1,8-diazabicyclo-[5.4.0]-undec-7-en (DBU) are good choices for the dissolution of cellulose also.[73]

3.1.3.5.2 Dissolution of lignin in ionic liquids

Switchable ionic liquids (SILs) are excellent solvents to successfully solubilize lignin and hemicelluloses from lignocellulosic material, becoming an alternative way for the pulping of wood.[113–118] SILs are solvents based on an amine base, such as 1,8-diazabicyclo-[5.4.0]-undec-7-ene (DBU), and an alcohol, such as 1-hexanol, which changes from nonpolar to polar properties by bubbling, and acid gas, such as carbon dioxide, as shown in Figure 3-3. SILs were first described by Jessop and co-workers.[119] Subsequently, the design and use of switchable ionic liquids based on DBU glycerol and carbon dioxide/sulfur dioxide for the processing of wood was demonstrated by Anugwom and co-workers.[113,117]

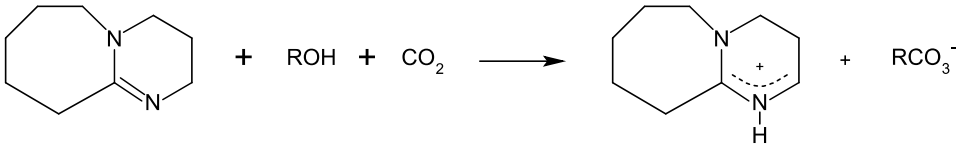

Figure 3-3. Example of switchable ionic liquids;
Adapted from Jessop et al., 2005.[119]

In this regard, the use of DBU-glycerol-CO_2 for the fractionation of lignocellulosic biomass at 100°C for five days allowed for the extraction of 83% of the hemicelluloses, maintaining most of the cellulose and lignin in the treated biomass. Moreover, the reuse of the solvent was probed for four consecutive cycles.[48,117] Alternatively, the change of the alcohol to monoethanolamine (MEA) and the selection of sulfur dioxide as the triggering gas allowed for the synthesis of the SIL DBU-MEA-SO_2. The use of this ionic liquid in the treatment of birch and Norway spruce favored the reduction of the lignin content from 22 to 5 wt.% and 27 to 6 wt.%, respectively when the biomass was processed at 120°C for one day.[116] Regarding hemicelluloses, the content in the treated biomass was reduced by half in both species, while most of the cellulose remained in the treated biomass. Anugwom demonstrated in his thesis that SILs are a possibility for treating wood to produce pulp, since most of the lignin and hemicelluloses can be selectively fractionated by selection of the appropriate solvent.[48]

3.1.3.5.3 Hydrolysis of LCC in ionic liquids

One of the main features of ionic liquids is that they serve not only for the dissolution of polysaccharides, but also for the hydrolysis of carbohydrates and catalyze further reactions towards the production of bio-based building blocks. In this regard, acidic ionic liquids show great potential for the one-pot conversion of biomass into desired products, not only due to their dissolving ability, but also for their capacity to catalyze chemical reactions. Ionic liquids presenting Brønsted acidity in the cation are of particular interest to achieve this goal. Solvents based on sulfoalkyl methylimidazolium cations together with chloride anions effectively hydrolyze cellulose. The use of 1-(3-sulfopropyl)-3-methylimidazolium chloride (Figure 3-4) allowed for the obtaining of 62 wt.% of total reducing sugars from cellulose. Consequently, the production of monomers demands the efficient dissolution of cellulose in the ionic liquid via formation of hydrogen bonds between the cellulose fibrils and the chloride anions. Subsequently, the hydrolysis is catalyzed by the sulfonic groups that are present in the cation of the ionic liquid. In this regard, the cation of the ionic liquid should be flexible enough to interact with cellulose chains, similarly to the cellulose active domain present in cellulose degrading enzymes.[107]

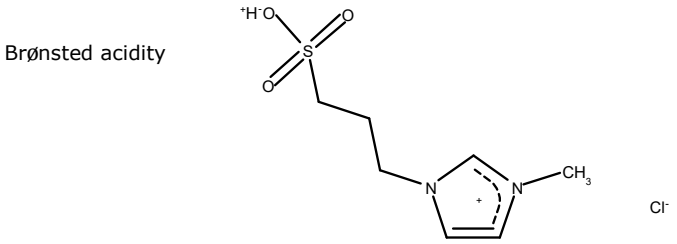

Figure 3-4. Acidic ionic liquid;
Adapted from da Costa Lopes and Bugel-Łukasik, 2014.[107]

The depolymerization of lignin has also been investigated in ionic liquid systems. The model molecules guaiacylglycerol-β-guaiacyl and veratrylglycerol-β-guaiacyl ethers reacted successfully in the presence of methylimidazolium chloride, via cleavage of the β-O-4 bonds. However, in the case of lignin, the acidity of the ionic liquid did not prove to be the most controlling parameter for the release of guaiacol units since the acidity trend did not correlate to the guaiacol yield. Instead, the dissolution ability of the ionic liquid via formation of hydrogen bonds between the anion and the hydroxyl groups of lignin was the most determining parameter. Subsequently, the experiments showed that the presence of water in the ionic

liquid system was also necessary for the depolymerization of lignin, indicating that the hydrolytic mechanism of depolymerization may take place in the presence of 1-hexyl-3-methyl-imidazolium chloride ([HMIM$^+$][Cl$^-$]).[107]

3.1.3.6 Enzymatic digestion

Enzymes are various types of proteins capable of catalyzing biochemical reactions with a high specificity. Concerning the fractionation of biomass, enzymes can catalyze the depolymerization of lignocellulose by cleavage of specific bonds of the major biomass constituents.

The depolymerization of cellulose involves the synergic action of several different enzymes which are grouped into endoglucanases (EGs) and exoglucanases (cellobiohydrolases, CBHs). At the first stage, EGs randomly catalyze the cleavage of intramolecular β-1,4 glycosidic linkages of low crystallinity cellulose to produce cellulose oligosaccharides. Accordingly, CBHs act by cleavage of the cellulose backbone in the reducing end of the chain releasing cellobiose units. Both reactions take place in the solid-phase of the cellulose fibers. Additionally, β-glucosidases (BGs) catalyze the cleavage of the cellobiose unit to produce glucose in the liquid phase. All the reactions mentioned above have a hydrolytic catalytic mechanism, in which water acts as a substrate cleaving for each reacting glycosidic bond.[103,120] New findings in the cellulose degrading mechanism have reported the existence of swelling proteins, capable of non-hydrolytically opening the highly ordered crystallized structure of cellulose and allowing for the action of endoglucanases to further depolymerize the cellulose fibrils. Many different microorganisms can produce cellulose degrading enzymes, which are classified under the glycosyl hydrolase type of enzymes according to the CAZy database.[121] Among these microorganisms, the main cellulose-degrading enzyme producers belong to the genus of *Aspergillus*, *Bacillus*, and *Trichoderma*.[103] Recently a new type of cellulose degrading enzymes acting via oxidative mechanisms has been discovered, receiving the name of lytic polysaccharide monooxygenases (LPMOs).[122]

On the other hand, the depolymerization of hemicelluloses occurs by action of the so-called hemicellulases, which are a broad group of enzymes involving among others, xylanases, galactanases, glucanases, arabinases, and mannases, which also have glycosyl hydrolase activity.[122,123] Since hemicelluloses comprise hetero-polysaccharides and side chain substituents, different types of enzymes are involved in the depolymerization of these molecules. Fungi are also an important source of hemicellulose degrading enzymes, especially within the genus of *Aspergillus*.[122]

In the case of pectins, these molecules are hydrolyzed by different types of enzymes. The hairy structure of pectins needs a different set of complementary enzymes as those of hemicellulose and cellulose degrading

enzymes. One of the main building blocks of pectins are sugars acids, as described in section 2.2.4. Consequently, the backbone can be cleaved via hydrolysis using polygalacturonases or by non-hydrolytic mechanisms using β-elimination, by the action of pectin and pectate lyases. Polygalacturonases act by both exo and endo mechanisms, as for in the case of rhamnogalacturonan hydrolytic enzymes. The cleavage of polysaccharides containing uronic acids is carried out by the action of polysaccharide lyase types of enzymes, which produce an unsaturated hexuronic acid and a new reducing end.[122]

The aromatic nature of lignin provides high stability to the molecule which is rather difficult to be degraded.[124] Consequently, multiple types of enzymes act in the depolymerization of this polymer in mechanisms which are not yet fully understood by scientists. Essentially, the enzymes involved in the depolymerization of lignin belong to the group of peroxidases and laccases, both acting via oxidative mechanisms.[124–126] Some peroxidases are capable of degrading lignin or lignin fragments, but others exhibit the action of oxidative mediators which are capable of penetrating the structure of lignin and producing the cleavage of bonds.[124] In the recent years, different fungi (white root fungi) and bacteria have been reported to produce lignin-degrading enzymes.[124–126]

3.1.4 Other lignocellulosic fractionation processes

Other treatments for the fractionation of biomass consist of the use of microwaves, ultrasound, and pulse electric energy to improve the disruption and bond cleavage of the lignocellulose matrix. Alternatively, processes using ozone to oxidize the lignin fraction and microorganisms, such as white rot fungi for partial digestion of the biomass, have been proposed for the fractionation of lignocelluloses.[74,127]

3.2 Fractionation of algae biomass

Algae biomass has quantitatively less lignin compared to terrestrial plants. Thus, the arrangement of the cell wall of algae offers fewer barriers for the fractionation of its constituents. The most common fractionation processes are described below, with focus on the industrial application for the extraction of hydrocolloids.

3.2.1 Physical processes

3.2.1.1 Mechanical comminution

Admittedly macroalgae contain less cellulose compared to lignocelluloses, though it is the main carbohydrate constituent in algal tissue.[128] Still, in the

case of brown and red algae the cell wall comprises crystalline cellulose and alginate and agar, respectively, which results in a relatively strong matrix of polysaccharides. Consequently, the mechanical comminution of the biomass is required to reduce the crystallinity of cellulose and increase the surface area for subsequent extraction and depolymerization processes. Different works dealing with the production of bioethanol from seaweeds have utilized mechanical comminution for this type of biomass as an initial step prior to the use of physicochemical pretreatments and enzymatic saccharification of the biomass.[128–134]

3.2.1.2 Thermoconversion processing

Thermoconversion processing of macroalgae remains a promising possibility for the generation of energy from biomass, mainly due to the high presence of hydrocolloids. Different types of algae, especially fast-growing species belonging to the group of brown algae, have been subject to pyrolysis, gasification and combustion experiments.[135–138] However, suitable demineralization techniques must be developed for lowering the mineral content that may affect the conversion yields.[139] Additionally, proper control measures should be taken for preventing ash deposition, fouling, corrosion, and ultimately releasing of metals into the environment.[135]

3.2.1.3 Microwave and ultrasound processing

The use of microwave and ultrasound has become a novelty way for the fractionation of algae, in particular for the extraction of bioactive constituents from algae.[128,135] In the case of microwaves, the electromagnetic frequency in the range of 300 MHz and 300 GHz causes the disruption of hydrogen bonds and the migration of dissolved ions. Therefore, an increase in the porosity of the biological matrix is obtained, facilitating the accessibility of the solvent for the extraction of algal constituents such as fucoidans, carotenoids and minerals.[140]

Regarding the ultrasound-assisted extraction of algal constituents, mechanical waves at a frequency of 20 kHz are used for the partial disruption of the cell wall. These waves propagate through the algal tissue causing vaporization of the liquid contained in the cells, and subsequently produce cavitation of bubbles. The implosion of these bubbles causes significant perturbation in microporous particles, which results in an increment of the internal diffusion, facilitating the extraction of bioactive components.[140] The use of ultrasound has been effective in the extraction of isoflavonoids from *Sargassum* spp.,[135,141] as well as for the extraction of carotenoids and pigments from different types of microalgae.[142]

3.2.2 Chemical processes

Processes including supercritical and pressurized liquid extraction have gained attention for the extraction of selected bioactive compounds such as carotenoids, pigments, and polyphenols from different marine algae.[140] Still, the industrial applications for the extraction of algal constituents are mainly limited to the extraction of hydrocolloids, where the use of alkali treatments are the primary choices.

3.2.2.1 Alkali processing

3.2.2.1.1 Extraction of agarose

The extraction of agar from red seaweeds is a well-established extraction process which dates to the 1930 decade. *Gracilaria* and *Gelidium* species are the main sources of agar, whose extraction is principally exploited in Indonesia and Chile. In 2009, agar was commercialized at a price of 18 US$ kg^{-1}, being the most expensive of the main algal hydrocolloids.[20] Agar is extracted from *Gelidium* via dilute acid extraction in pressurized cookers, under temperatures in the range of 105–110°C for 2–4 hours. In the case of *Gracilaria*, agar is obtained via a pretreatment consisting of 2–5 wt.% sodium hydroxide solution heated under temperatures in the range of 85–90°C for 1 h, followed by extraction under temperatures in the range of 95–100°C for 2–4 h.[143] The alkali process allows for the conversion of galactose 6-SO_4 to 3,6-anhydrogalactose, which enhances the gelling properties of the molecule. Agar from *Gelidium* is preferred for biotechnological applications, while agar from *Gracilaria* and other species are used as food additives.[20,143]

3.2.2.1.2 Extraction of carrageenan

Most of the carrageenans are extracted from *Kappaphycus alvarezii* and *Eucheuma denticulatum* for producing the gel-forming κ-carrageenan. *Gigartina skottsbergii* and *Sarcothalia crispata* are among the most valuable species harvested from Chilean coasts for obtaining μ- and ν-carrageenan. These two molecules allow for the replacement of the commercially unavailable non-gelling λ-carrageenan.[20,143] By 2009, carrageenan obtained via extraction from red algae was commercialized at a price of 10.5 US$ kg^{-1}.[143]

κ-carrageenan can be obtained via alkali extraction with sodium hydroxide for several hours, depending on the species. Alkali is used for transforming galactose 6-SO_4 to 3,6-anhydrogalactose in the same way as for agar, increasing the gelling properties of the molecule. κ-carrageenan produces gels in the presence of potassium ions, while ι-carrageenan produces salts in the presence of calcium ions.[143] Most of the uses of carrageenan are related to dairy products and toothpaste preparations.[20,143]

3.2.2.1.3 Extraction of alginate

Alginate in brown algae cell wall is present in the form of calcium, sodium, magnesium, strontium and barium salts. Sodium alginate is the only salt which is soluble in water, whereas the rest remain insoluble in water. The extraction process of alginate starts with a pre-extraction where hydrochloric acid (pH 4) is used for removing salts. Subsequently, the extraction is carried out in the presence of sodium carbonate at pH 10 and in heating at 80°C for 2 h, with a biomass loading of around 5 wt.%. Consequently, the extraction is carried out by cation exchange to sodium alginate. After the solubilization of alginate, the remaining biomass is filtered, and the solution containing the sodium alginate is treated with calcium chloride to precipitate it back to calcium alginate. Subsequently, calcium alginate is converted to alginic acid exchanging the calcium cations with protons, which is done via subsequent washings with hydrochloric acid (pH 2). Finally, alginic acid is treated again with sodium carbonate in a solution containing 50:50 vol.% water-alcohol to produce sodium alginate.[144,145]

The alginate extraction process is also commercialized producing small quantities of alginic acid, salts of calcium, ammonium, and potassium, as well as, ester and propylene glycol alginate. The price of alginate in 2009 was 12 US$ kg^{-1}.[20] The main uses of alginate serve the textile and food industries, where it is used as a thickener for pastes containing dyes for the printing on canvas as well as in sauces, syrups, and toppings for ice cream.[143]

3.2.2.2 Enzymatic digestion of marine carbohydrates

Currently, there are no industrial applications in which enzymes of marine nature are used for the fractionation of algal biomass. Some efforts have been placed particularly in the depolymerization of alginate, aiming for the fermentation of uronic acids to produce bioethanol, even though literature is still scarce in this field. However, many marine microorganisms contain several unexplored enzymes, such as glycoside hydrolases (GHs) and polysaccharide lyases (PLs) that take part in important metabolic pathways in nature. While GHs utilize water molecules to break down glycosidic bonds, PLs are specific to polysaccharides containing uronic acids acting by the β-elimination mechanism.[146] The finding of marine-degrading enzymes is an additional pathway for a biorefinery based on marine biomass since the specificity of these enzymes towards carbohydrates can lead to selective fractionation of the different cell wall constituents.

Regarding glycoside hydrolases of marine nature, they present activity in polysaccharides such as agar. According to the CAZy database, α-agarases belonging to the GH96 and GH117 families, β-agarases pertaining to the GH16, GH50, GH86, and GH118 families have been discovered so far. α-agaroses belonging to the GH117 family are exo-enzymes which hydrolyze

3,6-anhydro-L-galactose from the non-reducing end of agarose oligosaccharides. In turn, β-agaroses act both via endo and exo hydrolytic mechanisms. Endo-β-agarases from *Zobellia galactanivorans* produce mainly agarose tetramers and hexamers. These enzymes belong to the GH16 family and catalyze the hydrolysis of agarose via a mechanism that facilitates the preservation of the stereochemistry at the anomeric carbon while utilizing two glutamate units. Instead, the exo-β-agarase from *Sacchaophagus degradans* that belongs to the GH50 family releases agarobiose dimers from the non-reducing end of agarose oligosaccharides produced by endo-β-agarases.[147]

The presence of sulfate groups in marine polysaccharides has forced nature to develop proteins capable of binding to negatively charged sites. In most of the reported sulfated polysaccharide active enzymes, the guanidine group of an arginine binds to the sulfate group of the polysaccharide, providing specificity to the substrate.[147] In the case of ulvan, a β-glycoronyl hydrolase belonging to the GH105 family was isolated from the bacteria *Nonlabens ulvanivorans*. These enzymes act on the oligosaccharides produced by ulvan lyases,[147,148] and they will be described later.

On the other hand, marine carbohydrate-active lytic enzymes act by β-elimination reaction to cleave the glycosidic bond, releasing an unsaturated 4,5- monomer at the new reducing end of the product.[146] The main examples of these types of enzymes are found in alginate degrading enzymes, particularly alginate and oligoalginate lyases. In the case of alginate lyases, they are grouped into the PL7, PL14, PL15 and PL17 families. Alginate lyases from the PL7 family perform similarly to agarases from the GH16 family, acting outside the cell of the microorganism through endo cleavage of the molecule producing alginate oligosaccharides, which are further degraded by oligoalginate lyases. This second type of lyases belongs to the PL15 and PL17 families. The oligoalginate lyase from *Agrobacterium tumefacens* cleaves the glycosidic bond from the non-reducing end of the oligosaccharide. A conformational change of the enzymes locks the guluronate residues of the alginate chain between two tyrosine residues of the enzyme, allowing for the action of a histidine residue as a base and a tyrosine as an acid to engage the sugar residue leading to the cleavage of the bond and the release of the substrate.[147]

Ulvan lyase degrading enzymes isolated from the ulvanoluytic bacteria *N. ulvanivorans* act by a β elimination mechanism and cleave the glycosidic bond that links 3-sulfated rhamnose to either glucuronic or iduronic acid residues. The cleavage of the β-(1->4) glycosidic bond is produced by the abstraction of the proton located at C5 of the uronic acid with a β eliminative mechanism resulting in the formation of a reducing end on one fragment and an unsaturated ring on the non-reducing end of the second fragment. Later on, additional ulvan lyases were isolated from *Alteromonadales* bacteria, which

were proved to act differently than *N. ulvanivorans* lyases by specific cleavage of the β-(1->4) glycosidic bond joining 3-sulfated rhamnose to glucuronic acid.[148]

4 Aim and scope of the work

As a summary, algal biomass contains many highly interesting molecules for the biorefinery industry. Algal biomass grows at very high rates compared to terrestrial plants, but more interestingly, algae almost entirely lack lignin. This feature is important, since milder conditions are required in fractionating the biomass. The open literature covering the fractionation of algal biomass under a biorefinery concept is scarce compared to terrestrial plants. In this thesis, two algal species have been selected to assess their potential in a biorefinery concept: the brown algae *Macrocystis pyrifera* and the green algae *Ulva rigida*. Both types of biomasses are rich in different types of extractives and carbohydrates that are potentially valuable for the chemical industry. Several constituents of marine nature have medicinal properties that are of enormous interest to the pharmaceutical industry. In this thesis, we cover the main issues dealing with the extraction of marine constituents, as well as the chemical and biochemical conversion of carbohydrates into monosaccharides. Consequently, this work provides an interesting starting point for the research in the fractionation of algal biomass and subsequent valorization of its fractions.

5 Materials and analytical methods

5.1 Materials

5.1.1 Biomass

Macrocystis pyrifera were collected by scuba diving 30 km southwest of Puerto Montt, Chile. The samples were harvested in November 2011 (M1), March 2013 (M2) and June 2013 (M3). Regarding *Ulva rigida* (C. Aghard 1823 *Chlorophyta*, *Ulvaceae*), the biomass was kindly donated by Prof. Mario Edding from the Research and Technological Center in Applied Phycology (CIDTA) Northern Catholic University, Chile. The algae were collected in 2009 from submerged marine rocks located in La Herradura de Guayacán Bay, in the city of Coquimbo in Northern Chile. Algae were dispersed on plastic carpets and left to air dry for 48 h avoiding contact with sunlight. As the next step, algae were further dried in an oven at 40°C overnight and finally milled to 90% - # 30 mesh in a cross-beater mill Retsch SK10. Once received, both algae samples were stored in a freezer and freeze-dried before analyses.

5.1.2 Chemicals

The chemicals used in the different analysis techniques will be described directly in section 0. The chemicals utilized for the experiments were used as received unless otherwise mentioned: 1-ethyl-3-methylimidazolium acetate ([EMIM$^+$][OAc$^-$], Sigma, 97%), 1,1,3,3-tetramethylguanidine (TMG, Sigma Aldrich, 99.0%), 1,8-diazabicyclo-[5.4.0]-undec-7-ene (DBU, Sigma Aldrich, 99.0%), cellulases from *Trichoderma resei* (Celluclast 1.5L, Sigma), acetone (AcOH, J.T. Baker®, ≥ 99.3%), alginate lyase (Sigma, ≥ 10,000 unit/g) *Amberlyst™*70 (A70, kindly donated by Rohm and Haas®, now part of DOW Chemicals), chloroform (Rathburn, HPLC grade), ethanol (Etax Aa, Altia Oyj., ⩾ 99.5%), ethyl acetate (J.T. Baker®, ≥ 99.6%), hexane (Sigma-Aldrich, 99%), hydrochloric acid (HCl, J.T. Baker®, 37-38 wt.%), methanol (MeOH, J.T. Baker®, 99.8 wt.%), monoethanolamine (MEA, from Sigma Aldrich, 99.0%), propionic acid (CO_2Et, Acros Organics, 99.0%), *Smopex*®101 (S101, Johnson Mattey, UK), sulfur dioxide (SO_2, AGA, 99.998%, H_2O < 3 ppm), sulfuric acid (H_2SO_4, J.T. Baker®, 95-98%) and β-glucosidase (cellobiase from *Aspergillus niger*, Novozyme 188, Sigma).

5.2 Analytical methods

Several approaches were used for the characterization of the fresh algae and the products obtained from the processing of the biomass. The methods were classified into chemical and physical and physicochemical techniques. Figure 5-1 depicts a scheme where the general procedure for the treatment of the algae is provided, and the different analytical techniques used for the characterization of the products are given.

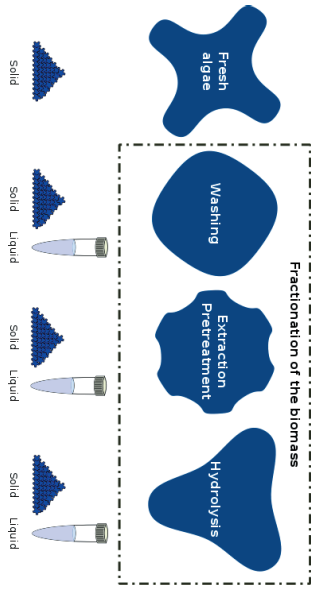

Chemical characterization								
Proximate	X							
OEA	X	X	X					
Extractives								
Spectrophotometry	X		X	X	X			
ICP-OES	X	X	X	X	X			
LC-ESI-MS/MS				X				
IC				X				
Carbohydrates and monomers								
Spectrophotometry				X	X			
GC	X	X	X	X	X			
HPLC				X				
Physical and physicochemical characterization								
TGA	X	X		X				
TEM	X			X				
SEM	X							
HPSEC	X			X				
FTIR	X			X				

Figure 5-1. General scheme of the processing of the biomass and list of the analytical techniques used for the characterization of the products.

5.2.1 Chemical characterization techniques

5.2.1.1 Proximate analyses

The moisture, protein, lipid, ash and fiber contents of both *M. pyrifera* and *U. rigida* were quantified following the official methods of the Association of Official Analytical Chemistry (AOAC): 930.04, 978.04, 991.36, 930.05 and 962.09, respectively.[149] The carbohydrate content was calculated from the difference between the initial mass and the total content of proteins, humidity, lipid and ash.[150]

5.2.1.2 Organic elemental analysis (OEA)

The organic elemental analyses were performed on fresh and treated *U. rigida* biomass to quantify the content of nitrogen, carbon, hydrogen, sulfur, and oxygen, respectively, using a Flash 2000 Thermo Scientific equipment. About 2.00 mg of standards and samples were weighed into tin cups. Helium (He) and oxygen (O_2) gases were used in the experiment. The instrument was calibrated using a commercial cysteine standard. Also, the commercial standard 2,5-(Bis(5-tert-butyl-2-benzo-oxazol-2-yl) thiophene (BBOT, Sigma-Aldrich, ≥ 99%) was used as the reference sample.

5.2.1.3 Inductively coupled plasma optical emission spectrometry (ICP-OES)

Inductively coupled plasma optical emission spectrometry (ICP-OES) for the quantification of Ag, Al, As, Ba, Be, Bi, Ca, Cd, Co, Cr, Cu, Fe, K, Li, Mg, Mn, Na, Ni, P, Pb, Rb, S, Se, Si, Sr, Tl, U, V, and Zn was performed to the fresh and processed biomass. The samples were weighed into Teflon bombs, and subsequently, 5 ml HNO_3 (65%) + 1,2 ml H_2O_2 (30%) was added and dissolved in a microwave oven (Anton Paar, Multiwave 3000). The dissolved samples were diluted to 100 ml before the ICP-OES (PerkinElmer, Optima 5300 DV) analysis. The acids used in the analyses were of supra pure grade from Merck.

5.2.1.4 Determination of total phlorotannin concentration

The total phlorotannins concentration (TPC) in the extracts was determined according to the Folin–Ciocalteu assay,[151] adapted to 96-well plates. A set of standards containing gallic acid (GAE, Sigma, ≥ 97.5) in concentrations in the range of 20-100 mg L^{-1} wase prepared to quantify the concentration of phlorotannins in the extracts. The samples and the standard (20 µL) were introduced separately into 96-well plates, each containing 100 µL of Folin–Ciocalteu's reagent diluted with water (10 times) and 80 µL of a solution containing 7.5% w/v sodium carbonate (Merck, ⩾ 99.9% purity). The plates were mixed and incubated at 45°C for 15 min. The absorbance was measured

at 765 nm using a UV–visible spectrophotometer (Asys, UVM 340). The phlorotannin concentration was determined by the regression equation of the calibration curve expressed as GAE mg equivalent 100 g^{-1} dry solids (DS).

5.2.1.5 Determination of the total anti-oxidant activity

The free radical scavenging activity (total anti-oxidant activity, TAA) was quantified using the modified method of von Gadow *et al.*[152] Consequently, 40 µL of a solution containing 0.4 M 1,1-diphenyl-2-picryl-hydrazyl (DPPH, Aldrich, 97.5%) in ethanol was added to 50 µL of the sample, complemented with 110 µL of ethanol. The plates were mixed and allowed to stand for 30 min in the absence of UV light to avoid decomposition. The absorbance was measured at 520 nm using a UV–visible spectrophotometer (Asys, UVM 340) against an ethanol blank. Calibration curves of Trolox ((±)-6-Hydroxy-2,5,7,8-tetramethylchromane-2-carboxylic acid, Aldrich, 97%) in the concentration range of 0–24 mg L^{-1} were prepared, and the results were expressed as mg of equivalents of Trolox per 100 g of DS (mg TE 100 g^{-1} DS).

5.2.1.6 Analysis for the identification of phlorotannins

A volume of 14 ml of the phlorotannins extract obtained under the best extraction condition was concentrated at RT in a vacuum concentrator (SpeedVac, Savant Instruments Inc., NY-USA). Consequently, the concentrated extract was re-suspended in 4.5 ml of water, and a volume of 20 µL was analyzed using a Liquid Chromatography-Electrospray Ionization Tandem Mass Spectrometric (LC-ESI-MS/MS) system. The equipment consisted of an HP1100 liquid chromatography (Agilent Technologies Inc., CA-USA) connected to a mass spectrophotometer (Esquire 4000 ESI-Ion Trap LC/MS(n) system, Bruker Daltonik GmbH, Germany). A Luna C18 150 × 4.6 mm, 5 µm and 100 Å analytical column (Phenomenex Inc., CA-USA) was used in the analysis; at the exit of the column, a split divided the eluent for simultaneous UV and mass spectrometry detection. The mobile phase used was 1% v/v formic acid in deionized water (solvent A) and acetonitrile (solvent B). The mobile phase was fed at a flow rate 1 mL min^{-1} according to the following elution gradient: 0–15 min, 5% B; 15–75 min, 5–100% B; 75–85 min, 100% B and 85–90 min, 100–5% B.[153] The detection wavelength was set at 280 nm. The mass spectral data were acquired in positive and negative modes; ionization was performed at 3000 V assisted by nitrogen as a nebulizing gas at 3.1 bar, drying gas at 345°C and flow rate 10 L min^{-1}. All the scans were performed in the range of 20–2200 m/z. The trap parameters were set in ion charge control using the default parameters defined by the manufacturer. The collision-induced dissociation was performed by monitoring collisions with the helium background gas present in the trap and automatically controlled through the SmartFrag option.

5.2.1.7 Chlorophyll analyses of fresh and processed algae

The chlorophyll content was analyzed to fresh and IL-processed *U. rigida* samples. The experiments were carried out in duplicate using N,N-dimethylformamide (DMF, from VWR, ≥ 99.8% purity) as the solvent. 120 mg of the sample and 2.5 mL DMF were disposed in a flask and left in a refrigerator for 72 h, as described by Schumann *et al.*[154] The flasks were covered with aluminum foil to prevent the decomposition of chlorophyll by UV. The samples were homogenized in a vortex every 24 h. Once the extraction time was completed, the solution was filtered and analyzed in a spectrophotometer (Shimadzu, UV-2550) at 646.8, 663.8 and 750.0 nm for quantification of the concentration of chlorophyll using the equation proposed by Porra *et al.*[155]

5.2.1.8 pH determination

The pH of the extracts was analyzed right after sampling and quenching of the samples with running water. A pH meter (pH 100 L pHenomenal®, VWR) was used for the analysis and performed at RT.

5.2.1.9 Sulfate content

An amount of 600 mL of Milli-Q water was heated to 90°C in a 1 L glass reactor. Once the set temperature was reached, 30 g of freeze-dried algae washed at RT for 20 min was added to the reactor. Samples of about 7 mL were withdrawn after 1, 5, 10, 30, 60 and 120 min, respectively, and immediately stored in a freezer. Subsequently, the samples were quenched at RT, and 5 mL of sample was mixed with 10 mL of ethanol (Etax Aa, Altia Oyj., ⩾ 99.5%). The samples were stored for 72 h in a freezer to allow for the precipitation of carbohydrates. Then the samples were centrifuged, filtered, and washed with additional ethanol to remove the non-ulvan associated sulfate groups. Eventually, the precipitate was freeze-dried and stored in a freezer in sealed test tubes before characterization.

The sulfate content in the ulvan extracts was analyzed by following the same procedure as described by Ray and Lahaye.[156] About 8–12 mg of the precipitate was placed into test tubes, and 3 mL of 2 M trifluoroacetic acid (Sigma-Aldrich, ⩾ 99% purity) was added. The samples were incubated at 100°C for 3 h, to maximize the release of sulfate groups. Subsequently, the samples were centrifuged, diluted, and filtered through a 0.22 µm nylon syringe filter before injection to the chromatograph. The quantification of sulfates was performed using a Metrohm ion chromatograph (881 Compact IC pro) coupled to a suppressor module. The column was a Metrosup A Supp 5-100 (100 mm ×4 mm) featuring a polyvinyl alcohol resin with quaternary ammonium groups, operated at RT. The eluent was an aqueous solution

containing 1.3 mM of sodium carbonate and 2.0 mM of sodium bicarbonate (Sigma Aldrich, ⩾ 99.7% purity) and operated at a flow rate of 0.8 mL min^{-1}.

5.2.1.10 Carbohydrate analyses

The concentration of carbohydrates was measured using the following two methods:

5.2.1.10.1 Acid methanolysis method

The concentration of hemicelluloses and pectins was determined following the acid methanolysis method.[157] 2 mL of methanolysis reagent containing 2 M of hydrochloric acid (HCl, J.T. Baker®, 37-38 wt.%) in anhydrous methanol (MeOH, J.T. Baker®, 99.8 wt.%) was added to 10 mg of freeze-dried algae samples and a calibration solution containing the following monomers: L-(+)-arabinose (Sigma, ⩾ 99% purity), D-(+)-galacturonic acid (Fluka, ⩾ 93% purity), D-(+)-galactose (Fluka, ⩾ 99.5% purity), D-(+)-glucose anhydrous (Fluka, ⩾ 98% purity), D-glucuronic acid (Sigma, ⩾ 98% purity), L-iduronic acid (LC Scientific Inc.), D-(+)-mannose (Fluka, ⩾ 99% purity), L-rhamnose monohydrate (Danisco, ⩾ 99% purity) and D-(+)-xylose (SAFC, ⩾ 99% purity). As the next step, the tubes were inserted into an oven operating at 100°C, for 3 h for liquid samples and 5 h for solid samples. Once the reaction was completed, 200 µL of pyridine (from Aldrich, ⩾ 99.0% purity) was added to neutralize any excess of HCl, and 1 mL of each internal standard solutions containing 0.1 mg mL^{-1} of sorbitol and resorcinol in methanol, respectively, were added to each sample. After mixing, methanol was evaporated at 50°C under a nitrogen stream, and the sample was further dried under a vacuum oven (Heraeus VTR 5022) operating at 42°C and below 50 mbar for 20 min before the derivatization of the samples.

5.2.1.10.2 Acid hydrolysis method

The cellulose content was determined using the acid hydrolysis method. 200 µL 72 vol.% sulfuric acid was added to each 10-mg algae sample. Also, 10 mg of cellulose powder (microcrystalline cellulose, Aldrich) was used as a standard. The standard and the algae samples were placed in a vacuum oven (Heraeus VTR 5022) at 42°C and degassed until 50 mbar of pressure was reached. This step was repeated three times. As the next step, the samples were stored under a fume hood for 2 h, whereupon 0.5 mL of deionized water was added to each sample. Again, 4 h later 6 mL of distilled water was added to each sample and stored under a fume hood overnight at RT. The next day, samples were placed in an autoclave, at 125°C for 90 min and then cooled down to RT. Once finished, two droplets of bromocresol green (Sigma-Aldrich, 95%) were added to each sample as an indicator of the pH, and barium carbonate (Aldrich, 99.98%) was added to neutralize the samples

until the liquid phase turned blue. 1 mL of internal standard containing 5 mg mL^{-1} of D-sorbitol (Sigma, ≥ 98%) in deionized water was added to each sample, and then centrifuged at 1200 rpm for 10 min. 1 mL of liquid phase was taken from each sample and transferred to another test tube, where 1 mL of acetone was added. Finally, the samples were evaporated under a nitrogen gas stream at 60°C and further dried in a vacuum oven (Heraeus VTR 5022) operating at 42°C below 50 mbar for 15 min before the derivatization of the samples.[158]

5.2.1.10.3 Derivatization of samples

Once the samples were completely dry, the derivatization was commenced by adding 150 µL of pyridine, 150 µL of hexamethyldisilazane (HDMS, Fluka, ⩾ 99.0%), and 70 µL of chlorotrimethylsilane (TMCS, Aldrich, ⩾ 99.0%), followed by a thorough mixing using a high-sheer vortex mixer. Further, the samples were left in a fume hood overnight, and the clear liquid phase was analyzed to determine the sugar content of the samples by gas chromatography.[157]

5.2.1.10.4 Gas chromatography

About 1 µL of a silylated sample was injected via a split injector (260°C, split ratio 1:15) into a 30 m / 0.32 mm i.d. column coated with dimethyl polysiloxane (HP- 1, Hewlett Packard) with a film thickness of 0.17 pm. The column temperature program was set as follows: a temperature ramp from 100 to 175°C (4°C min^{-1}), followed by a ramp of 175 to 290°C (12°C min^{-1}). The detector (FID) temperature was 290°C. Hydrogen was used as the carrier gas.

5.2.1.11 Monosaccharide analyses

The analysis of monosaccharides and uronic acids was performed using the following methods.

5.2.1.11.1 Gas chromatography method

The liquid samples from which the heterogeneous catalyst was separated were analyzed using gas chromatography before derivatization. The samples were left to quench, centrifuged, and 100 µL of sample was transferred to test tubes and freeze dried at -50°C and 0.1 mbar vacuum overnight. Separately, two calibration samples containing 1 mL of a solution comprising 0.1 mg mL^{-1} of each monosaccharide described in section 5.2.1.10.1 in a volume ratio 9:1 methanol-water were evaporated at 50°C under a nitrogen stream. Subsequently, 1 mL of an internal-standard solution consisting of 0.1 mg mL^{-1} of xylitol (Sigma, ≥ 99%) in methanol was added to each sample including the calibration samples. After mixing, methanol was evaporated at 50°C under a nitrogen stream, and the sample was dried further in a vacuum oven

(Heraeus VTR 5022) operating at 42°C below 50 mbar for 20 min. Once the samples were completely dry, they were silylated by adding 150 µL of pyridine, 150 µL of HMDS and 70 µL of TMCS, followed by a thorough mixing using a high-sheer vortex mixer. Further, the samples were left in a fume hood overnight, and the clear liquid phase was analyzed to determine the sugar content of the samples by gas chromatography.[159]

5.2.1.11.2 High Precision Liquid Chromatography (HPLC) method

HPLC was used for analyzing the samples processed with the homogeneous catalyst. The samples were withdrawn from the freezer and left to quench at RT, centrifuged, and 100 µL was transferred into 200 µL glass inserts disposed inside 1.5 mL HPLC vials. The analyses were performed in an HP-1100 HPLC (Agilent Technologies®, CA, USA) coupled to a refractive index detector HP-1047A (Hewlett Packard®, CA, USA). The system featured an Aminex™-HPX-87H (Bio-Rad, CA, USA) column (300 x 7.8 mm) operated at 55°C. The mobile phase was 5 mM of sulfuric acid at a flow of 0.3 mL min^{-1}. The injection volume was 10 µL.

5.2.2 Physical and physicochemical characterization techniques

5.2.2.1 Thermogravimetric analysis of fresh and processed algae

The thermogravimetric analyses of fresh and processed *U. rigida* biomass were performed under synthetic air with a SDT Q600 (V20.9 Build 20) instrument. About 6–8 mg of each sample was weighed to carry out the analyses. The sample was inserted in a platinum pan and heated up from RT to 625°C with a 10°C min^{-1} ramp. The purge gas rate fed into the system was 100 ml min^{-1}.

5.2.2.2 Transmission electron microscopy (TEM)

The comparative transmission electron microscopy analyses were performed for fresh *U.rigida* biomass, and *U. rigida* processed with ionic liquids. The samples were fixed with 5% glutaraldehyde in 0.16 mol L^{-1} s-collidine buffer, pH 7.4, and post-fixed with 2% OsO_4 containing 3% potassium ferrocyanide for 2 h. Subsequently, the samples were dehydrated in a series of increasing ethanol concentrations (70%, 96% and twice at 100%) and embedded in 45359 Fluka Epoxy Embedding Medium kit. Thin sections were cut with an ultramicrotome to a thickness of 70 nm, stained with 1% uranyl acetate and 0.3% lead citrate. The sections were examined with a JEOL JEM-1400 Plus transmission electron microscope operated at 80 kV acceleration voltage and with a resolution of 0.38 nm using a Quemesa 11 MPix bottom mounted digital camera.

5.2.2.3 Scanning electron microscopy analysis and energy dispersive X-ray analysis

The morphology of the fresh algae was studied by scanning electron microscope (SEM, Zeiss Leo 1530 Gemini) equipped with a ThermoNORAN vantage X-ray detector. The energy-dispersive X-ray analysis (EDXA) was carried out with the same instrument.

5.2.2.4 Molecular size distribution determination

The molar mass distribution of the ulvan extracts was determined using high-performance size-exclusion chromatography (HPSEC) in online combination with a multi-angle laser light scattering (MALLS) instrument (miniDAWN, Wyatt Technology, Santa Barbara, USA) and a refractive index (RI) detector (Shimadzu Corporation, Japan). The system featured two-columns in series, 2×UltrahydrogelTM linear 7.8×300 mm (Waters, Milford, USA). 100 mM sodium nitrate ($NaNO_3$, Merck, $\geqslant$ 99.5% purity) was used as the elution solvent, with a flow rate of 0.5 mL min^{-1}. The samples were first diluted to a concentration of around 3 mg mL^{-1} and subsequently filtered through a 0.22 µm nylon syringe filter before injection. A sample of 100 µL was injected into the column. The refractive index utilized dn/dc for calculations was equal to 0.146 mL g^{-1}, used by other authors.[160,161] The Astra software (Wyatt Technology, Santa Barbara, USA) was used for analyzing the data.

5.2.2.5 Fourier transform infrared spectroscopy (FTIR)

The IR spectra obtained from the extracts were recorded on an ATI Mattson Infinity Series IR spectrometer at room temperature. The samples were freeze-dried before the FTIR analyses and blended in a 3% w/w ratio with potassium bromide (KBr, Sigma-Aldrich, ≤ 100%) powder, followed by tableting (10 tons for 1 min) before measurement. A region of 4,000–400 cm^{-1} was used for scanning.

6 Experimental procedures

6.1 Extraction of phlorotannins [I]

Before obtaining the extracts, the dry seaweed (M1 dried at room temperature) was pretreated according to the procedure described by Koivikko, *et al.*[162] The pretreatment consisted of washing the alga with hexane (solid/liquid ratio of 1:5 w/v) three times to remove pigments and lipids. Additionally, 5.0 g of dry algae washed with hexane was dispersed separately in 50 ml of different solvents (methanol, ethanol, water, water/methanol 50:50, hexane/ethanol 88:12, ethanol/water 25:75 or 80:20, ethyl acetate/water 50:50, water/acetone 20:80 or 30:70 and methanol/chloroform 66:33% v/v),[141,162–166] and incubated on a platform at 200 rpm and 40°C for 2 h. The mixture was centrifuged at 2000 rpm at 4°C for 20 min, and the supernatant was stored at − 20°C before further analysis for the quantification of the total phlorotannin content (TPC) and the total antioxidant activity (TAA).

6.1.1 Evaluation of the effect of the drying temperature on the total phlorotannin content and the total antioxidant activity

The best drying conditions were determined using fresh algae (M2) dried at four temperatures 30, 40, 50 and 60°C.[167] The experiments were performed in a horizontal dryer with hot air flow (Tray dryer, Armfield UOP8) at an airflow speed of 1.3 m s^{-1}. After drying the samples were milled (1.4–2 mm) and stored at 4°C before the extraction.

As the next step, 0.5 g of alga (dried and pretreated) was placed in a test tube containing distilled water at a solid/liquid ratio of 1/10 and incubated on a platform shaker at 200 rpm and 40°C for 2 h. The sample was centrifuged at 7000 rpm for 10 min at 4°C, and the supernatant was stored for further analyses. The best drying temperature was determined in terms of the highest TPC and TAA obtained.

6.1.2 Evaluation of the effect of the extraction parameters on the total phlorotannin content and the total antioxidant activity

The different extraction variables, namely the extraction time, the extraction temperature, the solid/liquid (S/L) ratio and the particle size of the algae were simultaneously evaluated using a Taguchi orthogonal array L9, 3^4. The schedule considered the realization of nine experiments, with a total of four factors and three working levels.[168] The seaweed M3 was previously dried at

40°C, washed with hexane, and water was used as an extractant. Further, Table 6-1 describes the conditions evaluated for each experimental run. The best extraction conditions were determined in terms of the highest TPC and TAA values measured after the extraction.

Table 6-1. The conditions evaluated for the extraction of phlorotannins

Runs	Time h	Temperature °C	Solid-to-liquid ratio -	Particle size mm
1	2	25	1/10	< 1.4
2	2	40	1/15	2.0–1.4
3	2	55	1/20	> 2.0
4	3	25	1/15	> 2.0
5	3	40	1/20	< 1.4
6	3	55	1/20	2.0–1.4
7	4	25	1/20	2.0–1.4
8	4	40	1/10	> 2.0
9	4	55	1/15	< 1.4

6.2 Ionic liquid extraction of carbohydrates [II]

Three ionic liquids were used in the algal processing. DBU-MEA-SO_2 (SIL) was prepared by mixing the superbase DBU and monoethanolamine followed by exothermic reaction upon bubbling of sulfur dioxide, as described by Anugwom *et al.*[116] The second IL used was TMG propionate ($[TMGH^+][CO_2Et^-]$), prepared by simple acid-base neutralization reaction, as described by King *et al.*[169] The third IL used was the protonated 1,8-diazabicyclo-[5.4.0]-undec-7-ene 2,2,3,3,4,4,5,5-octafluoro-1-pentoxide ($[HDBU^+][5OF^-]$), which was kindly provided by The Institute of Heavy Organic Synthesis "Blachownia" (ICSO, used as received). After treatment with IL, several washing and precipitation steps for the recovery of the solubilized fractions were performed, as described in the following sections.

6.2.1 Switchable ionic liquid (SIL)

A total of 2.00 g of freeze-dried algae was added to a 100 mL reactor where 18.00 g of the SIL DBU-MEA-SO_2 was added. The experiments were performed at 100 and 120°C. The reactor was placed in an oil bath at the required temperature with continuous magnetic stirring for 6 h. All the experiments were carried out in duplicate unless otherwise stated.

6.2.2 Distillable ionic liquid (DIL)

A total of 10.95 g of TMG and 7.05 g of propionic acid were slowly added to a 100 mL reactor. The DIL formation took place upon mixing. Once mixed and cooled down, 2.0 g of freeze-dried algae were disposed into the reactor. The experiments were performed at 100, 120, 140 and 160°C, respectively. The

reactor was placed in an oil bath at the required temperature with continuous magnetic stirring for 6 h. All the experiments were carried out in duplicate unless otherwise stated.

6.2.3 Low viscosity ionic liquid (LVIL)

A total of 100 mg of freeze-dried algae was added to a 15 mL test tube where 900 mg of the LVIL was added. The test tube was placed in an oil bath at 120°C with continuous magnetic stirring for 6 h. The experiments were carried out in duplicate.

6.2.4 Filtering and washing of fibers

Once the preset treatment time was reached, 50 mL of deionized water (Milli-Q, Millipore) was added to the reactor to facilitate the removal of the ionic liquid. As the next step, the undissolved material was removed by using glass fiber filters and washed twice with 50 mL of deionized water. The samples treated with LVIL were filtered without the help of water due to its very low viscosity. Subsequently, a total of 20 mL of deionized water (Milli-Q, Millipore) was added for further IL removal. Due to its higher density compared to water, the LVIL decanted at the bottom of the funnel, allowing for a better IL removal from the undissolved material. The remaining solids were freeze dried at -50°C and 10 mbar of vacuum overnight and kept in a freezer before the FTIR analysis, acid methanolysis, acid hydrolysis or any other further analyses and treatments. The liquid filtrates (ionic liquid and washing water) were kept in a freezer until further analyses were performed.

6.2.5 Precipitation of dissolved algae biomass in ionic liquids

The water in the ionic liquid phase was evaporated using a Büchi R114 Rotavapor at 40°C under vacuum. Once the viscosity of the samples notably increased because of water removal (especially for SIL and DIL), and vacuum was below 0.1 mbar, and the treatment was continued for additional 20 min for maximum water removal. Subsequently, 40 mL of ethanol (Aa grade) was added, and the mixture was gently stirred for 30 min (in the case of LVIL 5 mL of ethanol was used). The precipitated mass was separated by filtration using glass filters and further washed with 20 mL ethanol for the removal of trace ionic liquids (in the case of LVIL 5 mL of ethanol was used). Once filtered, the solid precipitate was dried in a furnace at 70°C for 1 h and then left in freeze drying equipment at -50°C and 10 mbar of vacuum overnight.

6.2.6 Precipitation of dissolved algae biomass in wash water

The water in the washing liquid was evaporated using a Büchi R114 Rotavapor at 40°C under vacuum. Once a thin layer of solid was seen in the

balloon and vacuum was below 0.1 mbar, samples were left for additional 20 min for maximum water removal. Subsequently, 20 mL of ethanol (Aa grade) was added, and the mixture was gently stirred for 30 min (in the case of LVIL 5 mL of ethanol was used). The precipitate was separated by filtration using glass filters and further washed with 10 mL ethanol to ensure the removal of any ionic liquid traces (in the case of LVIL, 5 mL of ethanol was used). Once filtered, the solid precipitate was dried in a furnace at 70°C for 1 h, and then left in freeze drying equipment at -50°C and 10 mbar of vacuum overnight.

6.2.7 Aqueous carbohydrate extraction

In addition to ionic liquid processing, experiments using aqueous solvents were performed to study carbohydrate dissolution yields. Two experiments in duplicate were carried out using Milli-Q water and dilute sulfuric acid 1.0 vol.% in an autoclave at 125°C for 1 h. 200 mg of freeze-dry alga *U. rigida* was added to 15 mL test tubes at 10 wt.% mass loading. The test tubes were placed in an autoclave, and once the pretreatment temperature was achieved the reaction was continued for 60 min. Upon finish, the autoclave was turned off, and the pressure allowed to decrease to atmospheric condition. Subsequently, the test tubes were removed from the autoclave and allowed to cool down. The samples were filtered, and the undissolved fraction and the liquid phase were kept in a freezer before the carbohydrate analyses were performed.

6.3 Aqueous extraction of carbohydrate experiments [III]

6.3.1 Washing of algae

The removal of salts from the algae was studied by washing of the algae. The influence of the washing time was investigated as follows: 5.5 g of algae was placed in a glass reactor containing 110 mL of Milli-Q water, at room temperature. The mixtures were stirred at 650 rpm for 20 min and 16 h. Accordingly, the mixture was centrifuged in a Cellsep 6/720R centrifuge (MSE®, UK) at 4000 rpm at room temperature. Consequently, the liquid phase was filtered, and both the liquid and the solid phases were stored in a freezer for subsequent analyses.

6.3.2 Aqueous extraction of ulvan experiments

An amount of 60 g of algae was disposed into a glass reactor containing 1.2 L of Milli-Q water and stirred at 650 rpm for 20 min. The washed algae were filtered and thoroughly washed with Milli-Q water to remove remaining salts. As the next step, the algae were freeze-dried overnight. Subsequently, 110

mL of Milli-Q water was placed in a 250 mL glass reactor and heated to the desired temperature (60, 70, 80 and 90°C). The glass reactor was equipped with a thermometer and a cooling system. Once the set point temperature was reached, 5.5 g of the washed algae were disposed into the reactor. Samples were withdrawn at 1, 5, 10, 30, 60 and 120 min of extraction and stored in a freezer for subsequent analyses. The experiments carried out at 110 and 130°C were performed in an autoclave, where 15 g of washed algae were disposed together with 100 mL of MilliQ water. Subsequently, 200 mL of Milli-Q water was heated to 150°C in a preheater coupled to the autoclave. The experiment was initiated (time zero) by letting the water in the pre-heater to enter the autoclave by opening the valve located in the line connecting both vessels. In this set of experiments, samples were withdrawn after 1, 5, 10, 20, 30, 45, 60 and 120 min. The samples were stored in a freezer before their further characterization.

6.4 Enzymatic saccharification of brown algae [IV]

6.4.1 Dilute sulfuric acid pretreatment

0.5 g of dry *M. pyrifera* was pretreated with 1.5 ml of sulfuric acid (2 vol.%) or water. Algae and solvent were introduced into glass vials, placed in a thermostatic oil bath at 120°C for 1 h. This temperature was chosen because previous data at 80°C and 120°C showed higher yield at 120°C (data not shown). After incubation, the tubes were removed from the oil bath, and the algae were washed with water six times and oven-dried at 37°C for three days.

6.4.2 Ionic liquid pretreatment

Three different ionic liquids (ILs) were used: 1-ethyL-3-methylimidazolium acetate ($[EMIM^+][OAc^-]$), 1,5-diazabicyclo-[4.3.0]-non-5-ene acetate ($[DBNH^+][OAc^-]$), prepared as described by Parviainen *et al.*, 2013, and DBU–MEA–SO_2–SIL, prepared as described by Anugwom *et al.*, 2012.[113,170]

The algae and the solvent were introduced into glass vials, placed in a thermostatic oil bath at 120°C for 1 h. After incubation, the tubes were removed from the oil bath, and the algae were washed with water six times and over-dried, at 37°C for three days.

6.4.3 Saccharification with cellulases

For the saccharification with cellulases, samples containing 0.1 g of algae were incubated with a commercial cellulase enzyme complex (Celluclast; 10 FPU g^{-1} algae was determined as described by Ghose),[171] and β-glucosidase (10 unit g^{-1} algae; 1 unit of activity was defined as the amount of enzyme

required to hydrolyze 1 μmol of p-nitrophenyl β-D-glucopyranoside (Aldrich, 99%) per min at pH 4.0 and 37°C). The optimum pH was determined using a McIlvaine buffer (citric acid(Sigma-Aldrich, ≥ 99.5)/disodium hydrogen phosphate (Sigma, ≥ 99%)),[172] in a pH range of 4.8 to 7.5, incubated for 4 h at 50°C. The effect of temperature on the activity of the enzymes was analyzed. The samples were incubated for 4 h in a McIlvaine buffer pH 5.2 at 28.5, 37 and 50°C. The standard condition for saccharification of cellulose was pH 5.2 at 50°C under constant agitation (200 rpm). Once the reaction time was completed, the samples were centrifuged. The enzymatic saccharification of algae was performed in triplicate, and the quantification of glucose was performed using the Kit RandoxGluc-PAP.

6.4.4 Saccharification with alginases

For the saccharification with alginases, samples containing 0.1 g of algae were incubated with 3 unit g^{-1} algae of alginate lyase (an endo-type enzyme, 1 unit was defined as the amount of enzyme required to produce an increase equal to 1.0 in the absorbance measured at 235 nm per minute per ml of sodium alginate solution, at pH 6.3 and 37°C). Additionally, 4 unit g^{-1} algae of an oligoalginate lyase (an exo-type of enzyme, 1 unit was defined as the amount of enzyme required to liberate 1 μmol of uronic acid per minute at pH 7.5 and 37°C) kindly provided by BAL Company was added.

The optimum pH was determined in a McIlvaine buffer adjusted to a pH in the range of 5.4-8.0 and incubated for 2 h at 37°C. The effect of the temperature on the activity of the enzyme was analyzed. The samples were incubated for 2 h in a McIlvaine buffer at pH 7.5 at 28, 32, 37 and 50°C. The standard conditions for the saccharification were pH 7.5 at 37°C under constant agitation (200 rpm) followed by centrifugation. The saccharification of alginate with alginate lyase and oligoalginate lyase produces mainly uronic acid (monomers) and some oligoalginates with different molecular weights. The enzymatic saccharification of the algae was performed in triplicate, and the quantification of the concentration of uronic acid (unsaturated uronate) was performed as described by Milner *et al.* and Nelson.[173,174] The absorbance of each sample was measured at 600 nm. A standard curve was prepared using D-glucuronic acid (Sigma, ⩾ 98% purity).

6.5 Hydrolysis processing [V]

The hydrolysis of carbohydrates present in *U. rigida* biomass was performed following two different approaches: in-situ hydrolysis of the alga, in the presence of the catalyst, and pre-extraction of carbohydrates coupled to the subsequent hydrolysis of the extract.

6.5.1 One-pot hydrolysis of the biomass

The one-pot hydrolysis of carbohydrates present in the alga was carried out isothermally in a 250 mL glass jacketed reactor, equipped with an agitator (800 rpm), thermometer and reflux condenser. Initially, 200 mL of deionized water (DI, Millipore) was added to the reactor and heated to obtain the preset temperature. Once the required temperature was reached the catalyst was loaded into the reactor in a concentration in the range of 4.3- 100 mM H^{+}_{eq}, and subsequently 2 g of freeze dry alga was added. Three catalysts were used in the experiments: hydrochloric acid (HCl), *Amberlyst™*70 and *Smopex*®101, and the acidity loading was calculated using the acid capacity provided by the manufacturer. When the temperature was set to 120°C, an autoclave was used for carrying out the experiments (see section 6.5.3). Samples were withdrawn periodically to follow the hydrolysis kinetics. The reaction was carried out during 120 h, and thereafter, the mixture was allowed to cool-down to room temperature. Subsequently, the liquid was filtered using glass fiber filters, and the remaining fibers together with the solid catalyst were washed ten times with 50 mL deionized water. In the case of *Amberlyst™*70, the solid particles were separated from the remaining fibers due to their larger size and higher density. Both the hydrolysate and the remaining fibers containing the solid catalyst were kept in a freezer for further analyses.

6.5.2 Extraction of the ulvan fraction

The extraction of ulvan was carried out at 90°C in a 1 L glass reactor coupled to a reflux condenser, which was surrounded by an ISOPAD™ LG2/ER (Aldrich®, MO, USA) heating mantle connected to an ISOPAD™ TD 2000 (Aldrich®, MO, USA) temperature controller. Since the thermocouple was not in contact with the mixture, an analog thermometer was used for controlling the extraction temperature. Thereby, the reactor was loaded with 37.5 g of washed alga and 600 mL of deionized water (DI, Millipore). Concurrently, the temperature was set to 90 ± 3°C and the extraction time was 4 h. Upon the extraction time was completed, the mixture was left to quench and subsequently centrifuged at 4000 rpm at room temperature. Afterwards, the solid fibers were discarded, and the liquid phase was vacuum filtered and stored in borosilicate bottles in a freezer before characterization and further processing.

6.5.3 Hydrolysis of the ulvan fraction

The hydrolysis of ulvan was performed in a 300 mL 316 stainless steel autoclave (Autoclave Engineers®, PA, USA) equipped with an electric heating mantle, an internal cooling coil and an external heat exchanger (pre-heater). The system was equipped with a MagneDrive® agitator (Autoclave Engineers®, PA, USA) coupled to a Dispersimax™ straight blade turbine

stirrer (Autoclave Engineers®, PA, USA). The temperature, pressure, and stirring were controlled by PID through a Eurotherm® 2416 controller (Eurotherm®, VA, USA). Additionally, the autoclave was equipped with gas inlet and outlet lines connected to a nitrogen cylinder to modify the pressure inside the autoclave and the preheater, respectively. Similarly, the autoclave had a sampling line to follow the hydrolysis kinetics. Accordingly, the autoclave was loaded with 100 mL of ulvan extract and the respective amount of catalyst to give a final acidity loading between 50 and 100 mM H^{+}_{eq}. Concurrently, the preheater was loaded with deionized water to complete a final volume of 200 mL, depending on the humidity of the resins used as heterogeneous catalysts (Smopex®101) and the amount of hydrochloric acid added as the homogeneous catalysts, respectively. The temperature of the preheater was set according to the temperature of the reaction medium in the autoclave, and the temperature set for the hydrolysis reaction. The reaction temperatures evaluated in this work were 90, 100, 105, 110 and 120°C, respectively. The time zero of the reaction was set upon transfer of the content of the preheater to the autoclave. The reaction time was 48 h. Therefore, samples were withdrawn at 0, 1, 2, 4, 7, 12, 24, 36 and 48 h, respectively, and collected in 2x1.5 mL vials. Upon sampling, the vials were stored in a freezer before subsequent analyses.

7 Results and discussion

7.1 Composition of the alga [I], [II], [IV]

The algal biomass main constituents are carbohydrates, proteins, lipids, and ashes. Figure 7-1 depicts the proximate composition of the algal species used in the present study. Figure 7-1-A, B, and C show the composition for different *Macrocystis pyrifera* batches harvested in March 2011, November 2011, and June 2013, respectively. Accordingly, Figure 7-1-D illustrates the composition for *Ulva rigida* collected in December 2009. The variations between different algal species regarding their composition are noticeable. *M. pyrifera* (brown algae) has an evident higher ash content compared to *U. rigida* (green algae), and the difference may be explained by the distinct environments where the species were harvested as well as the variations of the cell wall polysaccharides to be described later. At the same time, the protein content was also different between both species, which is an indication of the structural dissimilarities of the cell wall. Brown algae belong to the phylum *Stramenopiles*, including protists and diatoms organisms. This phylum evolved independently from the *Archeaplastida* phylum, which includes green and red algae species, as well as, land plants. Consequently, brown algae developed plant-like structures that have a different root than plants, resulting in distinct cell wall components.[49] Another interesting observation is the high seasonal oscillation reported in the proximate composition of *M. pyrifera*. These results are in line with those reported previously for these species and are closely associated with the seasonal variations of the photosynthetic rate and the nutrient availability in near shore environments.[175–177]

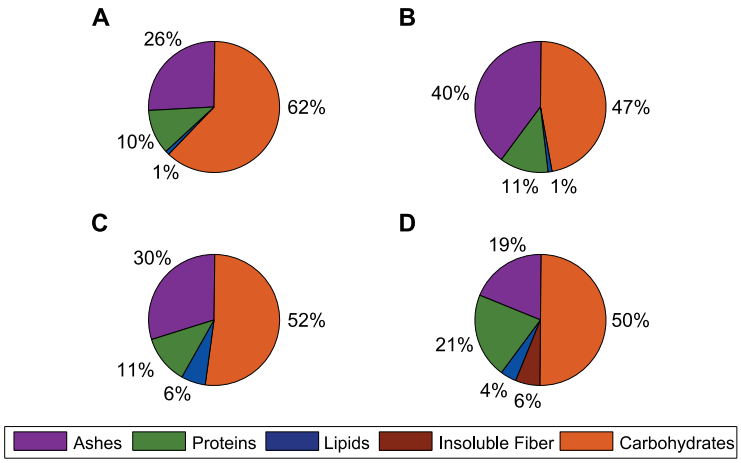

Figure 7-1. The proximate composition of the algae species used in this work; A. *M. pyrifera*–March 2011, B. *M. pyrifera*–November 2011, C. *M. pyrifera*–June 2013 and D. *U. rigida*–December 2009,

Regarding the carbohydrate composition, important differences are observed between brown and green algae species. While *M. pyrifera* is rich in uronic acids originating from alginate, as illustrated in Figure 7-2-A and B, *U. rigida* is rich in glucose coming from cellulose and starch, as depicted in Figure 7-2-C. *M. pyrifera* has a minor content of glucose, which is also coming from cellulose in addition to laminarin, a β-1,3-glucan that develops in brown algae species. Both species contain L-deoxy-sugars (L-rhamnose and L-fucose), which are present in the backbone of sulfated polysaccharides: fucans and ulvans. The occurrence of a high content of uronic acids explains the presence of ionic polysaccharides, such as alginate and ulvan, which were closely associated with the salts that were reported as ashes in the proximate analyses.

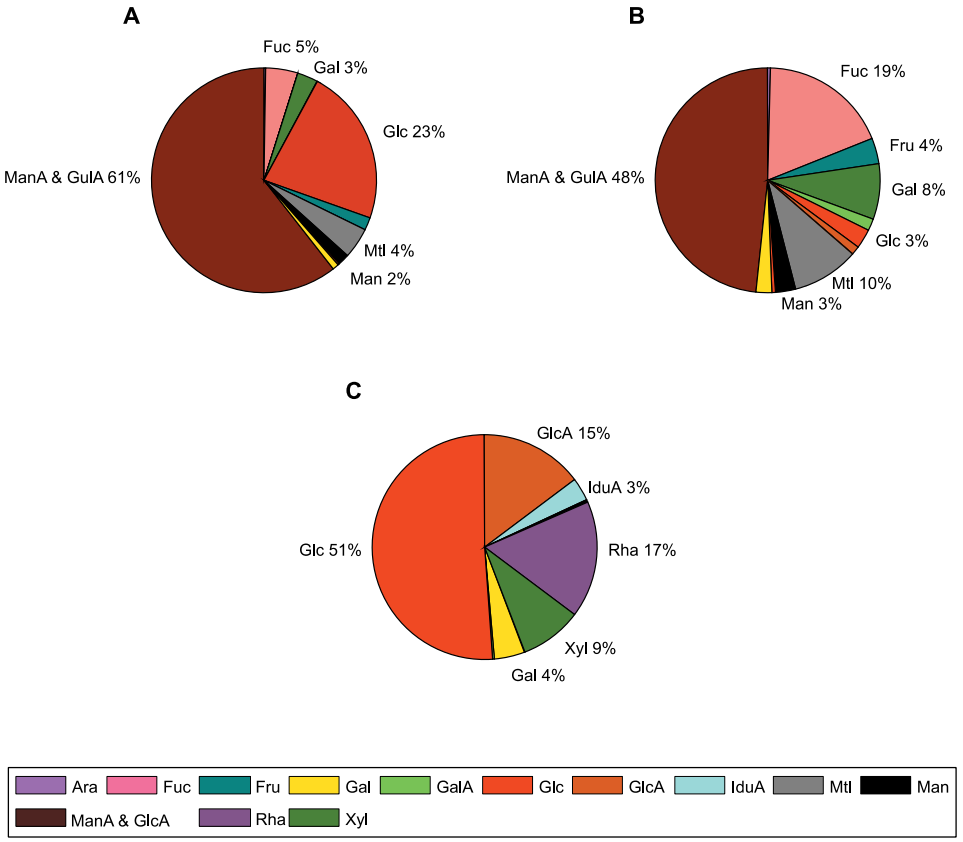

Figure 7-2. The composition of monomers of Macrocystis pyrifera *and* Ulva rigida*;*

The monomers content was expressed as wt.% of the total carbohydrate content calculated via acid hydrolysis and acid methanolysis methods. A. *M. pyrifera*–June 2012, B. *M. pyrifera*–December 2013 and C. *U. rigida*–December 2009.

The analyses of the fresh biomass performed with the scanning electron microscopy technique (SEM) revealed the abundant presence of salts in the biomass. The white spots marked for *U. rigida* fresh alga (see Figure 7-3, B), showed an increased content of salts, especially sodium chloride. In the case of *M. pyrifera*, the SEM image (see Figure 7-3, A) also shows white stops with a high concentration of salts attributed to the presence of sodium, chloride, and potassium, as determined in the EDXA analysis of the sample.

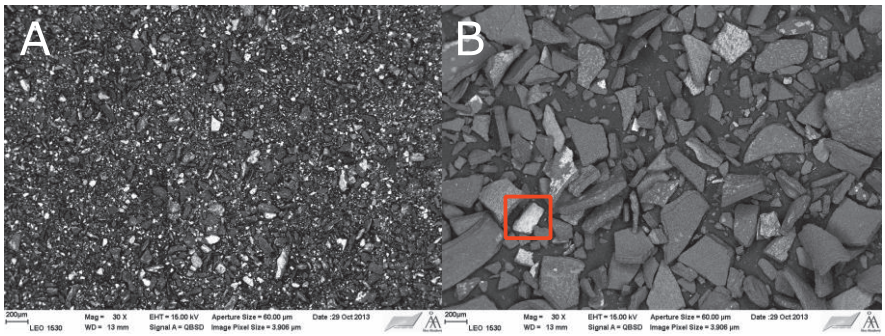

Figure 7-3. Scanning electron microscopy of fresh algae;
A. *Macrocystis pyrifera* (unpublished data), B. *Ulva rigida* (Paper II).

The thermogravimetric analyses of the fresh algae biomasses demonstrated a rather similar initial degradation profile of the alga. However, the end of the analyses showed a major difference in the final residues of both algae, as illustrated in Figure 7-4. While the treatment of *U. rigida* left a residue of 16 wt.%, the treatment of *M. pyrifera* left a residue of 40 wt.%. These results were in line with the proximate analyses, which revealed a major difference in the ash content of both algae.

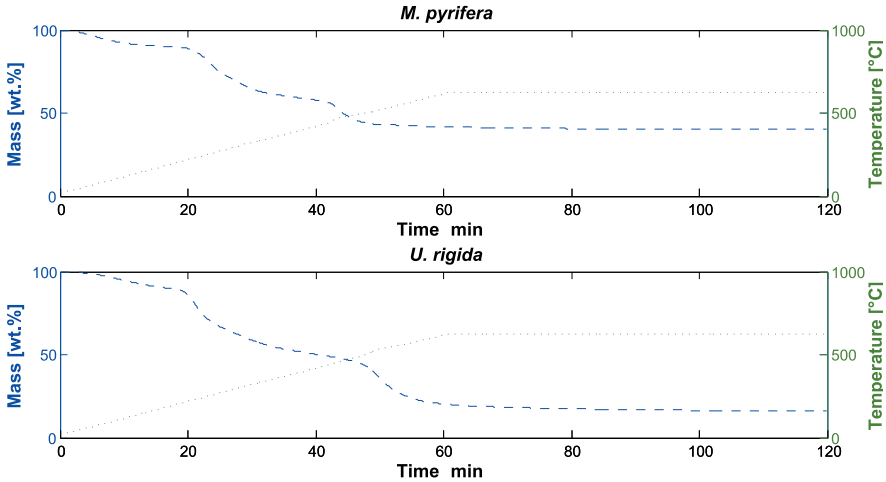

Figure 7-4. Thermogravimetric analyses of the fresh algae samples;
Upper picture *M. pyrifera*, lower *U. rigida*.

Large differences were also observed in the elemental composition of the ashes analyzed through ICP-OES (Table 7-1). *M. pyrifera* is particularly rich in Ca, K, Na, and Sr, which are common cations associated with alginate.[145] The Fe content is higher in *U. rigida* than in *M. pyrifera*, which may be due to the higher content of proteins reported in *U. rigida* compared to *M. pyrifera*. Regarding the organic analysis, both algae exhibited substantial amounts of C and O, with 58 and 72 wt.%, respectively, being characteristic for biomass with high carbohydrate content. The content of sulfate is especially high for the case of *U. rigida*, in line with the occurrence of the sulfated polysaccharide ulvan,[160,178–180] which is one of the main constituents of the cell wall in this alga.

Table 7-1. The results of the chemical analyses conducted for Macrocystis pyrifera *and* Ulva rigida

Organic elemental analysis

Specie	N [wt.%]	C [wt.%]	H [wt.%]	S [wt.%]	O [wt.%]	Others [wt.%]
M. pyrifera	1.7 ± < 0.1	27.9 ± 0.3	4.0 ± 0.1	1.6 ± 0.2	30.1 ± 0.4	34.8 ± 0.1
U. rigida	3.6 ± 0.1	37.0 ± < 0.1	5.7 ± < 0.1	3.6 ± 0.2	34.9 ± 0.1	15.3 ± 0.3

ICP–OES

Specie	Al [mg kg^{-1}]	As [mg kg^{-1}]	B [mg kg^{-1}]	Fe [mg kg^{-1}]	Si [mg kg^{-1}]	Sr [mg kg^{-1}]
M. pyrifera	260 ± n.d.	70.0 ± n.d.	130 ± n.d.	150 ± n.d.	640 ± n.d.	1000 ± n.d.
U. rigida	120 ± n.d.	n.d. ± n.d.	70.0 ± n.d.	390 ± n.d.	500 ± n.d.	15.3 ± n.d.
Specie	Ca [wt.%]	K [wt.%]	Mg [wt.%]	Na [wt.%]	P [wt.%]	S [wt.%]
M. pyrifera	1.8 ± n.d.	10.0 ± n.d.	0.9 ± n.d.	4.5 ± n.d.	0.3 ± n.d.	1.8 ± n.d.
U. rigida	0.4 ± n.d.	1.6 ± n.d.	2.0 ± n.d.	2.6 ± n.d.	0.2 ± n.d.	0.4 ± n.d.

7.2 Extraction of phlorotannins [I]

Brown algae contain a substantial number of compounds bearing antioxidant activity, concurrently to red and green algae species in which these compounds are relatively scarce. One of the molecules bearing antioxidant activity are phlorotannins, which are aromatic compounds found principally in brown algae species. Even though they can be considered as algal extractives since they are present in physodes (vesicular intercellular inclusions) analogous to tannins in terrestrial plants, phlorotannins have also been suggested to play a structural role in the cell wall of brown algae.[49,65] Consequently, it is worth studying different solvents and conditions for extraction of algae to maximize the yield of phlorotannins.

7.2.1 The effect of the solvent

Many solvents differing on their polarity were used for evaluating the extraction of phlorotannins. The extraction yield was quantified as the total phlorotannins content (TPC), which was calculated as mg gallic acid

equivalent (GAE) 100 g^{-1} of dry solid (DS). Additionally, the extraction of phlorotannins was evaluated in terms of the total antioxidant activity, which was calculated as mg of Trolox equivalent (TE) 100 g^{-1} DS. The result of this evaluation is shown in Figure 7-5.

The highest TPC was obtained with water, accounting for 147 ± 2.9 mg GAE 100 g^{-1} DS. Figure 7-5 illustrates the values of TPC and TAA ordered according to an increasing polarity of the solvent, calculated as the weighted average of the polarity of the pure solvent with respect to the volume ratio of the solvents. TPC showed higher values when more polar solvents were used. The increase of the TPC values with respect to the polarity of the solvent was a relatively obvious result, since the structure of phlorotannins shows increasing polarity due to the presence of several hydroxyl groups in these molecules. However, the second highest value of TPC was observed when a mixture of Acetone/Water 70/30 was used, accounting for a yield of 125 ± 1.5 mg GAE 100 g^{-1} DS. This high TPC value was explained by the low polarity of acetone that may have allowed for the extraction of lipids and pigments resulting in an elevated TAA value,[181] as shown in Figure 7-5. Consequently, water was considered as the best solvent for the extraction of phlorotannins under the evaluated conditions. Similar results have been reported for the species *Scytosiphon lomentaria*, *Papenfussiella kuromo* and *Namecystus decipiens*.[182]

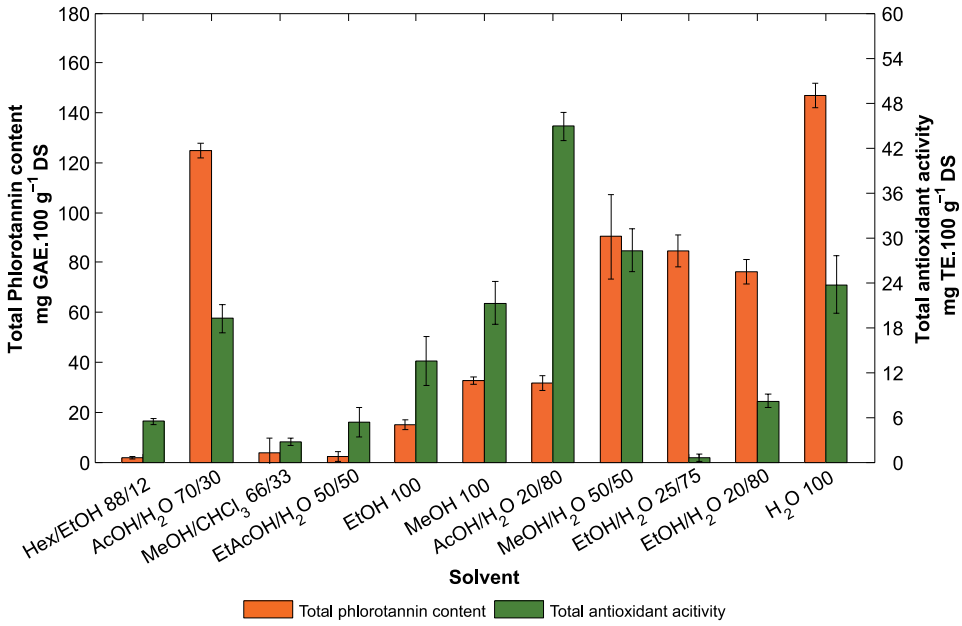

Figure 7-5. The effect of the solvent on the total phlorotannin content;
Hex: hexane, EtOH: ethanol, AcOH: acetone, MeOH: methanol, $CHCl_3$: chloroform and EtAcOH: ethyl acetate. Values in the abscise represent vol:vol ratio.

7.2.2 The effect of the drying temperature

A set of four drying temperatures were evaluated to study the drying time required to achieve final moisture content and subsequent TPC and TAA values obtained by extraction with water. When 30°C was used as the drying temperature for fresh algae, a much slower drying profile was observed compared to the temperature range of 40–60°C (see details in Paper [I]). TPC and TAA values decreased with respect to more elevated drying temperatures, as illustrated in Figure 7-6. The extraction of phlorotannins from fresh algae without drying showed the highest TPC and TAA values, accounting for 210 ± 20 mg GAE 100 g^{-1} DS and 115 ± 36 mg TE 100 g^{-1} DS, respectively. Consequently, a decrease on the TPC and TAA was observed upon extraction of dry algae. The effect of different drying techniques on the content of extractives obtained from terrestrial plants has been evidenced by various authors,[183,184] mainly due to the risks of oxidation of the extractive molecules.

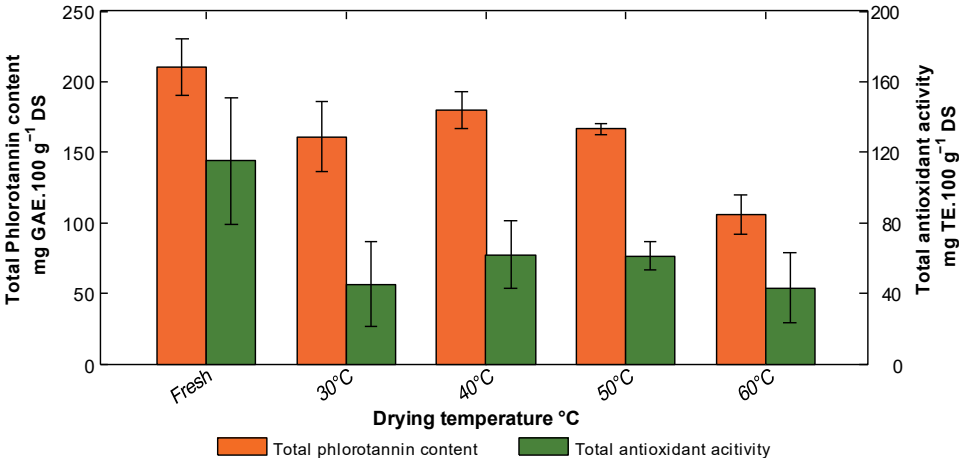

Figure 7-6. The effect of the drying temperature on the total phlorotannin content and total antioxidant activity.

7.2.3 Optimization of the conditions for the phlorotannin extraction

Different conditions regarding the extraction time, the extraction temperature, the solid to liquid ratio and the particle size of the algae were evaluated to optimize the extraction of phlorotannins from *M. pyrifera*. The best conditions were obtained upon 4 h of extraction with water at 55°C at a solid-to-liquid ratio of 1:15 and particle size of 100% < 1.4 mm, accounting for TPC and TAA of 200 ± 5.6 mg GAE 100 g^{-1} DS and 38.4 ± 2.9 mg TE 100 g^{-1} DS, respectively. The statistical evaluation of the different conditions evidenced that the solid-to-liquid ratio was the most determining factor in terms of the TPC and TAA values.

Table 7-2. The influence of extraction parameters on the total phlorotannin content and the total antioxidant activity

Runs	Time h	Temperature °C	Solid-to-liquid ratio	Particle size mm	TPC mg GAE 100 g^{-1} DS	TAA mg TE 100 g^{-1} DS
1	2	25	1/10	< 1.4	120.8 ± 11.3	42.7 ± 0.4
2	2	40	1/15	2.0–1.4	55.8 ± 4.0	29.1 ± 8.4
3	2	55	1/20	> 2.0	39.5 ± 3.1	14.4 ± 4.2
4	3	25	1/15	> 2.0	31.4 ± 18.1	27.3 ± 4.3
5	3	40	1/20	< 1.4	47.2 ± 5.9	42.0 ± 3.2
6	3	55	1/20	2.0–1.4	136.9 ± 20.8	55.6 ± 1.9
7	4	25	1/20	2.0–1.4	100.0 ± 6.3	20.8 ± 2.0
8	4	40	1/10	> 2.0	89.1 ± 9.3	46.1 ± 4.8
9	4	55	1/15	< 1.4	200.5 ± 5.6	38.4 ± 2.9

7.2.4 Characterization of the phlorotannin extract

The characterization of the phlorotannin extract was carried out via Fourier transform infrared (FTIR) spectra and HPLC-ESI-MS/MS analyses. The FTIR spectra of the phlorotannin extract obtained after the best extraction conditions and the FTIR spectra of standard phloroglucinol and alginic acid showed similar peaks between the band 1630-520 cm^{-1} (see Figure 7-7). The peaks between the band 1470-1450 cm^{-1} corresponds to the stretching of aromatic rings, while peaks around 1100–1000 cm^{-1} correspond to the stretching of glycosidic linkages and C-O-H bonds typical of carbohydrates. Additional stretching bands between 950 and 800 cm^{-1} and 1260-1240 cm^{-1} are typical for sulfate esters found both in the standard of alginate (possible contamination with sulfated polysaccharides from brown algae), and in the phlorotannins extract. Indeed, a substantial amount of fucose, 39.7 mg g^{-1} DS, and mannitol, 38.1 mg g^{-1} DS, were present in the phlorotannin extract. Both fucose and mannitol are residues found in fucoidans and at reducing ends of laminarin, respectively, and they are readily extracted with water at relatively low temperatures. Additionally, 23.4 mg g^{-1} DS of mannuronic and guluronic acid was obtained in the extracts. The total carbohydrate content found in the extracts accounted for 118 mg g^{-1} DS according to the acid methanolysis analyses.

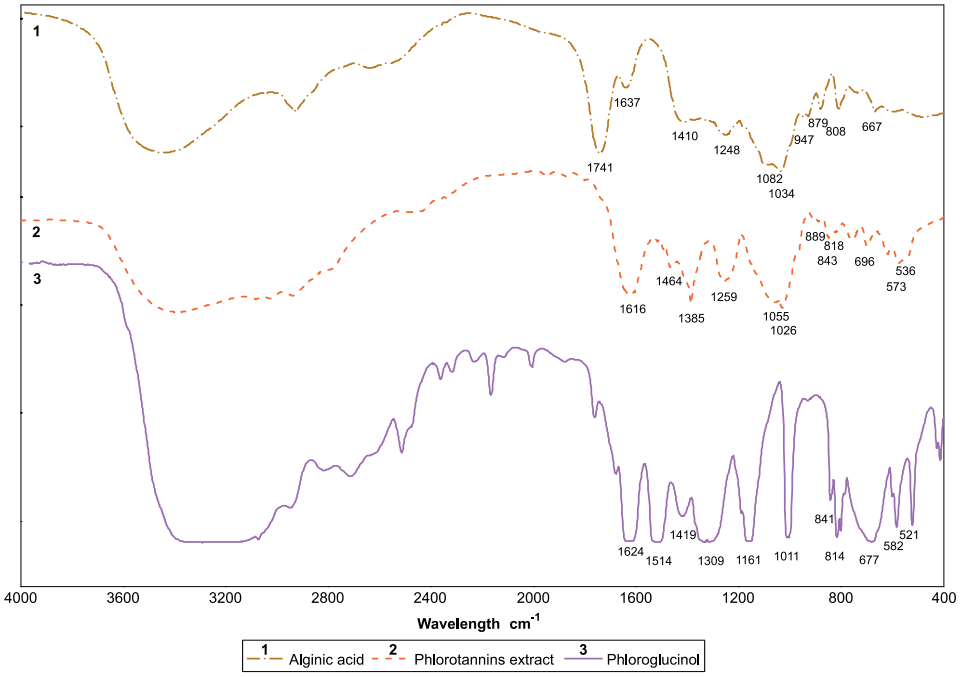

Figure 7-7. FTIR spectra of phlorotannin extracts from Macrocystis pyrifera *and standards of phloroglucinol and alginic acid.*

However, the HPLC-ESI-MS/MS gave two peaks at the retention times 34.4 and 52.1 min, with signal m/z 497 and 499, respectively. The fragmentation of the first peak gave m/z values of 478.2 and 245.8, which are likely to correspond to a derivative of phloroglucinol named phloroeckol. Furthermore, the fractionation of peak 2 gave signals m/z of 480.4, 235.9 and 245.8, which likely correspond to a tetramer of phloroglucinol isomer, namely difucophloroethol, fucodiphloroethol, tetrafucol or tetraphloroethol (see Figure 7-8).

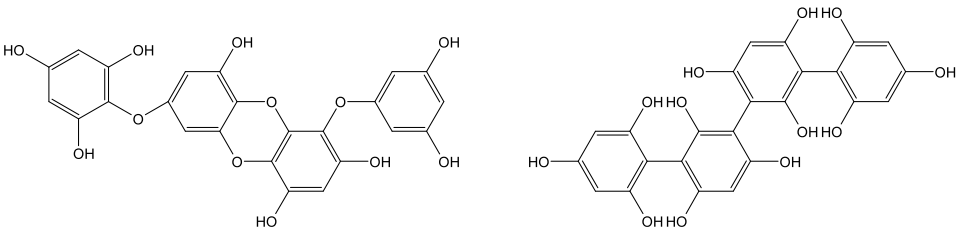

Figure 7-8. Possible molecules occurring in the phlorotannin extracts from Macrocystis pyrifera*.*

7.3 Extraction of ulvan [II], [III]

7.3.1 Selection of the solvent

The green macroalgae *Ulva rigida* was processed in ionic liquids whereupon the goal was to isolate carbohydrates that can be used in the production of platform chemicals or biofuels such as ethanol. The ionic liquids were selected based on their potential to dissolve different type of biomass constituents. The first IL tested was DBU-MEA-SO2 (1,8-diazabicyclo-[5.4.0]-undec-7-ene, monoethanolamine, sulfur dioxide), the so-called switchable ionic liquid (SIL). The term switchable stands for the ability of these types of solvents to be back switched from ionic form to a mix of molecular liquids by bubbling an inert gas (such as nitrogen) to obtain the starting materials (in this case a superbase and an alkanol amine). This IL has been successfully utilized in the solubilization of lignin and hemicelluloses.[118] The second IL used was 1,1,3,3-tetramethylguanidine (TMG) propionate ([$TMGH^+$][CO_2Et^-]), known as a distillable ionic liquid (DIL), capable of being distilled at temperatures around 130°C under relatively high vacuum. This IL has been shown to successfully dissolve microcrystalline cellulose (MCC) with dissolution times as short as 10 min.[169] The third IL used was a protonated 1,8-diazabicyclo-[5.4.0]-undec-7-ene 2,2,3,3,4,4,5,5-octafluoro-1-pentoxide ([$HDBU^+$][$5OF^-$]). This IL was selected because of its very low viscosity (LVIL), which allows for a better mixing and improvement of the mass transference compared to the high viscosity ILs. Further, the IL pertains more hydrophobic properties, since its anion is a bulky molecule containing fluoride groups, an organic molecule which facilitates its separation from water. Notwithstanding, this IL has not yet been reported in the literature as a biomass pretreatment or as a dissolution solvent. Figure 7-9 illustrates the chemical structure of the ionic liquids utilized in this work. Besides the ionic liquids, DI water and 1.0 vol.% sulfuric acid were used for a comparison.

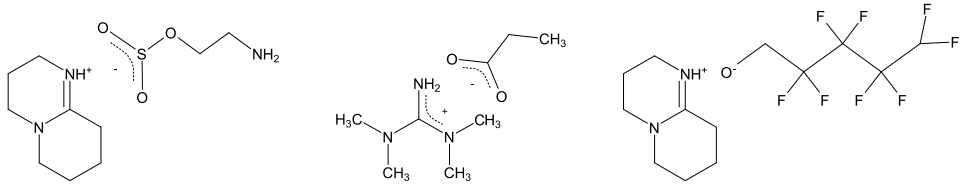

Figure 7-9. Ionic liquids utilized in the processing of green algae.

The results of the dissolution experiments carried out with ionic liquids are shown in Figure 7-10. The different fractions collected after the dissolution process revealed that a minimum of 85 wt.% of the biomass was recovered

either as a residue or as precipitated fractions from the ionic liquid and washing water fractions. Consequently, the mass balance of the process was successfully closed.

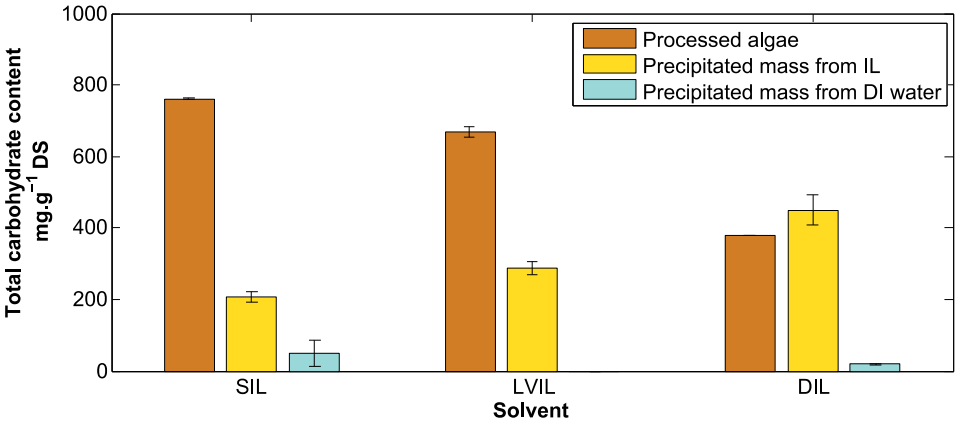

Figure 7-10. The effect of the solvent on the mass balance of the dissolution of Ulva rigida *biomass in ionic liquids at 120°C for 6 h;*
Bars represent the standard deviation of two replicates.

The results from the dissolution experiments show that the ionic liquids dissolved between 24 and 62 wt.% of the *U. rigida* biomass at 120°C for 6 h of reaction. Still, DIL was the best solvent among the ionic liquids used in the experiments in terms of *U. rigida* biomass dissolution, accounting up to 62 wt.% dissolution yield, as observed in Figure 7-10. Interestingly, up to 47 wt.% of the *U. rigida* biomass was recovered from the precipitated fractions when the alga was processed with DIL. Concurrently, SIL and LVIL dissolved only 26 and 29 wt.% of the biomass, while 79 and 66 wt.% of the biomass remained undissolved, respectively. These results show that DIL more efficiently dissolved algal constituents compared to SIL and LVIL, which may be explained for the solvation of cellulose with DIL, indicating its excellent properties of carbohydrate dissolution compared to SIL and LVIL.

According to these results, the dissolution of *U. rigida* biomass in DIL was evaluated at different temperatures in the range of 100–160°C, and the results are presented in Figure 7-11. The yield of the undissolved biomass was observed to decrease with increasing temperature, while the precipitated biomass from the ionic liquid increased at higher temperatures. Evidently, the temperature had a positive effect on the dissolution of algal constituents added to the disruption of the biomass cell wall. In the temperature range of 140–160°C, in the biomass dissolution, the efficiency was the same since the undissolved biomass, and the precipitated fraction from the ionic liquid and the washing water remained relatively stable. In this regard, the fresh and the processed biomasses with DIL at 120°C for 6 h were

also analyzed with transmission electron microscopy (Figure 7-12). The images revealed major biomass disruption in the processed biomass since most of the internal organs were absent and partial disruption of the cell wall was observed.

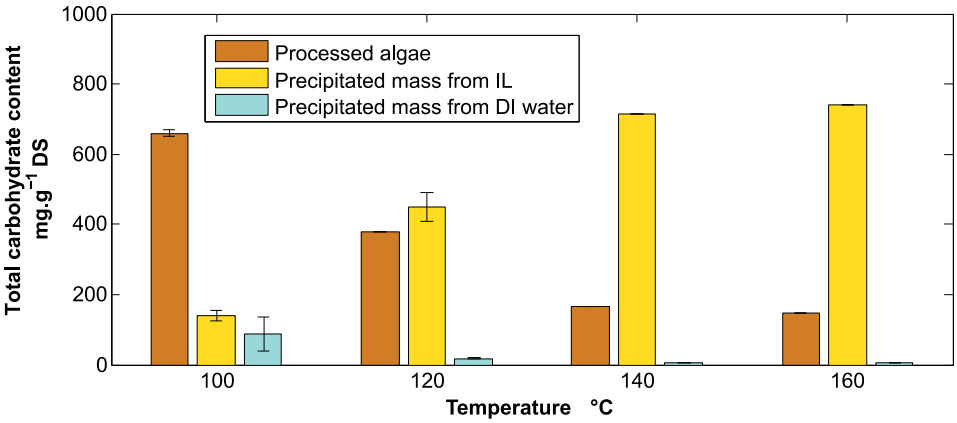

Figure 7-11. The effect of the temperature on the mass balance of the dissolution of Ulva rigida *biomass in DIL;*

Bars represent the standard deviation of two replicates. Only one experiment was performed for temperatures 140 and 160°C, respectively.

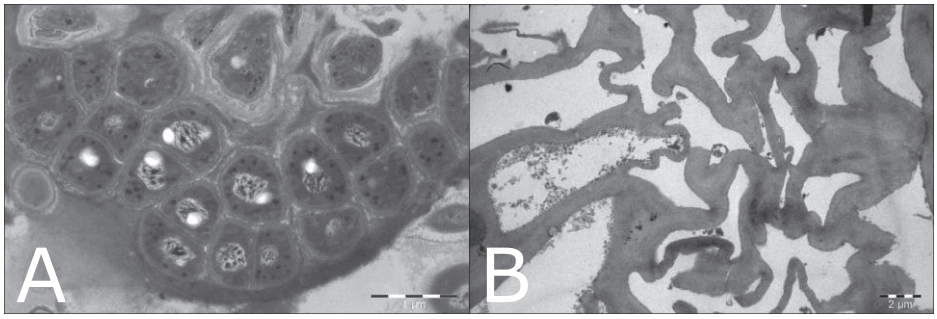

Figure 7-12. Transmission electron microscopy images of U. rigida *samples;*

A: Fresh *U. rigida*. B: Processed *U. rigida* with DIL at 120°C for 6 h

The undissolved and precipitated fractions from DIL obtained after processing of *U. rigida* at 120°C were analyzed through FTIR, resulting in prominent peaks in the bands corresponding to carbohydrates (1160–980 cm^{-1}) and sulfated carbohydrates (950–800 cm^{-1}), shown in Figure 7-13. This last band was especially prominent for the precipitated fraction from DIL, being consistent with the major presence of carbohydrates in this fraction (see Figure 7-14). In the case of proteins (1485–1425 cm^{-1}), more prominent peaks were observed in the undissolved portion rather than in the precipitated fraction from DIL, suggesting that proteins remained mainly in

the undissolved portion, which was consistent with OEA analyses of this fraction (see Figure 7-19).

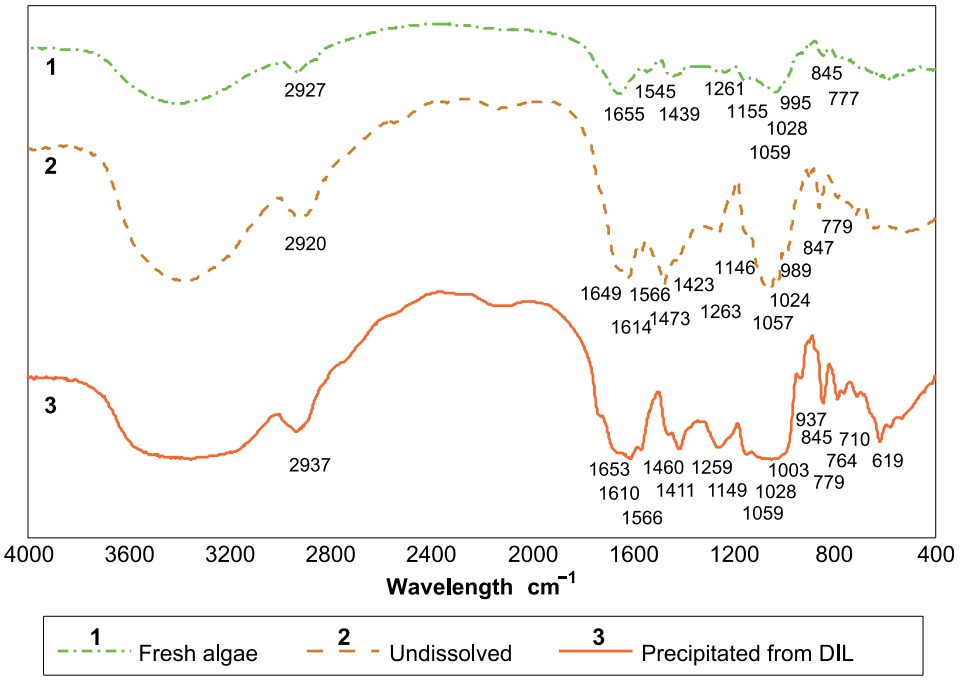

Figure 7-13. FTIR spectra of fresh alga and undissolved and precipitated fractions.

The results of the total carbohydrate dissolution show that the ionic liquids evaluated at 100°C (SIL and DIL) did not dissolve many carbohydrates (Figure 7-14). However, when the temperature was increased to 120°C, a maximum of 248 mg of carbohydrates g^{-1} fresh DS was recovered from the precipitated fractions. The dissolution of carbohydrates was observed to correlate with the dissolution of biomass, as seen in the decrease of the total mass and the total carbohydrate content of the undissolved fraction. However, when the alga was processed at 140 and 160°C, even though a major algal dissolution was observed, the total carbohydrate content of the precipitated fractions from the ionic liquid and the washing water decreased to 229 and 103 mg of carbohydrates g^{-1} fresh DS, respectively. This result confirmed the degradation of carbohydrates, which most probably underwent into sugars and different decomposition products. Interestingly, the use of Milli-Q water and dilute H_2SO_4 dissolved a major share of carbohydrates, since the liquid fraction accounted for 197 and 374 mg of carbohydrates g^{-1} fresh DS, respectively.

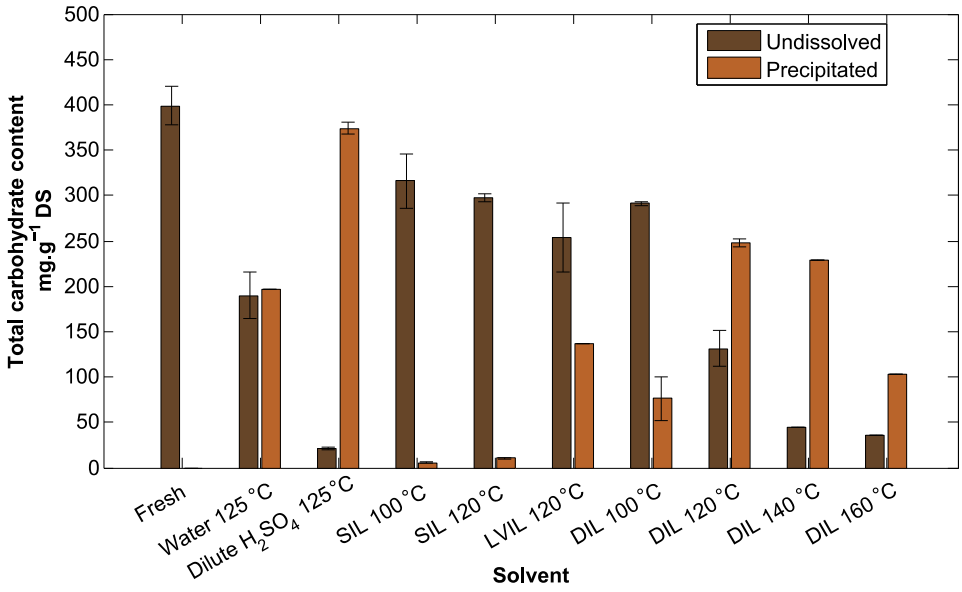

Figure 7-14. Total carbohydrate content in the undissolved and the precipitated fractions from ionic liquid and washing water obtained from the dissolution process;

Description in the abscise represents solvent and temperature in 6 h processing.

The quantification of the glucose and xylose contents in the undissolved and precipitated fraction is shown in Figures 7-15 and 7-16. The glucose content in the precipitated fraction accounted for 128 mg of glucose g^{-1} fresh DS, when the *U. rigida* biomass was processed with DIL at 120°C. Higher temperatures (140 and 160°C) resulted in lower glucose yields, which accounted for 107 and 56.4 mg of glucose g^{-1} fresh DS, respectively. Interestingly, the glucose obtained in the liquid phase of *U. rigida* biomass processed with water at 125°C for 2 h resulted in 30.1 mg of glucose g^{-1} fresh DS. Consequently, glucans showed better solvation properties in DIL compared to the use of water. Water is known to be a poor solvent for cellulose (major constituent in green algae cell wall), while as mentioned earlier DIL is efficient regarding cellulose dissolution. Conversely, dilute H_2SO_4 showed major glucan solubilization since 178 mg of glucose g^{-1} fresh DS was obtained in the liquid fraction, representing a maximum among all the dissolution experiments performed.

Regarding xylose, most of this sugar residue remained in the undissolved fraction when *U. rigida* was processed with deionized water. An analogous trend was observed with DIL. Xylose residues are present both in the ulvan backbone in the ulvanobiose units and in xyloglucans that occur in the cell wall of *Ulva* species. Additional analyses should, however, be performed to the precipitated fraction to study the nature of the extracted xylose.

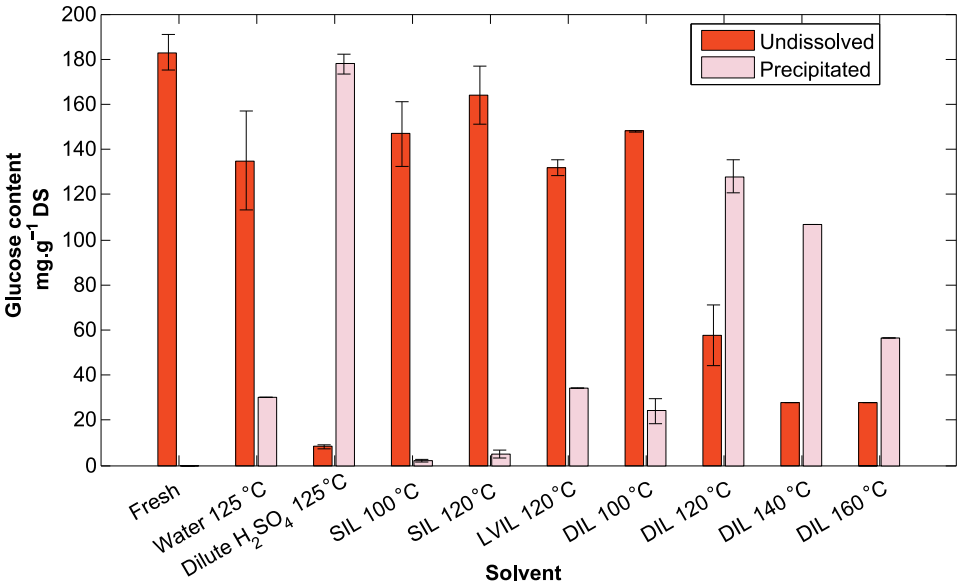

Figure 7-15. Glucose content in the undissolved and precipitated fractions from ionic liquid and washing water obtained from the dissolution process;
Description in the abscise represents solvent and temperature in 6 h processing.

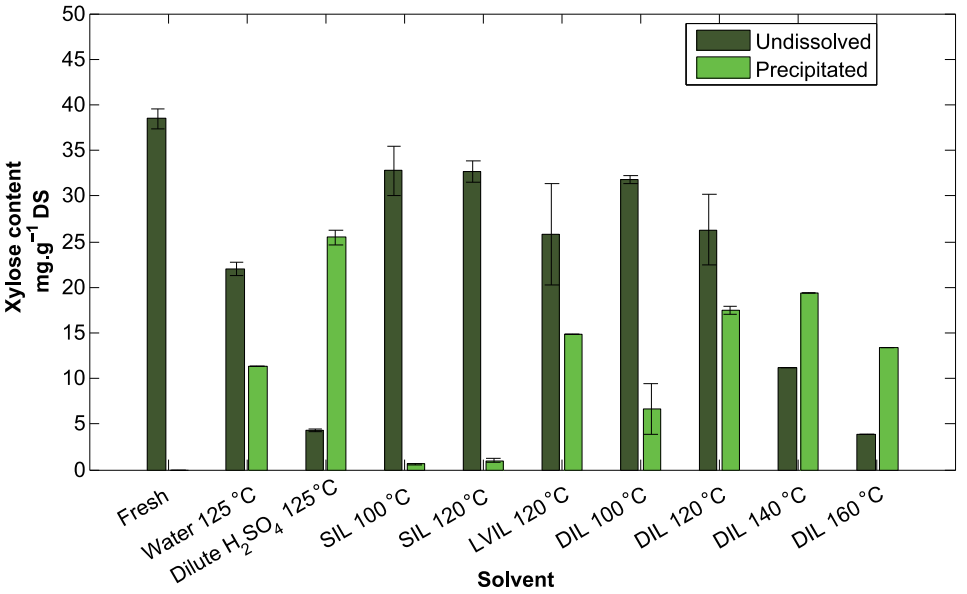

Figure 7-16. Xylose content in the undissolved and precipitated fractions from ionic liquid and washing water obtained from the dissolution process;
Description in the abscise represents solvent and temperature in 6 h processing.

The dissolution yields of the main constituents of ulvan, L-rhamnose, and D-glucuronic acid are shown in Figure 7-17, 18. Both deionized water and dilute

H_2SO_4 solvents dissolved significant amounts of rhamnose with 77.5 and 80.8 mg of rhamnose g^{-1} fresh DS, respectively. In the case of DIL at 120°C, 47.1 mg of rhamnose g^{-1} fresh DS was obtained in the precipitated fractions. Concurrently, a major fraction of glucuronic acid was also dissolved when the biomass was processed with deionized water and dilute H_2SO_4, accounting for 62.0 and 60.4 mg of glucuronic acid g^{-1} fresh DS, respectively. In the case of DIL at 120°C, 38.5 mg of glucuronic acid g^{-1} fresh DS was obtained in the precipitated fractions. Higher temperatures (140–160°C) in the case of DIL resulted in a major dissolution of carbohydrates composed of rhamnose and glucuronic acid, though a slight decrease in the precipitated fraction obtained at 140°C was observed. The extraction carried out at 160°C resulted, on the other hand, in a major degradation of rhamnose and glucuronic acid, since the precipitated fraction accounted only for 15.3 mg of rhamnose g^{-1} fresh DS and 7.7 mg of glucuronic acid g^{-1} fresh DS. Consequently, dilute H_2SO_4 and deionized water were the best solvents for the dissolution of ulvan. However, deionized water selectively dissolved ulvan, while glucans remained mainly in the undissolved fraction. The dissolution yield of ulvan obtained from the processing with deionized water accounted for 96 wt.%, while in the case of glucan the yield accounted for 16 wt.%. In the case of DIL, the dissolution yields of ulvan and glucans were relatively similar, accounting for 60 wt.% of ulvan and 70 wt.% of glucans.

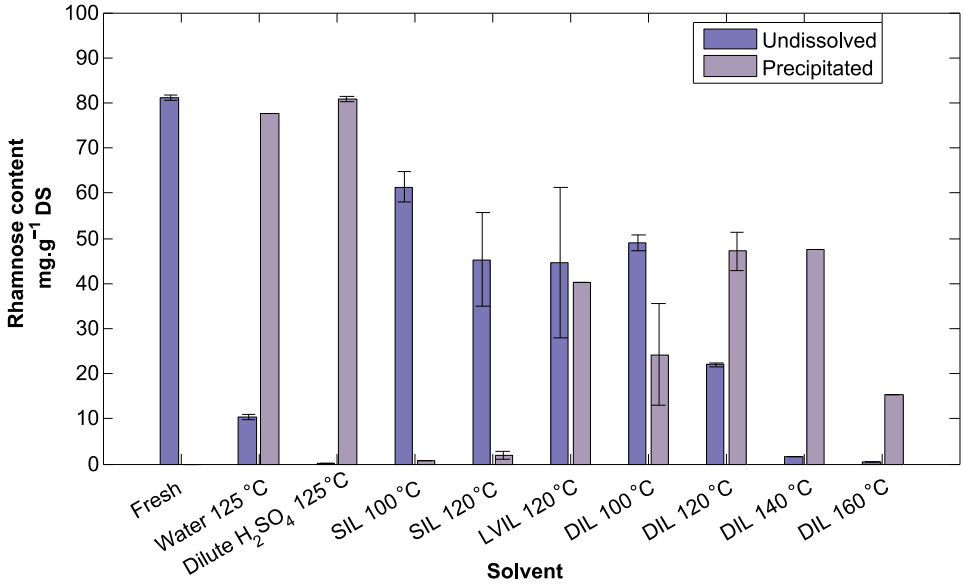

Figure 7-17. Rhamnose content in the undissolved and precipitated fractions from ionic liquid and washing water obtained from the dissolution process; Description in the abscise represents solvent and temperature in 6 h processing.

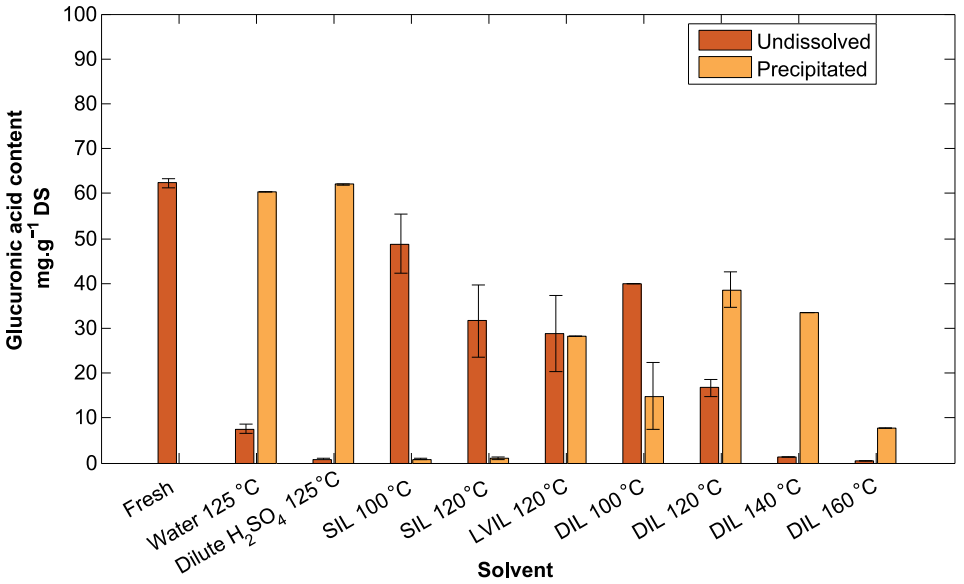

Figure 7-18. Glucuronic acid content in the undissolved and the precipitated fractions from ionic liquid and washing water obtained from the dissolution process;

Description in the abscise represents solvent and temperature in 6 h processing.

The mass balance for the major constituents for the dissolution of *U. rigida* biomass processed with SIL and DIL at 120°C is presented in Figure 7-19. The results show that SIL principally dissolves ashes and chlorophyll, accounting for 132 mg ash g^{-1} fresh DS and 859 µg chlorophyll g^{-1} fresh DS, respectively. Proteins and carbohydrates remained mainly in the undissolved fraction, accounting for 173 mg proteins g^{-1} fresh DS and 297 mg carbohydrates g^{-1} fresh DS, respectively. In the case of DIL, proteins remained mainly in the undissolved fraction, accounting for 106 mg proteins g^{-1} fresh DS, but 65.1 mg proteins g^{-1} fresh DS was observed in the precipitated fraction. It is worth noticing that glucuronan is a type of carbohydrate that is linked to proteins in the cell wall, which can explain the elevated protein content observed in the precipitated fraction. DIL dissolved a major fraction of the ashes as well as a high proportion of chlorophyll, accounting for 113 mg ash g^{-1} fresh DS and 846 µg ash g^{-1} fresh DS, respectively.

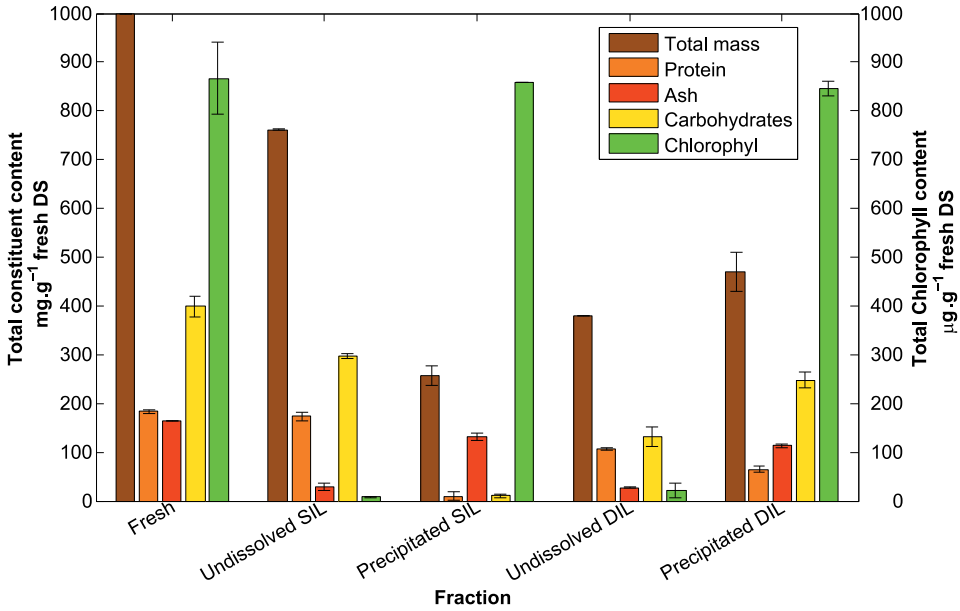

Figure 7-19. Mass balance for the dissolution of Ulva rigida *processed with SIL and DIL at 120°C for 6 h.*

7.3.2 Washing of the alga

Deionized water was selected as the solvent to study the kinetics of the extraction of ulvan, according to the evaluation of the different solvents. The reasons that justify this selection were: Firstly, the high yields obtained based on the extraction of rhamnose and glucuronic acid and; secondly, the high selectivity observed towards the extraction of ulvan constituents compared to polysaccharides containing glucose and xylose residues.

Before the kinetic study of the extraction of ulvan, the washing of the alga was examined to see the amount and type of ashes removed after the treatment. Two types of washing times were evaluated (20 min and 16 h) to compare the effects of a short and a prolonged washing step. The results of the carbohydrate and ash content after the washing of the biomass are shown in Figure 7-20. The removal of ash accounted for 63 and 67 wt.% for the washing performed for 20 min and 16 h, respectively. The salts removed in the washing were most probably residues from the marine nature of the biomass, and not chemically bonded to cell wall constituents. Although the yields for the removal of ashes were similar between the two washings steps, the weight losses reached 19 and 26 wt.% for the washings performed for 20 min and 16 h, respectively. Accordingly, these differences accounted for the loss of carbohydrates that were observed between the two treatments. The 20 min washing step resulted in a removal of 8.6 and 1.7 wt.% of ulvan and glucan, respectively. Conversely, the 16 h washing led to a removal of 20 and

16 wt.% of ulvan and glucan, respectively. Consequently, the 20 min washing step was preferred for the subsequent processing of the alga.

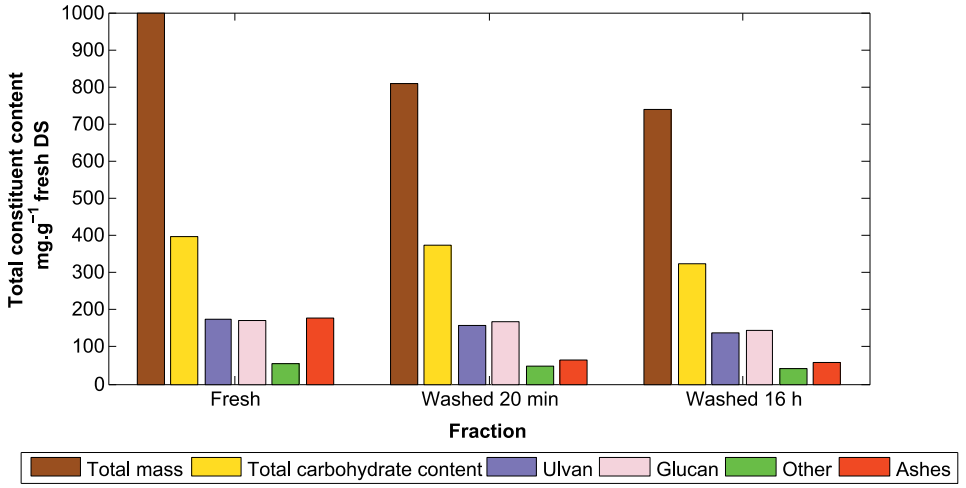

Figure 7-20. The effect of washing on the carbohydrate and ash contents of the alga.

7.3.3 Carbohydrate composition of the ulvan extracts

The kinetics of the aqueous extraction of ulvan from *U. rigida* biomass previously washed for 20 min were studied in the temperature range of 60–130°C for 2 h of extraction. The Figure 7-21 shows the carbohydrate composition of the ulvan extracts obtained after 1 and 120 min of processing at 60 (Figure 7-21-A, B), 90 (Figure 7-21-C, D) and 130°C (Figure 7-21-E, F), respectively. The results indicate that the ulvan content in the extract (rhamnose and glucuronic and iduronic acids) was the highest for the extract, obtained after 120 min at 60°C, accounting for 84 wt.%. Accordingly, the higher the temperature, the lower the purity of the ulvan extract, since the ulvan content in the extracts obtained after 120 min of extraction at 90 and 130°C accounted for 80 and 71 wt.%, respectively. This trend was explained due to the extraction of glucans, which increased from 6 wt.% after 120 min of extraction at 60°C, to 13 and 20 wt.% of glucans after 120 min of extraction at 90 and 130°C, respectively. Consequently, more elevated temperatures facilitated the undesired extraction of glucans.

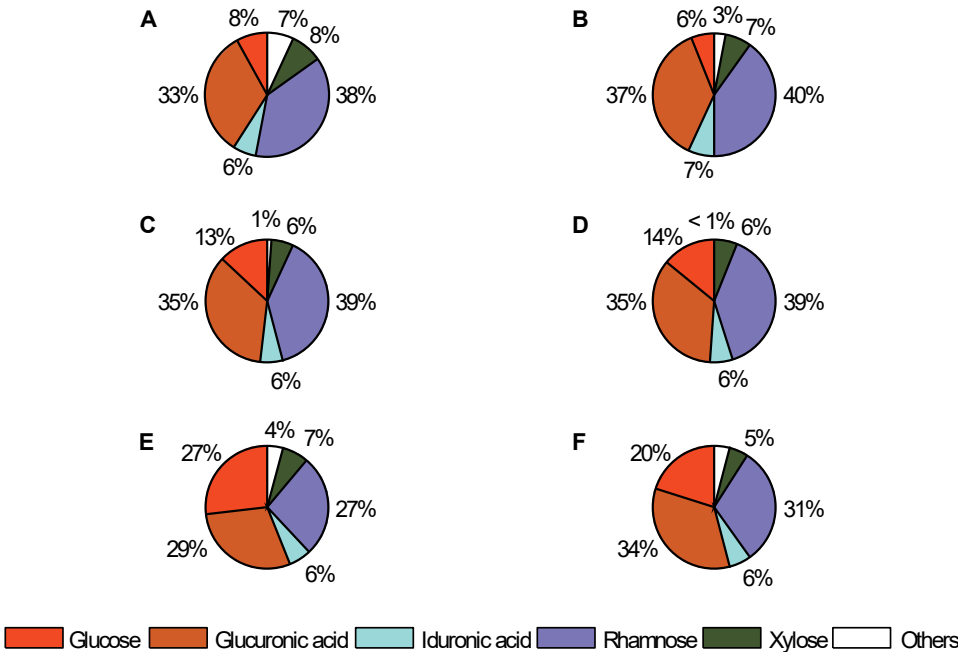

Figure 7-21. The monomer distribution of the ulvan extract obtained at 60–130°C at different sampling times;

Figures show the sugar composition of the extract at A: 60°C–1 min, B: 60°C–120 min, C: 90°C–1 min, D: 90°C–120 min, E: 130°C–1 min, F: 130°C–120 min. Other sugars comprise arabinose, galactose, galacturonic acid, fructose, and mannose.

7.3.4 Molecular size distribution of the extracts

The molecular size distributions of the ulvan extracts for the range of temperature between 60 and 110°C and extraction times in the range of 1–120 min are shown in Figure 7-22. The range of the molecular weight observed in the samples was between 237 and 709 kDa, which is within the range of molecular sizes reported for ulvan by other authors.[50,178] The extraction at 60°C did not release higher molecular weight fractions, although already at 70°C, an increment in the average molecular weight of the extract was observed, reaching values in the range of 550–650 kDa. However, when the temperature was raised to 80°C, the molecular weight distribution of the extract achieved a maximum of 709 kDa and then successively decreased to lower values upon increasing the temperature and extraction time. The trend obtained for the molecular weight in the sequence of ulvan extractions was explained by a partial collapse of the ultrastructure of the ulvan molecule. The ulvan backbone has been reported to have high molecular weight values up to 3,600 kDa.[50] However, the ulvan chains also tend to form aggregates between the fibers due to their necklace-like structure, similar to the one that DNA features, as reported by Robic and co-

workers.[160] Therefore, rather than a partial hydrolysis of ulvan producing shorter molecules, it might also be possible that the molecular weight decreased due to a collapse of this necklace type of ultrastructure of ulvan, resulting in a reduction in the overall molecular weight in prolonged extraction times and elevated temperatures.

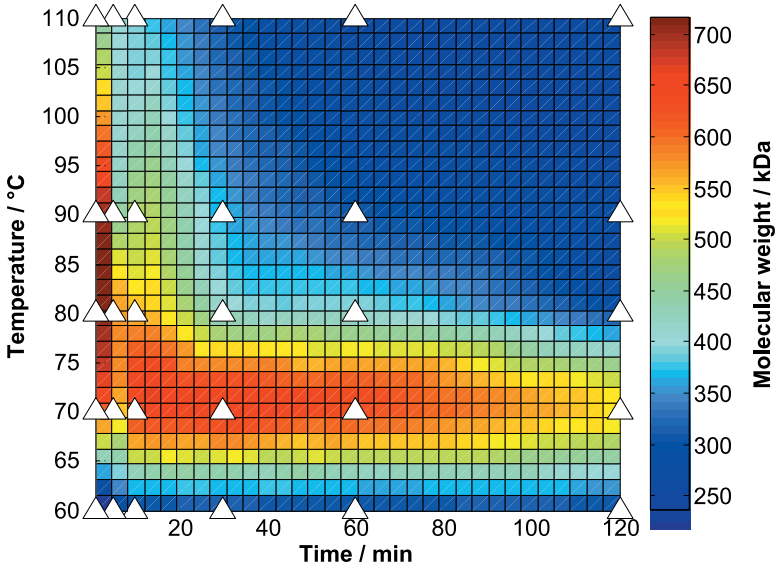

Figure 7-22. Molecular size distribution of the ulvan extracts as a function of time and temperature.

7.3.5 Sulfate content of the extracts

The sulfate content in the ulvan extract obtained by water processing of *U. rigida* at 90°C is illustrated in Figure 7-23. The results indicated that the sulfate content in the extracts increased from 14.9 mg g^{-1} of fresh alga (FA) after 1 min of extraction to 44.4 mg g^{-1} FA after 120 min, accounting for an increment of 41.3 wt.%. Consequently, it was evident that sulfate was co-extracted with rhamnose and glucuronic acid as the main constituents of ulvan. In fact, Lahaye and Ray demonstrated the presence of sulfate groups linked to O3-rhamnose.[185] The sulfate content increased at prolonged extraction times, which was an indication that more sulfate-rich ulvan fractions were extracted at extended times. Therefore, it might be reasonable to suggest that more sulfated ulvan fractions might be more associated with different cations, and consequently more cross-linked within different fibers requiring longer extraction times, as was also observed from the molecular size distribution results. However, more research should be carried out to study the composition of sulfates within the different ulvan fractions to confirm this hypothesis.

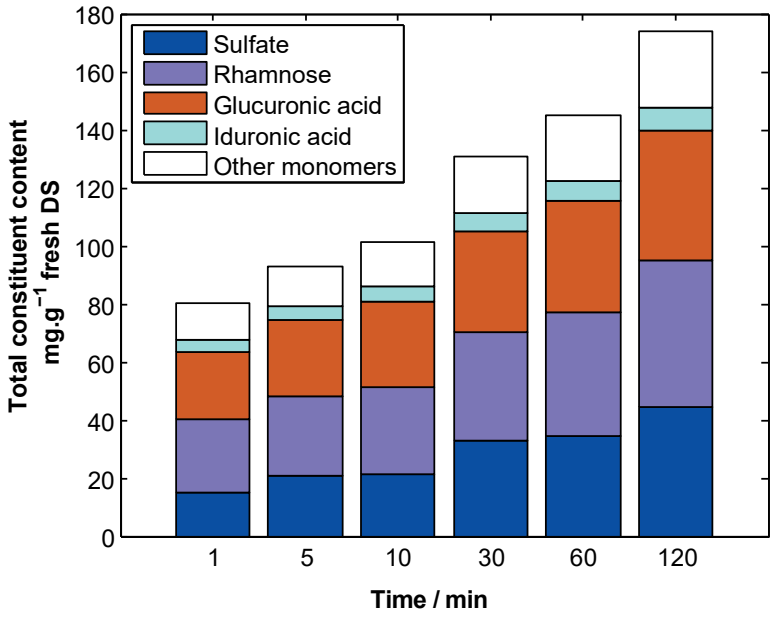

Figure 7-23. Sulfate content in the ulvan extracts obtained at 90°C using water as solvent.

7.3.6 Kinetics of the ulvan extraction

The kinetics for the extraction of ulvan in water in the temperature range of 60–130°C are presented in Figure 7-24. Not surprisingly, the extraction yield of ulvan increased at higher temperatures, which is logical in terms of the energy required to extract higher molecular weight fractions. The maximum yield of ulvan was 97.6 wt.% after 2 h of treatment at 130°C. In the case of rhamnose, glucuronic and iduronic acids, the yields were 99.8, 96.9 and 92.1 wt.% after 2 h of extraction at 130°C, respectively. These results are consistent with those reported in the open literature for the extraction of ulvan from different algae among the *Ulva* genera.[50,160,178,180,186–193]

The extraction of ulvan in the temperature range of 60–80°C was relatively slow, with a maximum yield of 40 wt.%. Even though the extraction kinetics was slow, the average molecular weight of the ulvan fractions extracted in the range of temperatures of 60–80°C was higher, as discussed in section 7.3.4. Successively, the largest increase in the extraction of ulvan was attained when the temperature was raised from 80 to 90°C. The extraction of ulvan at 90°C was enhanced 1.4 fold compared to that at 80°C, and 3.3 fold compared to the one at 60°C. This result suggested that there was a fraction relatively easy to be extracted during the very first contact of the fibers with water at 90°C and higher temperatures. After the initial rapid extraction within 1 min, the reaction rate appeared to be slower, suggesting that there might be higher molecular weight fractions that take a longer time

to be extracted compared to the extraction of shorter fractions. In this regard, different molecular weight fractions of the ulvan extract have been observed by other authors,[178] which may eventually have different kinetic behavior upon extraction.

Consequently, there was a distinct advantage in using temperatures above 90°C, since there was a boost in the extraction of ulvan. Robic and coworkers demonstrated the aggregation of ulvan into bead-like structures, and they also suggested that different cations, such as calcium or borate, allow these beads to agglomerate. Within the cell wall, these structures may form a gel-like structure linked by fiber-like material, such as ulvan, proteins or glucuronan.[160] This gel-like structure occurring in the cell wall may eventually collapse at a certain threshold temperature, and this phenomenon explains the difference observed between the extraction at 80 and 90°C. This hypothesis should be closer evaluated with additional experiments in future work. Henceforth, the kinetic modeling of this data was performed only for the period after 1 min of ulvan extraction, since it was clear that different kinetic behaviors were observed in the initial stages at the threshold value of 90°C and over.

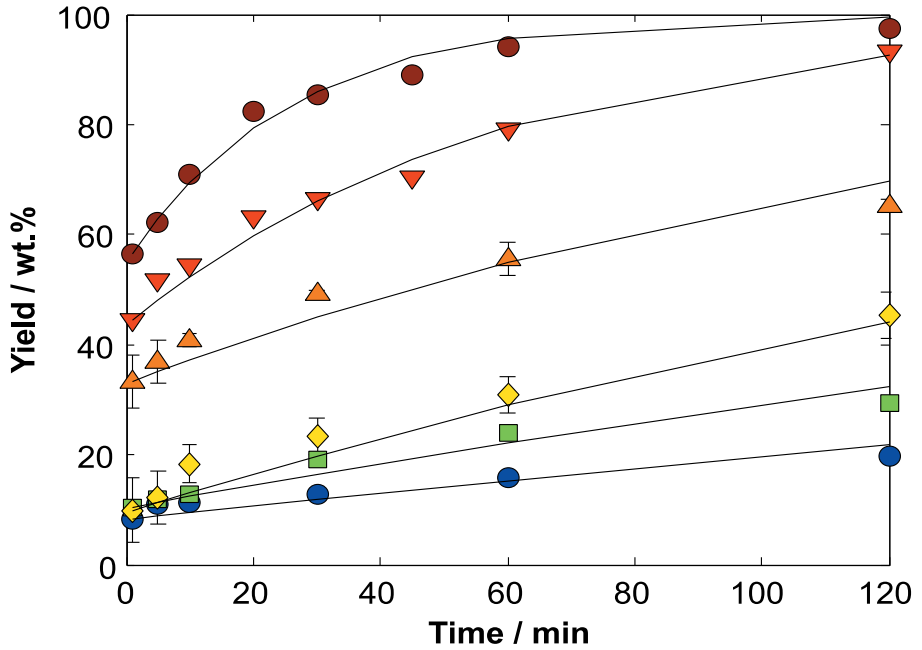

Figure 7-24. The extraction kinetics of ulvan in deionized water;
Ulvan was calculated as the sum of rhamnose, iduronic acid, and glucuronic acid residues. Lines represent the kinetics predicted by the model. Symbols: ● 60°C, ■ 70°C, ◆ 80°C, ▲ 90°C, ▼ 110°C and ● 130°C.

The correlation between the extraction yields of different monomers in the extraction of ulvan in water is depicted in Figure 7-25. The results showed that the yields of rhamnose and glucuronic acid increased at the same rate, obtaining a degree of explanation R^2 of 0.98 for this linear trend. Similar results have been achieved with the extraction yields of rhamnose and iduronic acid. It was evident that these three units were extracted at a similar rate in the temperature range of 60–130°C evaluated in this work. Interestingly, the xylose yields also showed a relatively high correlation with the extraction yields of rhamnose, which can be explained by its minor occurrence in the structure of ulvan (ulvanobiose dimer). Regarding glucose, a low correlation between the extraction yield of glucose with the extraction of the ulvan constituents was observed. This result was evident, since glucose is not a major unit in the structure of ulvan, and its occurrence is more related to the extraction of xyloglucans and cellulose.

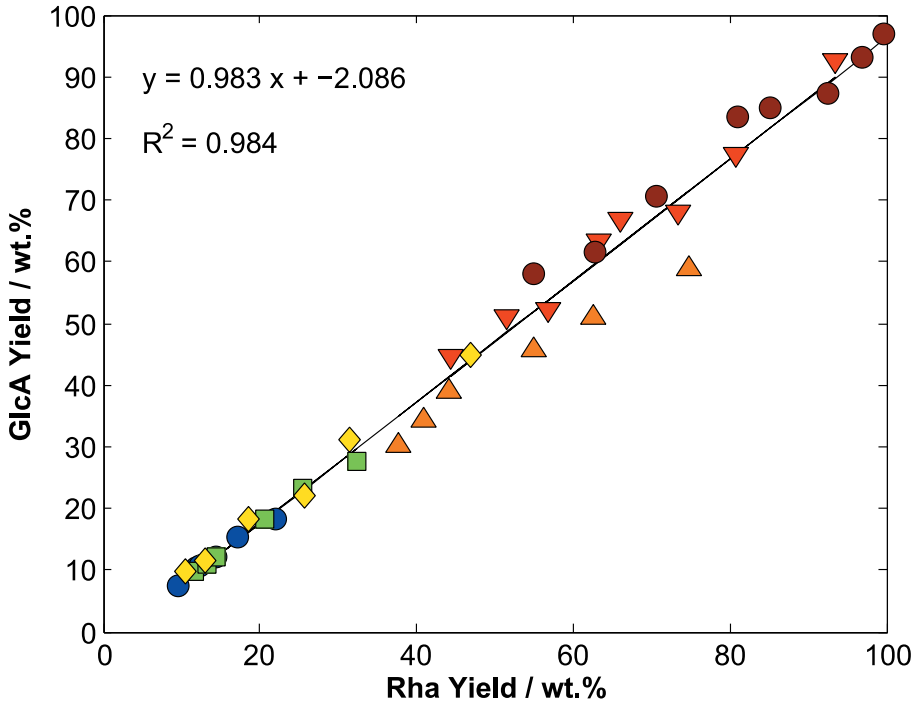

Figure 7-25. The correlation of the extraction yield for rhamnose vs. glucuronic acid using deionized water as solvent;

Symbols: ● 60°C, ■ 70°C, ◆ 80°C, ▲ 90°C, ▼ 110°C and ● 130°C.

7.4 Hydrolysis of marine carbohydrates [IV], [V]

The hydrolysis of marine carbohydrates was studied following two approaches: the first was the conventional hydrolysis of brown algae by use of enzymatic saccharification; and the second, hydrolysis of green algae using mineral acids and heterogeneous catalysis.

7.4.1 Enzymatic saccharification of brown algae

The enzymatic saccharification of the brown algae *M. pyrifera* was evaluated at different pH, temperatures, and pretreatments. The effect of these conditions on the hydrolysis yield was quantified according to the amount of D-glucose and uronic acids per g of fresh algae.

7.4.1.1 The effect of pH and temperature on the enzymatic hydrolysis of brown algae

The effect of the pH and the temperature on the liberation of glucose and uronic acids in the enzymatic hydrolysis of *M. pyrifera* pretreated with distilled water at 120°C for 60 min is shown in Figure 7-26. Not surprisingly, the highest conversion of *M. pyrifera* biomass into glucose was obtained at pH 5.2 and 50°C, accounting for 25.5 mg of glucose g^{-1} DS. This value of pH and temperature was within the range at which the activity of cellulases reaches a maximum, as described by many authors.[69,105,120,194,195] In turn, the enzymatic hydrolysis carried out with alginate lyases, and oligoalginate lyases achieved a maximum at pH 7.5 and 37°C, releasing 110 mg of uronic acids g^{-1} DS. Consequently, the optimum pH and temperatures at which the hydrolytic cellulases and alginate lyases maximize the release of glucose and uronic acids, respectively, differ importantly. Therefore, the enzymatic hydrolysis of both carbohydrates cannot be carried out simultaneously, and neutralization steps are required to perform the saccharification of the main carbohydrate constituents of the brown algae cell wall.

The main reason for such a difference in the conditions at which the activities of the enzymes are maximized, is the nature of the proteins that take part in these enzymatic cocktails. Consequently, nature has developed enzymes capable of the degradation of polysaccharides according to the environment where microorganisms and the substrate occurs. While cellulose occurs both in marine and terrestrial environments, alginate occurs exclusively in marine organisms. Additionally, the saccharification mechanism (hydrolytic for most of the cellulases and lytic for alginate lyases) is another reason behind why the operating conditions for the maximization of the release of sugars differ between cellulose and alginate. In a chemical process, it would be appreciated if these biocatalysts operated at similar conditions. Consequently, the research should focus on finding enzymes capable of working in all environments alike.

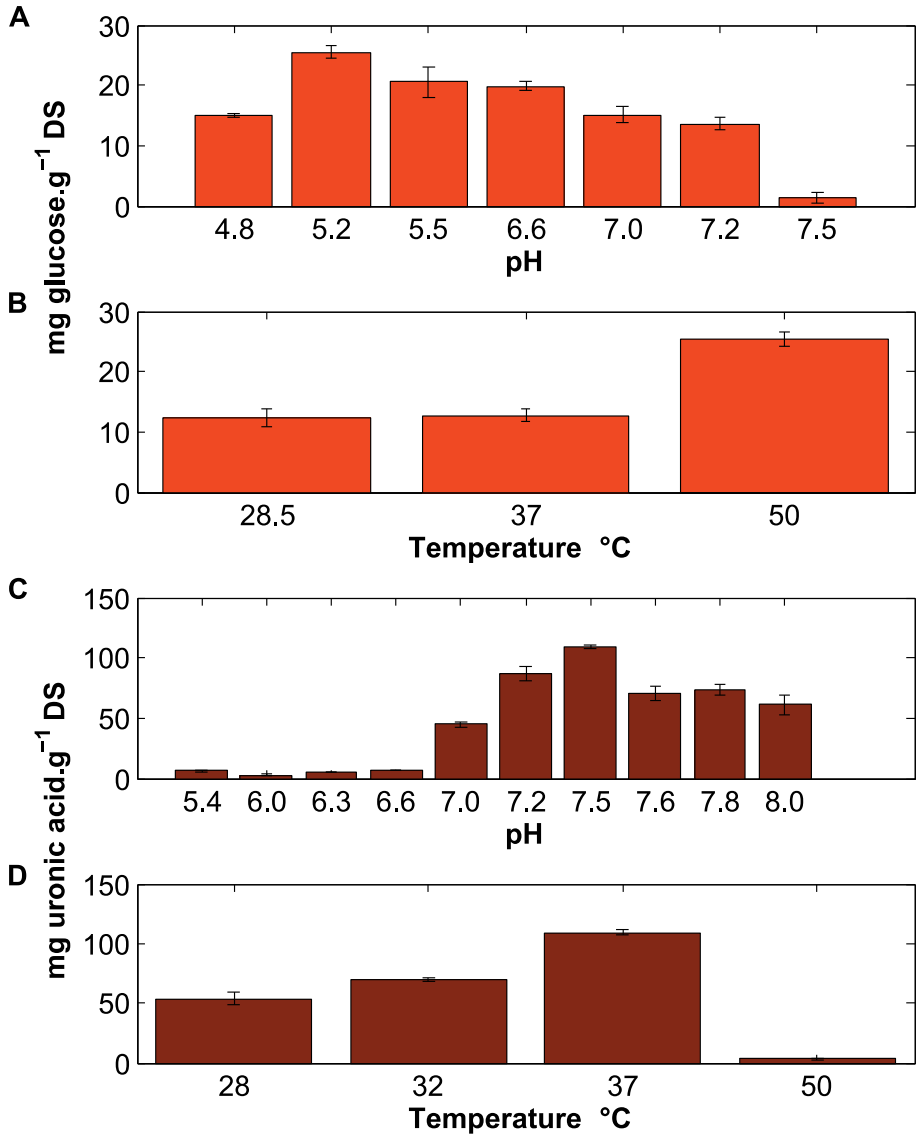

Figure 7-26. The effect of the pH and temperature on the saccharification of M. pyrifera*.*

The effect of pH on the enzymatic hydrolysis with A: cellulases, C: alginate and oligo alginate lyases. The effect of the temperature on the enzymatic hydrolysis with B: cellulases, D: alginate, and oligo alginate lyases.

7.4.1.2 The effect of the pretreatment on the enzymatic saccharification

The effect of the different pretreatments utilized on the enzymatic saccharification with cellulases and alginate and oligoalginate lyases in terms

of the concentration of monomers is illustrated in Figure 7-27. The results show that the pretreatment is required to efficiently depolymerize both cellulose and alginate, since only 5.2 mg of glucose g^{-1} DS and 41.4 mg of uronic acids g^{-1} DS were released upon the saccharification of the fresh non-pretreated biomass.

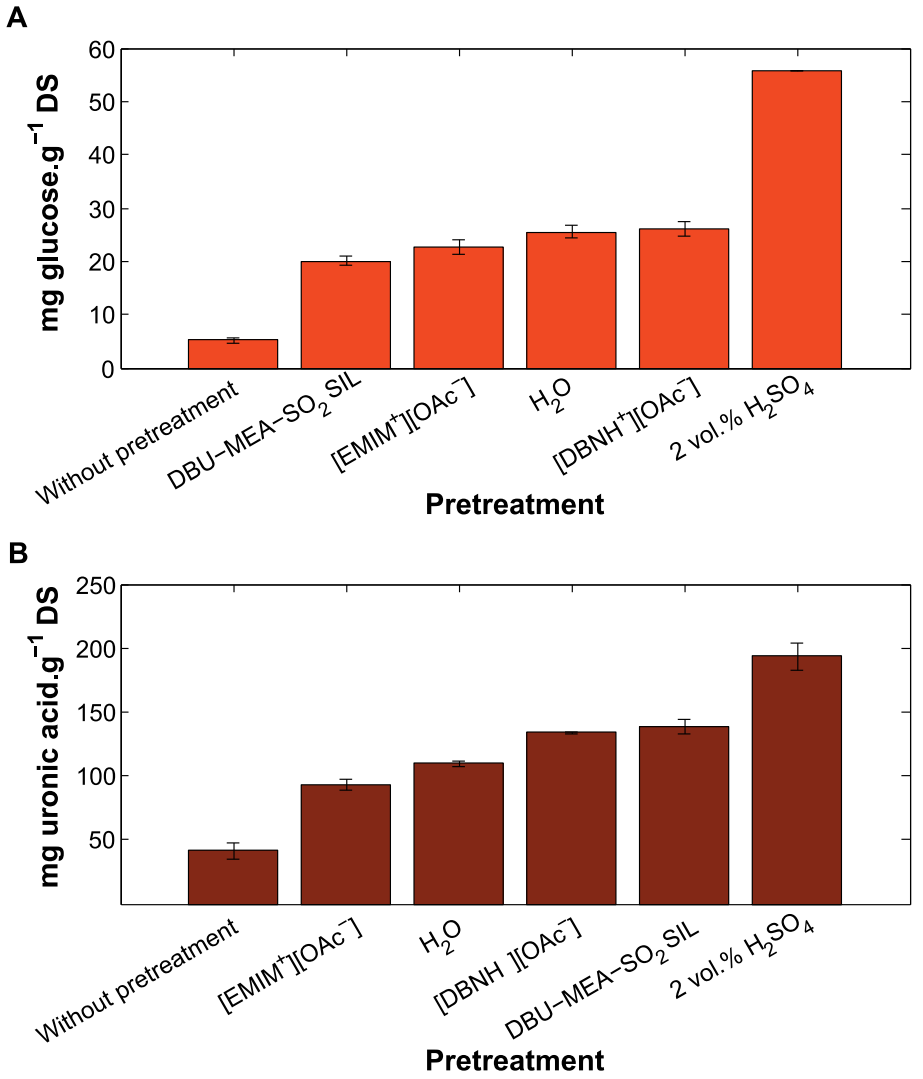

Figure 7-27. The effect of the pretreatment on the saccharification of M. pyrifera *pretreated with different solvents at 120°C for 1 h.*

A. Enzymatic saccharification with cellulases. B. Enzymatic saccharification with alginate and oligoalginate lyases.

The best pretreatment was the 2 vol.% H_2SO_4 which attained 55.7 mg of glucose g^{-1} DS and 194 mg of uronic acids g^{-1} DS in the saccharification with

cellulases and alginate lyases, respectively. These values represented an 11- and 4.7-fold increments in the saccharification yield of cellulose and alginate, respectively. However, there was a clear difference in the enzymatic saccharification yields upon the ionic liquids pretreatments. The ionic liquid [$DBNH^+$][OAc^-] was the second best pretreatment for the enzymatic saccharification of cellulases, accounting for 26 mg of glucose g^{-1} DS. This ionic liquid is known to be a good solvent for cellulose, since it allows for decreasing the crystallinity of cellulose and the consequent enhancement of the enzymatic saccharification with cellulases.[196] Still, this ionic liquid was better than DBU-MEA-SO_2, which is known to disrupt lignocelluloses dissolving lignins.[117,118] In this regard, sodium alginate is known to be soluble at pH around 10, similarly to Kraft pulping conditions for the removal of lignins. Such similarities raise the idea that ionic liquids, such as DBU-MEA-SO_2, are more suitable for the solubilization of alginate. The pretreatment of *M. pyrifera* with DBU-MEA-SO_2 resulted in being the second best pretreatment upon the enzymatic saccharification with alginate and oligoalginate lyases, attaining 139 mg of uronic acids g^{-1} DS. Consequently, DBU-MEA-SO_2 may have been a better solvent for the solubilization of alginate compared to the rest of the solvents tested in this work.

Literature about pretreatments for the saccharification of alginate is scarce. Still, the development of enzymes capable of fully hydrolyzing alginate into guluronic and mannuronic acid units has not been completely achieved. *Laminaria japonica* was pretreated with 0.06 wt.% H_2SO_4 at 170°C for 15 min and subsequently saccharified using alginate lyase, accounting for a 28 wt.% yield based on the uronic acid content of the algae.[197] In this work, a high-yield of 86 wt.% was obtained, although both alginate and oligoalginate lyases were used for fully hydrolyzing alginate.

The high yields achieved with 2 vol.% H_2SO_4 are presumably due to the cleavage of bonds that interconnect the biomass constituents in nature. In this regard, the susceptibility of the β-1,4-glycosidic bond in cellulose to hydrolysis catalyzed by sulfuric acid is well documented. Concerning alginate, the degradation of this polysaccharide at pH below 2 has also been reported by different authors.[144,145,198] Consequently, it is expected that 2 vol.% H_2SO_4 results in a good pretreatment for the saccharification of both cellulose and alginate, due to the disassembly of the cell wall constituents. However, the use of acids raises environmental concerns, and requires neutralization of the downstream process which makes this alternative unlikely to be industrially utilized. Accordingly, a more environmentally friendly method would be preferred to carry out the pretreatment before the saccharification of brown algae polysaccharides; however, challenges upon the selection of the right solvent and the development of enzymes capable of being coupled to the same saccharification process for the digestion of the different brown algae constituents remain open for optimization.

7.4.2 Chemical hydrolysis of green algae

Rhamnose is a high-value compound used in the cosmetic industry, although the availability of rhamnose-rich raw materials is scarce. In this regard, the green algae containing the polysaccharide "ulvan" becomes an interesting source to produce rhamnose. Consequently, it is of great importance to efficiently hydrolyze ulvan into its main constituents. Both the biochemical and the chemical routes for the hydrolysis of ulvan remain still unexplored.

The hydrolysis of ulvan was studied in this work using both heterogeneous and homogeneous catalysts. Sulfonated resins, such as *Amberlyst™* 70 and *Smopex*® 101, were used as heterogeneous catalysts, while hydrochloric acid was used as the homogeneous catalyst. *Amberlyst™* 70 is a macroporous resin consisting of polystyrene which is functionalized with sulfonic acid groups. This resin is commercialized in the form of beads of around 0.55 mm size, exhibiting a surface area of 36 m^2 g^{-1}, 200 Å pore diameter, and 2.55 mmol H^+_{eq} g^{-1} acidity. In turn, *Smopex*® 101 is a nonporous resin consisting of a polyethylene-graft polystyrene matrix, also functionalized with sulfonic acid groups. This resin is commercialized in the form of fibers with an acidity of 3.2 mmol H^+_{eq} g^{-1}.

The hydrolysis of the green alga was studied following a one-pot processing, where the alga was treated in the same pot with the catalysts. Additionally, different acidities and temperatures in the range of 4.3-100 mM H^+_{eq} and 90-120°C, respectively, were evaluated.

7.4.2.1 The effect of the acidity on the hydrolysis of the alga

The kinetics of the hydrolysis performed at 90°C with the acidity in the range of 4.3–100 mM H^+_{eq} were observed to be very slow. Figure 7-28 shows that the monomer yield of rhamnose accounted for 23 wt.% after 96 h of processing with A70 at 90°C and 100 mM H^+_{eq} acidity. In turn, the monomer yield of rhamnose accounted for 62 wt.% after 96 h of processing with HCl at 90°C and 100 mM H^+_{eq} acidity. Additionally, the carbohydrate yield of rhamnose in the treatment at 90°C and 4.3 mM H^+_{eq} acidity was much faster than the hydrolysis of the ulvan backbone, since 81 and 99 wt.% of rhamnose were attained after 2 and 48 h of processing, respectively. Consequently, it was evident that the pore structure of A70 hindered the hydrolysis of ulvan, since rapid extraction and slow hydrolysis kinetics were observed. Conversely, the kinetics of the one-pot hydrolysis of the alga with hydrochloric acid was faster than with A70, also supporting the suggestion that mass transfer limitations occurred in the case of the heterogeneous catalyst.

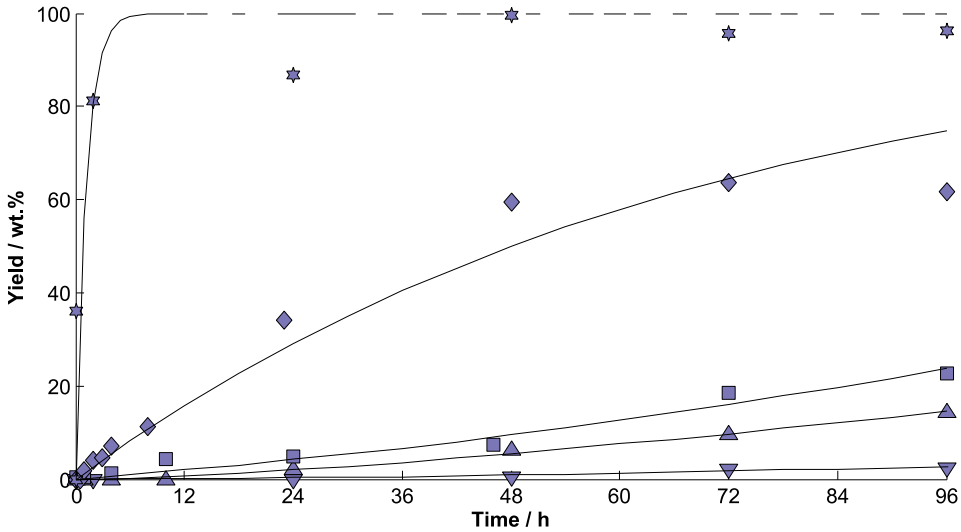

Figure 7-28. The effect of the acidity on the rhamnose yield of the hydrolysis of the alga;

The results are expressed in monomer yield of rhamnose wt.% unless otherwise indicated. Symbols: ▼ A70–4.3 mM H^{+}_{eq}, ✸ A70–4.3 mM H^{+}_{eq} (total rhamnose content: monomers + oligomers), ▲ A70–12.9 mM H^{+}_{eq}, ■ A70–100 mM H^{+}_{eq}, ◆ HCl–100 mM H^{+}_{eq}. Lines represent a mathematical model.

7.4.2.2 The effect of type of catalyst and reusability on the hydrolysis of the alga

The effect of the type and reusability of the catalyst on the monomer yield of rhamnose and glucuronic acid are shown in Figure 7-29. In the case of A70, the rise of the temperature from 90 to 120°C improved the monomer yield of rhamnose, which accounted 52 wt.% after 24 h. This boost in the yield of rhamnose represented a 16 fold increase compared to the yield obtained at 90°C after 24 h at the same acidity (100 mM H^{+}_{eq}, 3.3 wt.% yield). In turn, when the alga was processed with S101 at 100 mM H^{+}_{eq} acidity and 120°C, a rhamnose yield of 89 wt.% was attained, representing a 1.7-fold increase compared to A70 under similar conditions. This increase in the yield was explained by the non-porous and fibrous structure of S101, which reduced the mass transfer limitations for oligomers to access the catalytic sites of the catalyst. Regarding the glucuronic acid, the monomer yield was very low for both catalysts, which was an indication of degradation of this monomer. As to the reusability of the catalysts, it was clear that the yields attained were much lower than those obtained with the fresh catalysts. In the case of S101, the reuse of the catalyst at 120°C reduced the rhamnose yield to 42 wt.%, while in the case of A70 the yield was reduced to 6.6 wt.%. Consequently, the catalytic activity of the reused catalysts was severely hindered under the operating conditions.

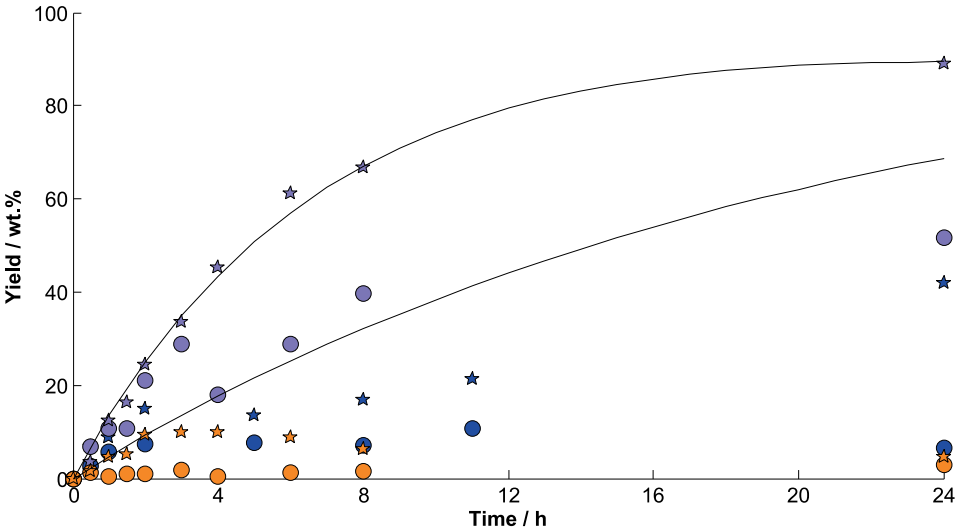

Figure 7-29. The effect of the catalyst on the monomer yield in the hydrolysis of the alga;

Hydrolysis of the alga using A70 and S101 at 100 mM H^{+}_{eq} acidity at 120°C. Results are expressed in monomer yield wt.%. Symbols: ● Rha, ● GlcA, A70–100 mM H^{+}_{eq}, ★ Rha, ★ GlcA, S101–100 mM H^{+}_{eq}, ● Rha, A70–100 mM H^{+}_{eq} (reused), ★ Rha, S101–100 mM H^{+}_{eq} (reused). Lines represent a mathematical model.

7.4.3 Chemical hydrolysis of the ulvan extract

The hydrolysis of the pre-extracted ulvan was carried out to obtain L-rhamnose and D-glucuronic acid as the main products in the hydrolysate. While the concept of one-pot extraction hydrolysis provided by the in-situ hydrolysis has positive aspects, such as making the process economically more feasible by reducing the number of steps for obtaining the final product. The presence of ash, proteins, and lipids may also contaminate the reaction medium and the catalyst. Otherwise, although the pre-extraction of ulvan results in an additional step, it has the advantage of working with a purer polysaccharide mixture (mainly L-rhamnose and D-glucuronic acid), leaving most of the cellulose in the treated biomass (spent solid) for further processing.

7.4.3.1 Homogeneous hydrolysis of the ulvan extract

The results of the homogeneous hydrolysis of the ulvan extract are presented in Figure 7-30. The results show that the kinetics is heavily dependent on the temperature. After 8 h of processing at 110°C, the maximum yield of rhamnose was 80 wt.%, while the glucuronic acid yield reached 40 wt.%. The kinetics show that rapid decomposition of the monomers occurred at 110°C, especially in the case of glucuronic acid. The HPLC chromatograms also showed the presence of low molecular weight organic acids and furfural

compounds in the hydrolyzate. The presence of these compounds may have triggered the degradation of rhamnose which was also observed in the kinetic curves (Figure 7-30-A).

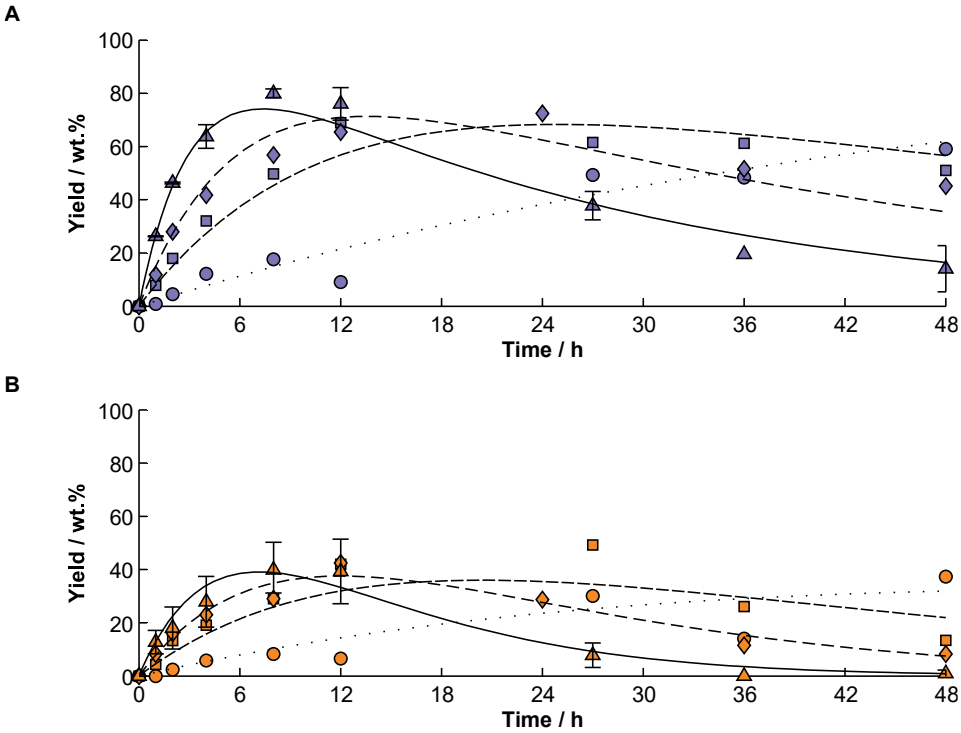

Figure 7-30. The effect of the temperature on the homogeneous hydrolysis kinetics of the ulvan extract;

Hydrolysis of ulvan extract performed with HCl at 100 mM H^{+}_{eq} acidity in the temperature range of 90–110°C. Data is expressed in monomer yield. A. Rha, B. GlcA. Symbols: ● Rha, ● GlcA at 90°C, ■ Rha, ■ GlcA at 100°C, ◆ Rha, ◆ GlcA at 105°C and ▲ Rha, ▲ GlcA at 110°C. Lines represent mathematical modeling of the kinetics.

7.4.3.2 Heterogeneous hydrolysis of the ulvan extract

The results of the heterogeneous hydrolysis of the ulvan extract are illustrated in Figure 7-31. The kinetics are heavily dependent on the temperature, since noticeable differences were observed in the rhamnose yields after 7 h of processing, accounting for yields of 6.1, 34 and 74 wt.% at the temperatures 100, 110 and 120°C, respectively. The maximum yields of rhamnose, around 80 wt.% were reached at 110 and 120°C after 48 h and 12 h of reaction, respectively. In this regard, the processing at 120°C benefited not only from faster kinetics, but also form faster degradation of the products, represented by the decrease in the rhamnose yield after 12 h. In turn, the processing at 110°C gave rise to slower kinetics, but not an evident

degradation of rhamnose. Regarding glucuronic acid, the yields were meager in all the evaluated conditions which were an indication of its severe deterioration. The most abundant repeating unit in the ulvan backbone is the ulvanobiuronic type A disaccharide, which comprises one unit of rhamnose and glucuronic acid, respectively. The cleavage of the glycosidic bond of the ulvan backbone should result in the release of rhamnose and glucuronic acid units in a molar ratio relatively close to 1:1. Due to the major difference observed in the yield of rhamnose and glucuronic acid, these results evidenced that glucuronic acid undergoes degradation under the conditions evaluated in this work.

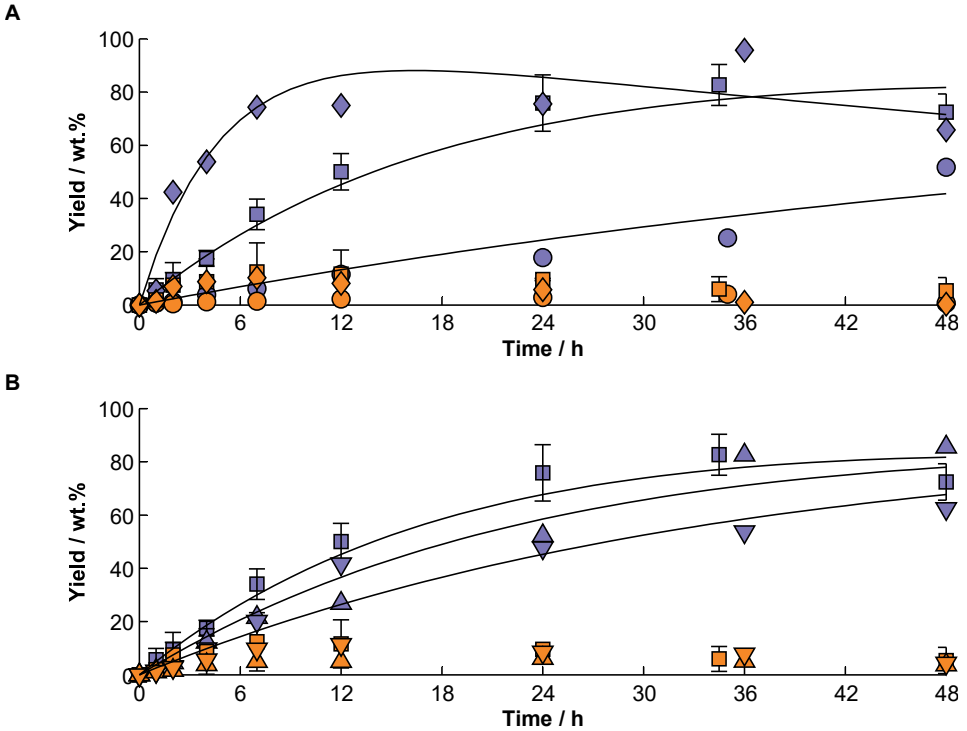

Figure 7-31. The effect of the temperature and acidity on the hydrolysis kinetics of the ulvan extract with S101;

The data are expressed in monomer yield. A. Temperature effect, B. Acidity effect. Symbols: ● Rha, ● GlcA at 100 mM H^+_{eq} and 100°C, ■ Rha, ■ GlcA at 100 mM H^+_{eq} and 110°C, ◆ Rha, ◆ GlcA at 100 mM H^+_{eq} and 120°C, ▼ Rha, ▼ GlcA at 50 mM H^+_{eq} and 110°C and ▲ Rha, ▲ GlcA at 75 mM H^+_{eq} and 110°C. The lines represent mathematical modeling of the kinetics.

The concentration of furfural and 5-hydroxymethylfurfural (HMF) in the hydrolyzate obtained with S101 at 100 mM H^+_{eq} acidity and 120°C is depicted in Figure 7-32. The concentration of furfural reached 25 mg L^{-1} after 24 h of reaction, while the concentration of HMF reached 3.0 mg L^{-1} after 48 h of

treatment. The increase in the concentration of these two compounds was in line with the decrease of the same for glucuronic acid, which accounted 3.8 mg L^{-1} after 48 h of reaction (0.28 wt.% yield).

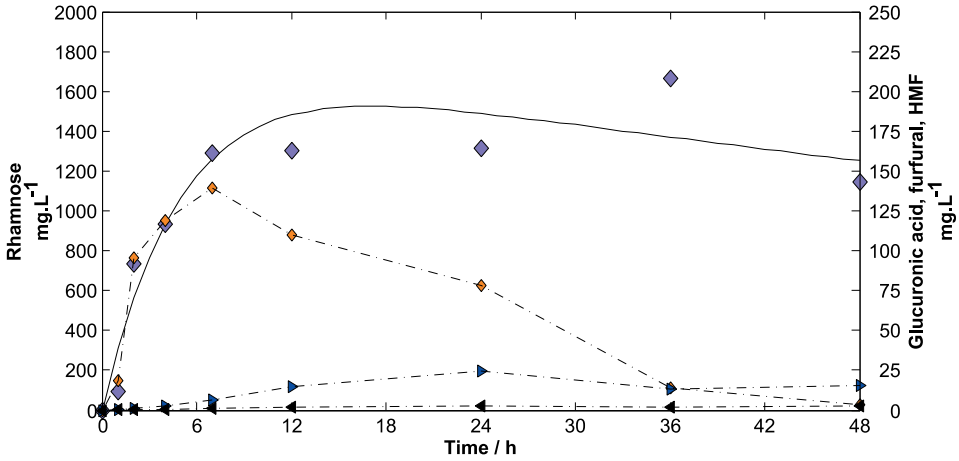

Figure 7-32. The concentration of furfural and 5-hydroxymethylfurfural in the hydrolysis of ulvan extract with S101 with 100 mM H^{+}_{eq} at 120°C;

Hydrolysis of ulvan extract performed with S101 at 100 mM H^{+}_{eq} acidity and 120°C. The data are expressed in concentration mg L^{-1}. The concentration of rhamnose is plotted on the left axis, whereas the concentrations of glucuronic acid, furfural and hydroxymethylfurfural are plotted on right axis. Symbols: ◆ Rha, ◆ GlcA, ▶ furfural and ◀ HMF. The solid line represents mathematical modeling of the kinetics, while dash-dot lines account for the trend of the data.

When comparing the results obtained in the homogeneous and heterogeneous catalysis of the hydrolysis of the ulvan extract, it was evident that the homogeneous catalysis benefited from faster kinetics compared to the heterogeneous catalysis. The maximum rhamnose yield of 81 wt.% was achieved after 8 h of processing with HCl, whereas the treatment with S101 gave the highest yield of rhamnose of 82 wt.% after 35 h, as shown in Figure 7-33. Consequently, external mass transfer limitations due to the fibrous nature of S101 cannot be avoided. In the case of the processing with HCl, the uronic acid molecule appeared to be more stable compared to the treatment with S101, since a maximum yield of 40 wt.% was attained with HCl compared to 12 wt.% yield obtained with S101. Accordingly, it was evident that the ionic resin favored the degradation of uronic acids.

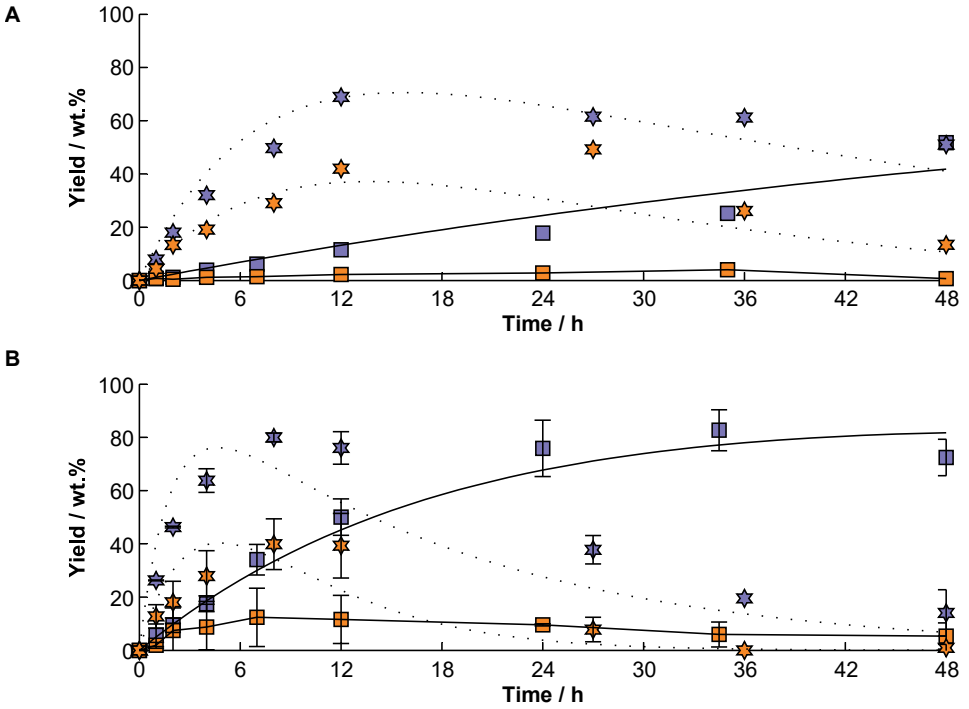

Figure 7-33. Comparison of the homogeneous and heterogeneous catalysis ulvan hydrolysis;

The data are expressed in yield wt.%. A: 100°C, B: 110°C. Symbols: ★ Rha, ★ GlcA, HCl at 100 mM H^{+}_{eq} acidity, ■ Rha, ■ GlcA, S101 at 100 mM H^{+}_{eq} acidity. The lines represent mathematical modeling of the kinetics, except for the case of GlcA obtained with S101.

The degradation of glucuronic acid was also investigated experimentally by performing two independent experiments in which HCl and S101 are added to the acid at the same acidity and temperature, 100 mM H^{+}_{eq} and 100°C, respectively. The results confirmed that the concentration of glucuronic acid decreases, while glucuronic acid γ-lactone (GlcA γ L) appears in the medium (Figure 7-34). Accordingly, a faster degradation of GlcA was observed when the reaction was carried out with S101 compared to HCl, as noted in the hydrolysis of the ulvan extract. This result confirmed that the resin did trigger faster degradation of the uronic acid. The carbon balance obtained at the beginning of the reaction showed, for both HCl and S101, that most of the glucuronic acid was transformed into glucuronic acid γ-lactone. Thus, the molar ratio GlcA: GlcA γ L was kept relatively constant throughout the timeframe of the reaction, indicating that there was an equilibrium between the two species. Subsequently, both GlcA and GlcA γ L were degraded into many different degradation compounds, from which levulinic, maleic and butyric acids and furfural were the most prominent ones identified by HPLC. However, some different pathways including isomerization, oxidation, and

deacetylation can occur in acidic environments.[199] In this regard, the equilibrium of uronic acids with lactones, and further degradation at elevated temperatures and in the presence of low pH has been reported by different authors.[198,200]

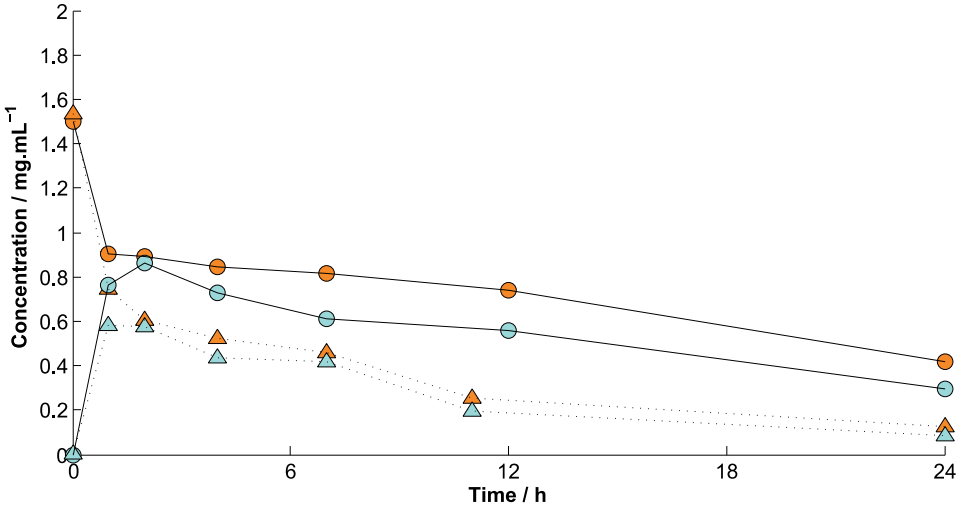

Figure 7-34. The degradation kinetics of glucuronic acid in the presence of HCl and S101;

The concentration of glucuronic acid in the presence of HCl and S101 at 100 mM H^{+}_{eq} acidity and 100°C. The data are expressed in concentration mg L^{-1}. Symbols: ● GlcA, ● GlcAγL, HCl at 100 mM H^{+}_{eq} acidity and 100°C, ▲ GlcA, ▲ GlcAγL, S101 at 100 mM H^{+}_{eq} acidity and 110°C. Lines represent the trend of the data.

8 Mathematical modeling

The kinetics of the extraction of ulvan from green algae biomass and the subsequent hydrolysis of ulvan using the one-pot and the pre-extraction processing with homogeneous and heterogeneous catalysis was quantitatively studied by mathematical modeling to estimate the kinetics parameters of the reactions.

8.1 Modeling of the ulvan extraction [III]

The experimental data obtained from the aqueous extraction of ulvan in the temperature range of 60–130°C showed very rapid extraction kinetics in the timeframe of 0–1 min, followed by a decrease in the reaction rate, resulting in two kinetics regimes. Consequently, the mathematical modeling for the extraction of ulvan comprised only of the kinetics regime evaluated between 1 and 120 min.

The extraction kinetics of ulvan considered the evaluation of the three most important monomers in the ulvan backbone: L-rhamnose, D-glucuronic acid, and L-iduronic acid. Therefore, ulvan was assumed as the sum of these three constituents. The model was based on the first-order kinetics with respect to the concentration of ulvan in the solid (Eq. (1)), and it took into account the temperature of the experiment (T). The reaction rate was modeled by a modified Arrhenius expression featuring a reference temperature (T_{ref}) (equal to 95°C). The model was based on the assumptions that no degradation of the sugars occurred and that the extraction was irreversible. The pH of the mixture was not included in the model since it remained relatively constant throughout the experiments. In Eq. (1), q stands for the oligomer concentration of component (i) in the solid (s) or the liquid (L) phase at time t. The parameter $k_{0,i}$ stands for the pre-exponential factor and $E_{a,i}$ stands for the activation energy for component (i), while R stands for the universal gas constant.

$$\frac{dQ_{i,S}}{dt} = -k_{0,i} \cdot e^{-\frac{E_{a,i}}{R}\left(\frac{1}{T}-\frac{1}{T_{ref}}\right)} \cdot \left(q_{i,0} - q_{t,i,L}\right) \quad (1)$$

The kinetic parameters were estimated by subsequent iterations of the objective function *FOB* minimized using the simplex method. The *FOB* was defined as the difference between the experimental (*exp*) conversion (y) and the conversion estimated by the model (*model*). The FOB included all the data obtained from the different monomers (i), the evaluated experimental conditions (j) and the sampling time (t) (Eq. (2) and Eq. (3)). The parameters for rhamnose, glucuronic acid, and iduronic acid were estimated all together in the same objective function (Eq. (2)), while ulvan was treated separately (Eq. (3)).

$$FOB_{monomers} = \sqrt{\sum_{i=1}^{i_{tot}} \sum_{j=1}^{j_{end}} \sum_{t=1}^{t_{end}} \left(Y_{i,j,t}^{model} - Y_{i,j,t}^{exp}\right)^2} \quad (2)$$

$$FOB_{ulvan} = \sqrt{\sum_{j=1}^{j_{end}} \sum_{t=1}^{t_{end}} \left(Y_{ulvan,j,t}^{model} - Y_{ulvan,j,t}^{exp}\right)^2} \quad (3)$$

The experimental data showed good fitting to the mathematical model, as observed in Figure 7-24, with a degree of explanation R^2 between 0.89 and 0.97 (see Table 8-1). The activation energies for the extraction of ulvan constituents were in the range of 52.9–57.6 kJ mol^{-1}. The similarity between the values was unequivocally due to the occurrence of these three residues in the ulvan backbone, as the dimers ulvanobiuronic type *A* and *B*.

Table 8-1. The kinetic parameters estimated for the extraction of ulvan from Ulva rigida

Sugar/Carbohydrate	Pre-exponential factor $k_0 \cdot 10^3$ a) min^{-1}	Activation energy E_a kJ mol^{-1}	Degree of explanation R^2 -
Rhamnose	9.47	53.8	0.97
Glucuronic acid	7.93	52.9	0.93
Iduronic acid	7.43	57.6	0.89
Ulvan	8.51	53.8	0.96

a) The pre-exponential factor was calculated at the reference temperature 95°C.

The activation energies estimated for the extraction of hemicelluloses from different lignocelluloses were in the range of 82–251 kJ mol^{-1}, as reported by various authors.[201–206] Therefore, the activation energies for the extraction of ulvan were lower than those reported for lignocelluloses. However, this seems rather logical, as the hemicelluloses in the cell wall of terrestrial plants are linked to lignin, which hinders their extraction, and consequently elevated temperatures are needed to obtain acceptable extraction yields. In contrast, algal cell walls do not contain lignin. Therefore, the conditions required for obtaining higher extraction yields are milder than those needed for terrestrial plants.

The results of the sensitivity analysis of the kinetic parameters for each of the main constituents of ulvan are depicted in Figure 8-1. The analysis was performed so that the value of one parameter was varied, while the values of the rest of the parameters were fixed to the optimized value estimated by the model. The contour plots demonstrated that the parameters were well defined under the experimental conditions evaluated in this work. and no severe correlation exists.

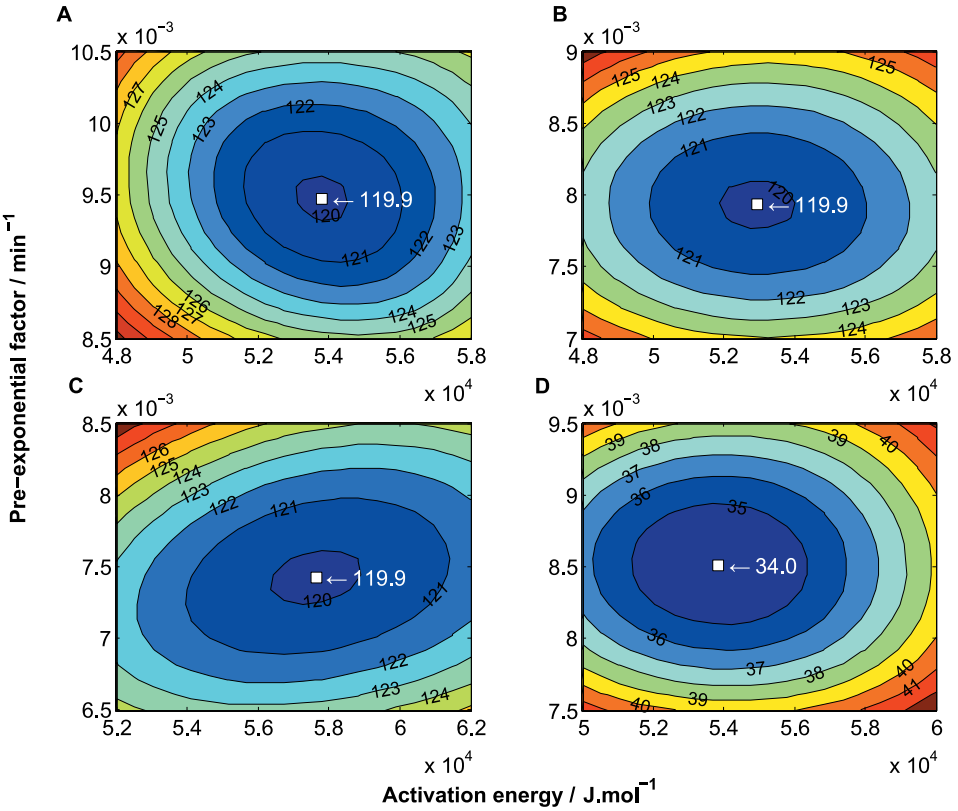

Figure 8-1. Sensitivity analysis of the FOB function to the kinetics parameters for the extraction of rhamnose, glucuronic and iduronic acids and ulvan.

A, B, C, and D show the contour plots of the FOB function for the activation energy and the pre-exponential factor for rhamnose, glucuronic acid, iduronic acid, and ulvan, respectively.

8.2 Modeling of the ulvan hydrolysis [V]

The hydrolysis of ulvan was modeled according to the mechanism showed in Eq. (4-9). The mechanism considers ulvan as a homopolymer, consisting in homorhamnan and homoglucuronan. In Eq (4), the extraction of ulvan from the solid (US) to the liquid phase (UL) is represented. In accordance with the experimental data obtained from the extraction and the hydrolysis experiments, the extraction rate was several orders of magnitude faster than the hydrolysis rate. Consequently, the kinetic expression for the extraction in the case of the one-pot processing was ignored. Eq (5) shows the protonation ($H_3O^+Z^-$) of the catalysts (H^+Z^-), which was assumed rapid equilibrium. Subsequently, Eq. (6) indicates the adsorption of the ulvan oligomers (U_L) onto the catalyst ($U_LH^+Z^-$), whereas the Eq. (7) exhibits the cleavage of the glycosidic bond of the ulvan backbone to produce the monomer (P) and leave the active site of the catalyst free. Eq (8) shows the adsorption of the

monomer (P) onto the active site of the catalyst (PH^+Z^-), whereas Eq. (9) describes the degradation reaction of the catalyst to produce the decomposition product (PX). The decomposition products were not directly quantified, but calculated from the mass balance.

$$U_S \rightarrow U_L \quad (4)$$

$$H^+Z^- + H_2O = H_3O^+Z^- \quad (5)$$

$$H_3O^+Z^- + U_L = H_2O + U_LH^+Z^- \quad (6)$$

$$H_2O + U_LH^+Z^- \rightarrow P + H^+Z^- \quad (7)$$

$$P + H^+Z^- = H_2O + PH^+Z^- \quad (8)$$

$$PH^+Z^- \rightarrow PX + H^+Z^- \quad (9)$$

The kinetics model was based on a previous work reported by Salmi and co-workers.[207] Both the homogeneous and the heterogeneous hydrolysis were modeled with the first-order kinetics with respect to the carbohydrate concentration (Eq. (10)). In the equations, *c* is the concentration, of water (*w*), catalyst (H^+) and monomer component (*i* = Rha, GlcA) at time zero (0), in the solid (*s*) or liquid (*L*) phase at time *t*. The concentration of water was kept constant in the modeling. The degradation products of component (*i*) were defined by (X_i). Additionally, *k* stands for the rate constant of reaction (*N*) of component (*i*) at the temperature (*T*).

$$\frac{dc_{i,L}}{dt} = k_{7,T,i} \cdot c_w \cdot c_{H^+} \cdot \left(c_{0,s,i} - c_{t,i,L} - c_{t,Xi}\right) - k_{9,T,i} \cdot c_{H^+} \cdot c_{i,T,L} \quad (10)$$

The model was implemented with the software MATLAB® 2010b. The system of ordinary differential equations was solved using Runge-Kutta method (MATLAB® function 'ode45'). The kinetic parameters were estimated by minimization of the objective function using the simplex method (MATLAB® function 'fminsearch') in Eq. 11, expressed as the error between the yield (*Y*) of Rha and GlcA (*i*) estimated by the model (*model*) and quantified analytically (*exp*) at the defined conditions of acidity and temperature (*j*) at the time (*t*).

$$FOB_{monomers} = \sqrt{\sum_{i=1}^{i_{tot}} \sum_{j=1}^{j_{end}} \sum_{t=1}^{t_{end}} \left(Y_{i,j,t}^{model} - Y_{i,j,t}^{exp}\right)^2} \quad (11)$$

8.2.1 Modeling of one-pot processing

The experimental data of the one-pot processing for the extraction and hydrolysis of ulvan showed very slow reaction kinetics. A clear autohydrolysis effect was observed in the experiments performed with A70 at low temperature (90°C), where the rate constant increased during the timeframe of the reaction (0–96 h). Consequently, to account for this effect

Eq. (10) was modified into Eq. (12), featuring the parameters α and β of the autohydrolysis as proposed by Salmi and co-workers.[207]

$$\frac{dc_{t,i,L}}{dt} = k_{7,i} \cdot \left(1 + \beta \cdot \frac{c_{t,i,L}+c_{t,Xi}}{c_{0,S,i}}\right)^{\alpha} \cdot c_w \cdot c_{H^+} \cdot \left(c_{0,s,i} - c_{t,i,L} - c_{t,Xi}\right) - k_{9,i} \cdot c_{H^+} \cdot c_{t,i,L} \quad (12)$$

The results of the modeling are presented in Table 8-2. The parameter estimation showed R^2 values higher than 0.9 for most of the experiments. The rate constants for the production of rhamnose for the experiments carried out with A70 at 90°C ($4.6 \cdot 10^{-7}$–$9.4 \cdot 10^{-17}$ L mol^{-1} min^{-1}) were at least 1 order of magnitude lower than that obtained with the homogeneous catalysis (HCl, $4.3 \cdot 10^{-6}$ L mol^{-1} min^{-1}). Consequently, mass transfer limitations due to the porosity of A70 were evident and hindered the rate constant at low temperatures. When the temperature was increased to 120°C, the enhancement in the reaction rate was evident, since the kinetic constant value increased by two orders of magnitude in the case of A70 ($1.5 \cdot 10^{-5}$ L mol^{-1} min^{-1}). Moreover, when the reaction was carried out with S101 at 120°C, the rate constant ($4.3 \cdot 10^{-5}$ L mol^{-1} min^{-1}) was 3-fold higher compared to that obtained with A70. This result confirmed the more obvious mass transfer limitations of A70 compared to S101.

Table 8-2. The estimated parameter values for the one-pot processing of ulvan

Homogeneous	$k_{7,Rha} \cdot C_{H^+} \cdot 10^4$ L mol^{-1} min^{-1}	$k_{9,Rha} \cdot C_{H^+} \cdot 10^4$ min^{-1}	β -	R^2 -
HCl – 100 mM H+eq – 90°C	0.043	-	-	0.960
Heterogeneous	$k_{7,Rha} \cdot C_{H^+} \cdot 10^4$ L mol^{-1} min^{-1}	$k_{9,Rha} \cdot C_{H^+} \cdot 10^4$ min^{-1}	β -	R^2 -
A70 – 4.3 mM H+eq – 90°C	9.4E-13	-	6.0e+09	0.992
A70 – 12.9 mM H+eq – 90°C	4.2E-07	-	3.3E+04	0.996
A70 – 100 mM H+eq – 90°C	4.6E-03	-	8.24	0.967
A70 – 100 mM H+eq – 120°C	0.15	0.6	-	0.796
S101 – 100 mM H+eq – 120°C	0.43	0.75	-	0.994

k_7 stands for the kinetic constant for the production of monomers, while k_9 stands for the kinetic constant for the degradation of monomers.

8.2.2 Modeling of the hydrolysis of the pre-extracted ulvan

The results of the modeling of the data acquired from the hydrolysis experiments of the pre-extracted ulvan are presented in Table 8-3. The R^2 values showed a good correlation of the experimental data to the model (above 0.9 for most of the experiments). The rate constant for the production of rhamnose was rather similar in the pre-extracted processing compared to the one-pot processing, since in the homogeneous hydrolysis performed at

90°C the rate constant of the one-pot and pre-extracted processing accounted for 4.3 and $6.0 \cdot 10^{-6}$ L mol^{-1} min^{-1}, respectively. A similar result was observed for the heterogeneous catalysis performed at 120°C, where the rate constant accounted for 4.3 and $3.0 \cdot 10^{-5}$ L mol^{-1} min^{-1}, for the one-pot and pre-extraction processing, respectively.

Table 8-3. The estimated parameters values for hydrolysis of pre-extracted ulvan

Homogeneous	$k_{7,Rha} \cdot C_{H^+} \cdot 10^4$ L mol^{-1} min^{-1}	$k_{9,Rha} \cdot C_{H^+} \cdot 10^4$ min^{-1}	R^2 -
HCl – 100 mM H^+_{eq} – 90°C	0.060	-	0.941
HCl – 100 mM H^+_{eq} – 100°C	0.25	2.55	0.948
HCl – 100 mM H^+_{eq} – 105°C	0.49	4.17	0.927
HCl – 100 mM H^+_{eq} – 110°C	0.96	6.74	0.958
Heterogeneous	$k_{7,Rha} \cdot C_{H^+} \cdot 10^4$ L mol^{-1} min^{-1}	$k_{9,Rha} \cdot C_{H^+} \cdot 10^4$ min^{-1}	R^2 -
S101 – 100 mM H^+_{eq} – 100°C	0.017	0.17	0.870
S101 – 50 mM H^+_{eq} – 110°C	0.038	0.19	0.943
S101 – 75 mM H^+_{eq} – 110°C	0.056	0.29	0.945
S101 – 100 mM H^+_{eq} – 110°C	0.075	0.39	0.978
S101 – 100 mM H^+_{eq} – 120°C	0.30	0.86	0.900

k_7 stands for the kinetic constant for the production of monomers, while k_9 stands for the kinetic constant for the degradation of monomers.

The rate constants for the production of rhamnose in the temperature range of 100–110°C in the homogeneous catalysis varied in the range $2.5 \cdot 10^{-5}$–$9.6 \cdot 10^{-5}$ L mol^{-1} min^{-1}. Conversely, in the case of the heterogeneous catalysis the rate constant for rhamnose varied in the range of $1.7 \cdot 10^{-6}$–$7.5 \cdot 10^{-6}$ L mol^{-1} min^{-1}, being one order of magnitude lower in the case of S101 compared to HCl. Consequently, the hydrolysis of ulvan benefited from faster rhamnose production in the case of HCl compared to S101. Regarding the decomposition rate, the higher the temperature, the higher the decomposition rate of rhamnose for both the homogeneous and the heterogeneous catalysis. However, the rate constant for the degradation of rhamnose at 110°C was greater in the case of HCl ($6.7 \cdot 10^{-4}$ min^{-1}) compared to S101 ($3.9 \cdot 10^{-5}$ min^{-1}).

The Arrhenius parameters estimated by the mathematical model are displayed in Table 8-4. The activation energy for the production of rhamnose was 160 kJ mol^{-1} in the case of the homogeneous catalysis, while for the heterogeneous catalysis the activation energy was 175 kJ mol^{-1}. The activation energy for the degradation of rhamnose was in the range of 100–116 kJ mol^{-1} for both the homogeneous and heterogeneous hydrolysis

Consequently, in the temperature range and the reaction time frame evaluated in this work, the homogeneous catalysts gave rise to faster kinetics upon the production of rhamnose, but also faster degradation of the monomers. Conversely, the heterogeneous processing benefited from conditions that were more easily controllable.

Table 8-4. The Arrhenius parameters for the hydrolysis of pre-extracted ulvan

Homogeneous	Parameter	Units	L-rhamnose	D-glucuronic acid
k_7	E_a	kJ mol^{-1}	160	134
	$k_0 \cdot 10^3$	L^2 mol^{-2} min^{-1}	0.49	0.26
k_9	E_a	kJ mol^{-1}	116	115
	$k_0 \cdot 10^3$	L mol^{-1} min^{-1}	3.64	11.3
Heterogeneous	Parameter	Units	L-rhamnose	D-glucuronic acid
k_7	E_a	kJ mol^{-1}	175	n.d.
	$k_0 \cdot 10^3$	L^2 mol^{-2} min^{-1}	0.075	n.d.
k_9	E_a	kJ mol^{-1}	116	n.d.
	$k_0 \cdot 10^3$	L mol^{-1} min^{-1}	0.39	n.d.

k_7 stands for the kinetic constant for the production of monomers, while k_9 stands for the kinetic constant for the degradation of monomers.

Concurrently to the mathematical modeling of the extraction of ulvan, the objective function of the hydrolysis data was evaluated at a different pair of kinetics parameters as depicted in Figure 8-2. No severe correlation of the kinetic parameters was observed, especially in the homogeneous hydrolysis. In the case of the degradation reaction for the heterogeneous catalysis, some correlation of the parameters was observed. The main explanation was attributed to the lack of experimental data of degradation products to which the modeling can compare with, resulting in a non-accurate prediction of the parameters.

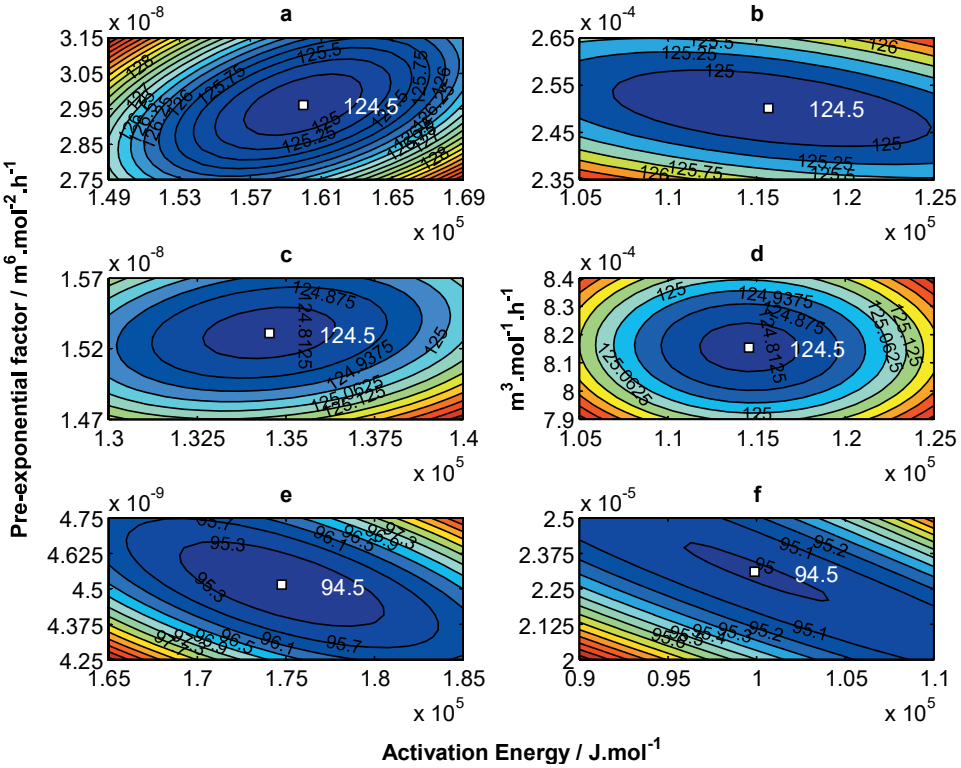

Figure 8-2. Sensitivity analysis of the FOB function to the kinetics parameters for the hydrolysis of ulvan.

A: production of rhamnose with HCl, B: degradation of rhamnose with HCl, C: production of glucuronic acid with HCl, D: degradation of glucuronic acid with HCl, E: production of rhamnose with S101 and F: degradation of rhamnose with S101.

9 Conclusions

The extraction and subsequent hydrolysis of marine carbohydrates from the brown algae *Macrocystis pyrifera* and the green alga *Ulva rigida* were investigated. The extraction of phlorotannins from *M. pyrifera* was studied using biomass particle sizes of 100% < 1.4 mm, 100% 2.0–1.4 mm and 100% > 2.0 mm, and drying temperatures between 30 and 60°C. Additionally, different extraction solvents varying in polarity, solid to liquid ratio of 1:20, 1:15 and 1:10 and extraction temperatures in the range of 25–50°C were evaluated. The drying of the biomass was found to be significantly slower at 30°C, compared to the drying in the temperature range of 40–60°C. The total phlorotannin content was found to be directly correlated to the polarity of the solvent. Thus, water was the most efficient solvent for the extraction of phlorotannins. The fractionation performed to the phlorotannins extract revealed the presence of phloroeckol and a tetramer of phloroglucinol.

Ionic liquids were demonstrated to extract carbohydrates from *U. rigida* biomass efficiently. Three ionic liquids were evaluated: DBU-MEA-SO2 (1,8-diazabicyclo-[5.4.0]-undec-7-ene, monoethanolamine, sulfur dioxide), 1,1,3,3-tetramethylguanidine propionate ([$TMGH^+$][CO_2Et^-]), and the protonated DBU 2,2,3,3,4,4,5,5-octafluoro-1-pentoxide ([$HDBU^+$][$5OF^-$]). The dissolution was studied in the temperature range of 100–160°C. Among the different solvents studied, [$TMGH^+$][CO_2Et^-] turned out to be the best solvent for the extraction of green algae carbohydrates, while the processing temperature of 120°C allowed for the extraction of 69 wt.% of carbohydrates. The mass balance of the main constituents of the alga was accomplished, and it revealed that most of the ashes were extracted to the ionic liquid phase, whereas most of the proteins remained in the solid phase. However, around 99 wt.% of the carbohydrates present in the fresh biomass was dissolved while processing with dilute sulfuric acid at 125°C, whereas water at the same conditions allowed for the selective extraction of 99 wt.% of the rhamnoglucuronan "ulvan" present in the fresh biomass.

Since water was an efficient and selective extractant for the ulvan, the kinetics of the extraction of this polysaccharide from *U. rigida* biomass was studied in the temperature range of 60–130°C at a solid-to-liquid ratio of 1:20. The results revealed that the extract obtained in this temperature range consisted of 65–84 wt.% ulvan. Higher temperatures 110–130°C allowed for the extraction of more glucan, reducing the relative content of ulvan in the extract. The maximum yield of 98 wt.% of ulvan was attained after 2 h of processing at 130°C. The kinetics was highly temperature dependent, since major differences in the extraction yields were observed among the set of temperatures evaluated. The molecular weight of the extracted fractions was also reliant on the temperature, which increased in the initial stages of the

reaction, but decreased at prolonged extraction times. The main reason behind this observation was the necklace-like ultrastructure of ulvan which collapsed in the temperature range of 80–90°C. The sulfate-rhamnose ratio was also observed to increase, indicating that more sulfated fractions were extracted at later stages of the treatment.

The saccharification of *M. pyrifera* carbohydrates was efficiently demonstrated using hydrolases (hydrolytic mechanisms) and lyases (β-elimination mechanism) at temperatures between 28 and 50°C in the pH range of 4.8–8.0. The best conditions for the hydrolysis of alginate were attained at 37°C, at pH 7.5, accounting for 109 mg uronic acids/g of fresh algae. These conditions were different from those of commercial cellulases (50°C, at pH 4.8–5.2), most probably due to the distinct nature of the microorganisms that synthesize these enzymes and the different cleavage mechanisms of these biocatalysts. The saccharification of *M. pyrifera* pretreated with ionic liquids at 120°C demonstrated to increase the production of uronic acids compared to the saccharification of fresh biomass by 2-5 -fold. The maximum yield of 86 wt.% of D-mannuronic and L-guluronic acids was attained in the saccharification of biomass pretreated with dilute sulfuric acid. In the case of ionic liquids, the saccharification of alginates was maximized with DBU-MEA-SO_2, whereas for glucans, the best ionic liquid was 1,5-diazabicyclo-[4.3.0]-non-5-ene acetate ($[DBNH^+][OAc^-]$).The different solvation properties of the ionic liquids towards alginate and cellulose may be an explanation for these results.

The hydrolysis of ulvan was studied using homogeneous (HCl) and heterogeneous catalysts (*Amberlyst™*70 and *Smopex*®101) to produce L-rhamnose. The hydrolysis kinetics were investigated in the temperature range of 90–120°C, using one-pot extraction and hydrolysis processing and hydrolysis of pre-extracted ulvan. The results showed very slow kinetics at 90°C with A70 due to the presence of internal mass transfer limitations caused by the porosity of the resin. The maximum yield of L-rhamnose of 80 wt.% was obtained after 8 h of processing with 100 mM H^+_{eq} HCl at 110°C. The use of S101 under the same conditions allowed for the obtention of a yield of L-rhamnose of 82 wt.% after 35 h of processing. Consequently, HCl allowed for the obtaining of higher yields in shorter reaction times, compared to S101. However, HCl induced more rapid degradation of L-rhamnose compared to S101 at the evaluated experimental conditions, since after 48 h the L-rhamnose yield decreased to 14 wt.%. Additionally, severe degradation of D-glucuronic acid was observed in the presence of S101. The degradation experiments of D-glucuronic acid in the presence of HCl and S101 at 100°C showed an equilibrium between D-glucuronic acid and glucuronic acid gamma lactone, which was favored in the presence of S101. Still, when using both HCl and S101, several low molecular weight organic acids were

observed in the hydrolysate, indicating that under these conditions uronic acids easily undergo degradation.

Mathematical modeling was used for predicting the aqueous extraction and the hydrolysis of ulvan kinetics in the presence of homogeneous and heterogeneous catalysts. Both the extraction and the hydrolysis of ulvan were modeled with the first-order kinetics. In the case of the extraction of ulvan, an activation energy of 54 kJ mol^{-1} was estimated. This value was substantially lower compared to what was reported for the extraction of hemicelluloses from terrestrial plants, which was explained by the absence of lignin in the algal cell wall favoring the fractionation of the biomass. Concerning the hydrolysis kinetics, the rate constants between the one-pot processing and the hydrolysis of pre-extracted ulvan showed minor differences, indicating relatively fast ulvan extraction under the evaluated conditions. The hydrolysis experiments performed at 90°C revealed that 80 wt.% of the ulvan was extracted within the first 2 h of processing, as was also observed in the ulvan extraction experiments. An activation energy in the range of 134–160 kJ mol^{-1} was estimated for the hydrolysis of ulvan in the presence of homogeneous catalysts, whereas for the heterogeneous catalysts, the activation energy of 175 kJ mol^{-1} was predicted.

The results show that it was possible to obtain a high yield of interesting molecules from the processing of algal biomass. Moreover, the use of water extraction, enzymes, and heterogeneous catalysts are processes that comply with the principles of a green chemistry concept. Still, several challenges are foreseen before algal biorefinery becomes a reality: cultivation/harvesting of the algae and valorization of the different fractions such as ashes, lipids, and proteins are still open fields of research.

10 Future work

The present work demonstrated that algae are an attractive feedstock to produce valuable chemicals. However, several challenges remain open before a biorefinery utilizing algae biomass can become a feasible alternative in the future. For instance, the efficient cultivation of algae to supply enough biomass for biorefineries is very important. The composition of algae is seasonable due to, among different factors, the temperature of water and the availability of nutrients. Consequently, the transformation into products of a major fraction of the biomass is a key for the feasibility of an industry of this kind. Concerning the fractionation of the biomass, the literature is scarce in details about the conformational disposition of the constituents inside the cell walls of the different algae species, and how they do interact with each other. More work concerning the understanding of the role that each constituent plays in the cell wall of algae would be of great value for the design of efficient fractionation processes.

The hydrolysis of L-sugar-containing polysaccharides has received little attention compared to the vast potential that these molecules may offer, particularly in the pharmaceutical sector. Due to the resemblance of deoxy-L-sugars to nucleotides present in DNA, these molecules (L-rhamnose and L-fucose) can serve for the design of vaccines, resulting in a significant development for the medical sector. However, the literature is scarce about the depolymerization techniques of polysaccharides of this kind. The presence of uronic acid in this pectin-type of polysaccharides represent a major challenge due to their instability in the presence of mineral acids and moderate temperatures. Consequently, the development of processes for a more efficient depolymerization of these types of polysaccharides would be welcome. Only a few research groups are involved in finding new ulvan-active enzymes. The development of these kinds of biocatalysts would be valuable for an efficient release of L-rhamnose from ulvan. Additionally, further advances in the development of ionic liquids capable of solubilizing and depolymerizing the backbone of marine polysaccharides would also provide a substantial progress for achieving this goal, since the research in this area has focused mainly on the solubilization and hydrolysis of terrestrial plant biopolymers}

Notation

Symbols

c	:	concentration
d	:	derivative
e	:	Euler's number
E_a	:	activation energy
FOB	:	objective function
H^+	:	proton
H^+Z^-	:	acidic catalyst
k_0	:	pre-exponential factor
k	:	rate constant
P	:	monomer product from hydrolyzed ulvan (Rha or GlcA)
PX	:	undefined degradation molecule from monomers
R	:	universal gas constant
q	:	oligomer concentration
t	:	time
T	:	temperature
T_{ref}	:	reference temperature
U	:	ulvan
Y	:	yield
α	:	parameter for autocatalytic effect
β	:	parameter for autocatalytic effect

Subscripts

0	:	initial state in the solid phase
eq	:	equivalent
i	:	monomer component (i)
j	:	number of experiment runs
L	:	liquid
s	:	solid
t	:	time
w	:	water

Superscript

exp	:	value analytically quantified
model	:	value estimated by mathematical modeling

Abbreviations

A70	:	*Amberlyst™* 70
AcOH	:	acetone
AOAC	:	Association of Official Analytical Chemistry
Ara	:	arabinose
BG	:	β-glucosidase
BBOT	:	2,5-(Bis(5-tert-butyL-2-benzo-oxazoL-2-yl) thiophene
CBH	:	cellobiohydrolase
$CHCl_3$	:	chloroform
CO2Et	:	propionic acid
DBN	:	1,5-Diazabicyclo-[4,3,0]-non-5-ene
DBU	:	1,8-diazabicyclo-[5,4,0]-undec-7-ene
DI	:	deionized
DIL	:	distillable ionic liquid
DMF	:	N,N-dimethylformamide
DPPH	:	1,1-diphenyL-2-picryL-hydrazyl
DS	:	dry solids
EDXA	:	energy dispersive X-ray analysis
EG	:	endoglucanases
EU	:	European Union
EMIM	:	1-ethyL-3-methylimidazolium
EtAcOH	:	ethyl acetate
EtOH	:	ethanol
FID	:	flame ionization detector
FOB	:	objective function
FPU	:	filter paper unit
Fru	:	fructose
Fuc	:	fucose
FTIR	:	Fourier transform infrared spectroscopy
GC	:	gas chromatography
Gal	:	galactose
GalA	:	galacturonic acid
GAE	:	gallic acid equivalent
Glc	:	glucose
GlcA	:	glucuronic acid
GlcAγL	:	glucuronic acid γ-lactone
GulA	:	guluronic acid
Hex	:	hexane
HCl	:	hydrochloric acid
HMDS	:	hexamethyldisilazane
HMF	:	5-hydroxymethyl furfural
HPLC	:	high performance liquid chromatography
LC-ESI-MS/MS	:	Liquid Chromatography Electrospray Ionization Tandem Mass Spectrometric
LCC	:	lignin-cellulose-hemicellulose matrix
HPSEC	:	high performance size-exclusion chromatography
ICP-OES	:	inductively coupled plasma optical emission spectrometry
IduA	:	Iduronic acid

IL	:	ionic liquid	POM	:	polyoxometalate
IR	:	infrared	Rha	:	rhamnose
LC/MS	:	liquid chromatography–mass spectrometry	RT	:	room temperature
			S101	:	*Smopex*® 101
LCC	:	lignin-carbohydrate complex	SEM	:	Scanning electron microscopy
LPMO	:	lytic polysaccharide monooxygenases	SIL	:	switchable ionic liquid
			TAA	:	total antioxidant content
LVIL	:	low viscosity ionic liquid	TE	:	Trolox equivalent
MALLS	:	multi-angle laser light scattering	Trolox	:	(±)-6-hydroxy-2,5,7,8-tetramethylchromane-2-carboxylic acid
Man	:	mannose			
ManA	:	mannuronic acid			
MCC	:	microcrystalline cellulose	TMCS	:	chlorotrimethylsilane
MEA	:	monoethanolamine	TMG	:	1,1,3,3-tetramethylguanidine
MeOH	:	methanol	TPC	:	total phlorotannins content
Mtl	:	mannitol	UV	:	ultraviolet
OAc	:	acetate	Xyl	:	xylose
OF	:	octafluoro			

Acknowledgments

The present work was carried out at the Laboratory of Industrial Chemistry and Reaction Engineering, John Gadolin Process Chemistry Centre, Faculty of Science and Engineering, Åbo Akademi University between 2013 and 2017. The main part of the work was funded by the Academy of Finland (AKA) (Grant number 268937, period 2013/09–2015/12) and with the scholarship provided by the National Commission for Scientific and Technological Research of the Government of Chile (CONICYT) (N°72170085, period 2016/06–2017/10). Moreover, in Sweden, the Bio4Energy program, the Kempe Foundations and the Wallenberg Wood Science Center are acknowledged. This research work is also a part of the activities of the Johan Gadolin Process Chemistry Centre (PCC), a center of excellence financed by Åbo Akademi University.

References

1. K. Svendsen, A. Kompaniets, in Regulation of the Russian Federation petroleum licensing regime, (Ed.: T. Hunter), Edward Elgar Publishing, Cheltenham, UK, **2015**, 306–339.
2. K. Aslanli, S. Isayev, Natl. Reports - Soc. Watch **2012**, 66–67, (last accessed on 2017-06-08), can be found under http://www.socialwatch.org/sites/default/files/SocialWatch-NationalReports2012_eng.pdf.
3. V. Rull, N. Cañellas-Boltà, O. Margalef, S. Pla-Rabes, A. Sáez, S. Giralt, *Front. Ecol. Evol.* **2016**, 4, 1–4.
4. Pacific Climate Change Science Program, "Current and future climate of Samoa", Samoa Meteorology Division, Ministry of Natural Resources and Environment, Australian Bureau of Meteorology, Commonwealth Scientific and Industrial Research Organisation, **2011**, (last accessed on 2017-06-08), can be found under http://www.pacificclimatechangescience.org/wp-content/uploads/2013/06/3_PCCSP_Samoa_8pp.pdf.
5. D. Stillman, D. Miller, "What are climate and climate change?," **2015**, (last accessed on 2017-06-08), can be found under https://www.nasa gov/audience/forstudents/5-8/features/nasa-knows/what-is-climate-change-58.html.
6. Directive 2009/28/EC of the European Parliament and of the Council of 23 April 2009, *OJ*. **2009**, L 140, 16-62.
7. COM(2016) 767 final/2 of 23.02.2017, " Proposal for a: Directive of the European Parliament and of the Council on the promotion of the use of energy from renewable resources (recast), (Ed. European Commission), Brussels, Belgium, **2017**, 1-116.
8. Energy Department, "Finland's national action plan for promoting energy from renewable sources pursuant to Directive 2009/28/EC", Ministry of Employment and the Economy of the Government of Finland, **2010**, (last accessed on 28.07.2017), can be found under http://www.buildup.eu/en/practices/publications/finland-national-renewable-energy-action-plan-accordance-directive-200928ec.
9. United Nations, "Paris Agreement", Conference of the Parties on its twenty-first session, **2015**, (last accessed on 28.07.2016), can be found under http://unfccc.int/paris_agreement/items/9485.php
10. United Nations, "C.N.735.2016.TREATIES-XXVII.7.d (Depositary Notification)", **2015**, (last accessed on 28.07.2016), can be found under http://unfccc.int/paris_agreement/items/9444.php
11. F. Cherubini, *Energy Convers. Manag*. **2010**, 51, 1412–1421.
12. L. Lange, B. Björnsdóttir, A. Brandt, S. K. Hildén, G. O. Hreggviðsson, B. Jacobsen, A. Jessen, E. N. Karlsson, J. Lindedam, M. R. Mäkelä, S. E. Smáradóttir, J. Vang, A. Wentze, *Development of the Nordic Bioeconomy - NMC reporting: Test centers for green energy solutions – Biorefineries and business needs*, Nordic Council of Ministers, Copenhagen, **2015**, DOI 10.6027/TN2015-582.
13. N. von Weymarn, "Metsä Group's Bioproduct Mill: A next generation wood biorefinery in Äaenoski, Finland," **2016**, (last accessed on 2017-06-08), can be found under https://www.slideshare.net/MetsaGroup/mets-groups-bioproduct-mill-a-next-generation-wood-biorefinery-in-nekoski-finland.
14. Metsä Group, "The next generation bioproduct mill," **2015**, (last accessed on 2017-06-08), can be found under http://bioproductmill.com/articles/metsa-group-to-build-next-generation-bioproduct-mill-in-aanekoski.
15. Suzano Pulp and Paper, "Institutional Presentation" **2011**, (last accessed on 2017-05-19), can be found under https://www.slideshare.net/Suzano_IR/institutional-presentation-10257194.
16. G. Roesijadi, S. B. Jones, Y. Zhu, *Macroalgae as a Biomass Feedstock : A Preliminary Analysis*, US Department of Energy, Richland, **2010**, (last accessed on 2017-05-31), can be found under https://www.osti gov/scitech/biblio/1006310/.
17. V. Smil, in *Power Density: A Key to Understanding Energy Sources and Uses*, The MIT Press, London, **2015**, 41–96.
18. P. T. Martone, J. M. Estevez, F. Lu, K. Ruel, M. W. Denny, C. Somerville, J. Ralph, *Curr. Biol.* **2009**, 19, 169–175.
19. FAO, *Fishery and Aquaculture Statistics 2014*, FAO, Rome, **2016**, (last accessed on 2017-05-31), can be found under http://www.fao.org/fishery/statistics/programme/publications/all/en
20. H. J. Bixler, H. Porse, *J. Appl. Phycol.* **2011**, 23, 321–335.
21. T. Werpy, G. Petersen, A. Aden, J. Bozell, J. Holladay, J. White, A. Manheim, D. Eliot, L. Lasure, S. Jones, M. Gerber, K. Ibsen, L. Lumberg, S. Kelley, *Top Value Added Chemicals from Biomass Volume I — Results of Screening for Potential Candidates from Sugars and Synthesis Gas*, US Department of Energy, Washington DC, **2004**, DOI 10.2172/15008859.
22. R. Pezoa, V. Cortinez, S. Hyvärinen, M. Reunanen, J. Hemming, M. E. Lienqueo, O. Salazar, R. Carmona, A. Garcia, D. Y. Murzin, J.-P. Mikkola, *Cellul. Chem. Technol.* **2010**, 44, 165–172.
23. T. Riitonen, V. Eta, S. M. Hyvärinen, L. J. Jönsson, J.-P. Mikkola, in *Chemical Engineering for Renewables Conversion, Volume 42*, (Ed.: D.Y. Murzin), Academic Press, San Diego, CA, **2013**, 3–73.
24. B. Li, F. Lu, X. Wei, R. Zhao, *Molecules* **2008**, 13, 1671–1695.
25. S. Kraan, in *Carbohydrates - Comprehensive Studies on Glycobiology*, (Ed.: C.-F. Chang), InTech, Rijeka, **2012**, 489–530.
26. S. Peat, J. R. Turvey, in Progress in the *Chemistry of Organic Natural Products XXIII*, (Ed.: L. Zechmeister), Springer-Verlag, Wien, **1965**, 1–45.
27. A. P. Imeson, in *Handbook of Hydrocolloids*, (Eds.: G.O. Phillips, P.A. Williams), Woodhead Publishing Limited, Cambridge, UK, **2000**, 87–102.
28. K. Draget, O. Smidsrød, G. Skjåk-Bræk, *Biopolym. Online* **2005**, 1–30.
29. L. E. Graham, L. W. Wilcox, *Algae*, Prentice-Hall, Inc., Upper Saddle River, NJ, **2000**.
30. V. Stiger-Pouvreau, N. Bourgougnon, E. Deslandes, in *Seaweed in Health and Disease Prevention*, (Eds.: I.A. Levine, J. Fleurence), Academic Press, London, UK, **2016**, 223–274.

31. E. Percival, *Br. Phycol. J.* **1979**, 14, 103–117.
32. K. A. Jung, S.-R. Lim, Y. Kim, J. M. Park, *Bioresour. Technol.* **2013**, 135, 182–190.
33. J. Kuszmann, in *The Organic Chemistry of Sugars*, (Eds.: D.E. Levy, P. Fügedi), CRC Press, Boca Raton, FL, **2006**, 23–50.
34. J.-P. Mikkola, R. Sjöhol,, T. Salmi, P. Mäki-Arvela, *Catal. Today* **1999**, 48, 73-81.
35. S. Oscarson, in *The Organic Chemistry of Sugars*, (Eds.: D.E. Levy, P. Fügedi), CRC Press, Boca Raton, FL, **2006**, 51–85.
36. M. Ochoa-Villarreal, E. Aispuro-Hernández, I. Vargas-Arispuro, M. Á. Martínez-Téllez, in *Polymerization*, (Ed.: A. De Souza Gomes), InTech, Rijeka, **2012**, 63–86.
37. J. Bidlack, M. Malone, R. Benson, in *Proceedings of the Oklahoma Academy of Science*, Oklahoma, US, **1992**, 51–56.
38. L. J. Gibson, *J. R. Soc. Interface* **2012**, 9, 2749–2766.
39. C. Gallis, M. Di Stefano, P. Moutsatsou, T. Sarjala, V. Virtanen, B. Holmbom, J. A. Buhagiar, A. Katalanos, in *Forest, trees and human health*, (Eds.: K. Nilsson, M. Sangster, C. Gallis, T. Hartig, S. de Vries, K. Seeland, J. Schipperijin), Springer, New York, US, **2011**, 41–76.
40. P. Hoffman, M. A. Jones, *Adv. Chem. Ser*. **1990**, 225, 35–65.
41. A. Baptista, I. Ferreira, J. Borges, in *Cellulose – Medical, Pharmaceutical and Electronic Applications*, (Eds.: T g.M. van de Ven, L. Godbout), InTech, Rijeka, **2013**, 67–82.
42. L. Axelsson, M. Franzén, M. Ostwald, G. Berndes, G. Lakshmi, N. H. Ravindranath, *Biofuels, Bioprod. Biorefining* **2011**, 5, 215–225.
43. J. George, S. N. Sabapathi, *Nanotechnol. Sci. Appl.* **2015**, 8, 45–54.
44. C. Laine, Ph.D. Thesis, Helsinki University of Technology, Helsinki, **2005**.
45. T. Koshijima, T. Watanabe, *Association between Lignin and Carbohydrates in Wood and Other Plant Tissues*, Springer Science & Business Media, New York, US, **2003**.
46. M. A. O'Neill, T. Ishii, P. Albersheim, A. G. Darvill, Annu. *Rev. Plant Biol.* **2004**, 55, 109–139.
47. N. Khodaei, S. Karboune, *Food Chem.* **2013**, 139, 617–623.
48. I. Anugwom, Ph.D. Thesis, Åbo Akademi University, Turku, **2014**.
49. E. Deniaud-Bouët, N. Kervarec, G. Michel, T. Tonon, B. Kloareg, C. Hervé, *Ann. Bot.* **2014**, 114, 1203–1216.
50. M. Lahaye, A. Robic, *Biomacromolecules* **2007**, 8, 24–30.
51. C. Bobin-Dubigeon, M. Lahaye, F. Guillon, J. L. Barry, D. J. Gallant, *J. Sci. Food Agric.* **1997**, 75, 341–351.
52. P. J. Moore, A. G. Darvill, P. Albersheim, A. L. Staehelin, *Plant Physiol.* **1986**, 82, 787–794.
53. S. Yu, M. Bojko, F. Madsen, C. E. Olsen, *Starch* **2002**, 54, 66–74.
54. R. Viola, P. Nyvall, M. Pedersén, *Proc. Biol. Sci.* **2001**, 268, 1417–1422.
55. G. Jiao, G. Yu, J. Zhang, H. S. Ewart, *Mar. Drugs* **2011**, 9, 196–233.
56. R. Armisén, F. Galatas, in *Handbook of Hydrocolloids*, (Eds.: G.O. Phillips, P.A. Williams), Woodhead Publishing Limited, Cambridge, UK, **2000**, 21–40.
57. M. Yanagisawa, K. Nakamura, O. Ariga, K. Nakasaki, *Process Biochem.* **2011**, 46, 2111–2116.
58. L. Cunha, A. Grenha, *Mar. Drugs* **2016**, 14, 42.
59. C. Andrieux, A. Hibert, A.-M. Houari, M. Bensaada, F. Popot, O. Szylit, *J. Sci. Food Agric.* **1998**, 77, 25–30.
60. A. Alves, R. A. Sousa, R. L. Reis, *J. Appl. Phycol.* **2013**, 25, 407–424.
61. P. Mäki-Arvela, T. Salmi, B. Holmbom, S. Willför, D. Y. Murzin, *Chem. Rev.* **2011**, 111, 5638–5666.
62. A. Leyton, R. Pezoa-Conte, A. Barriga, A. H. Buschmann, P. Mäki-Arvela, J.-P. Mikkola, M. E. Lienqueo, *Algal Res.* **2016**, 16, 201–208.
63. R. Pezoa-Conte, A. Leyton, I. Anugwom, S. von Schoultz, J. Paranko, P. Mäki-Arvela, S. Willför, M. Muszynski, J. Nowicki, M. E. Lienqueo, J.-P. Mikkola, *Algal Res.* **2015**, 12, 262–273.
64. R. Koivikko, PhD Thesis, University of Turku, Turku, **2008**.
65. I. P. Singh, J. Sidana, in *Functional ingredients from algae for foods and nutraceuticals*, (Ed.: H. Domínguez), Woodhead Publishing Limited, Cambridge, UK, **2013**, 181–203.
66. J. D. Murphy, B. Drosg, E. Allen, J. Jerney, A. Xia, C. Herrmann, *A Perspective on algal biomass*, IEA Bioenergy, **2015**, (last accessed on 2017-05-31), can be found under http://www.iea-biogas.net/files/daten-redaktion/download/Technical%20Brochures/AD_of_Algae_ebook_end.pdf
67. A. Peña-Rodríguez, T. P. Mawhinney, D. Ricque-Marie, L. E. Cruz-Suárez, *Food Chem.* **2011**, 129, 491–498.
68. D. Shuuluka, J. J. Bolton, R. J. Anderson, *J. Appl. Phycol.* **2013**, 25, 677–685.
69. A. Demirbas, *Biorefineries*, Springer-Verlag, London, UK, **2013**.
70. S. I. Mussatto, in *Biomass Fractionation Technologies for a Lignocellulosic Feedstock Based Biorefinery*, (Ed.: S.I. Mussatto), Elsevier Inc., Amsterdam, The Netherlands, **2016**, 169–185.
71. P. Sannigrahi, A. J. Ragauskas, in *Aqueous Pretreatment of Plant Biomass for Biological and Chemical Conversion to Fuels and Chemicals*, (Ed.: C.E. Wynam), John Wiley & Sons, Ltd., Chichester, UK, **2013**, 201–222.
72. S. Backa, M. Andresen, T. Rojahn, in *Biomass as Energy Source: Resources, Systems and Applications*, (Ed.: E. Dahlquist), CRC Press, Boca Raton, FL, **2012**, 141–150.
73. P. Mäki-Arvela, I. Anugwom, P. Virtanen, R. Sjöholm, J. P. Mikkola, *Ind. Crops Prod.* **2010**, 32, 175–201.
74. N. Demartini, A. Aho, M. Hupa, D. Y. Murzin, in *Chemical Energy Storage*, (Ed.: R. Schlögl), De Gruyter, Herndon, VA, United States, **2013**.
75. M. J. C. van der Stelt, H. Gerhauser, J. H. A. Kiel, K. J. Ptasinski, *Biomass Bioenerg.* **2011**, 35, 3748–3762.
76. F.-X. Collard, M. Carrier, G. F. Görgens, in *Biomass Fractionation Technologies for a Lignocellulosic Feedstock Based Biorefinery*, (Ed.: S.I. Mussatto), Elsevier Inc., Amsterdam, The Netherlands, **2016**, 81–101.
77. Y. Sun, J. Cheng, *Bioresour. Technol.* **2002**, 83, 1–11.
78. A. Duque, P. Manzanares, I. Ballesteros, M. Ballesteros, in *Biomass Fractionation Technologies for a Lignocellulosic Feedstock Based Biorefinery*, (Ed.: S.I. Mussatto), Elsevier Inc., Amsterdam, The Netherlands, **2016**, 349–368.
79. U. Merrettig-Bruns, B. Sayder, in *Biomass Fractionation Technologies for a Lignocellulosic Feedstock Based Biorefinery*, (Ed.: S.I. Mussatto), Elsevier Inc., Amsterdam, The Netherlands, **2016**, 461–481.

80. T. F. Carneiro, M. Timko, J. M. Prado, M. Berni, in *Biomass Fractionation Technologies for a Lignocellulosic Feedstock Based Biorefinery*, Elsevier Inc., Amsterdam, The Netherlands, **2016**, 385–407.
81. G. Hilpmann, N. Becher, F. A. Pahner, B. Kusema, P. Mäki-Arvela, R. Lange, D. Y. Murzin, T. Salmi, *Catal. Today* **2016**, 259, 376–380.
82. B. T. Kusema, T. Tönnov, P. Mäki-Arvela, T. Salmi, S. Willför, B. Holmbom, D. Y. Murzin, *Catal. Sci. Technol.* **2013**, 3, 116–122.
83. L. J. Konwar, Ph.D. Thesis, Åbo Akademi University, Turku, **2016**.
84. L. Vilcocq, P. C. Castilho, F. Carvalheiro, L. C. Duarte, *ChemSusChem* **2014**, 7, 1010–1019.
85. P. F. Siril, H. E. Cross, D. R. Brown, *J. Mol. Catal. A Chem.* **2008**, 279, 63–68.
86. B. T. Kusema, G. Hilpmann, P. Mäki-Arvela, S. Willför, B. Holmbom, T. Salmi, D. Y. Murzin, *Catal. Letters* **2011**, 141, 408–412.
87. J. Ahlkvist, Ph.D. Thesis, Umeå University, Umeå, **2014**.
88. G.-T. Jeong, S.-K. Kim, D.-H. Park, *Bioresour. Technol.* **2015**, 181, 1–6.
89. G.-T. Jeong, D.-H. Park, Korean Chem. Eng. Res. **2015**, 53, 478–481.
90. I. S. Tan, M. K. Lam, K. T. Lee, *Carbohydr. Polym.* **2013**, 94, 561–566.
91. J. Ahlkvist, S. Ajaikumar, W. Larsson, J. P. Mikkola, *Appl. Catal. A Gen.* **2013**, 454, 21–29.
92. I. S. Tan, K. T. Lee, *Carbohydr. Polym.* **2015**, 124, 311–321.
93. V. Pérez Martínez, Master Thesis, University of Valladolid, Valladolid, **2015**.
94. S. Tsubaki, K. Oono, M. Hiraoka, T. Ueda, A. Onda, K. Yanagisawa, J. Azuma, *Green Chem.* **2014**, 16, 2227.
95. J.-K. Xu, R.-C. Sun, in *Biomass Fractionation Technologies for a Lignocellulosic Feedstock Based Biorefinery*, (Ed.: S.I. Mussatto), Amsterdam, The Netherlands, **2016**, 431–459.
96. J. V. Rissanen, PhD Thesis, Åbo Akademi University, Turku, **2015**.
97. F. Carvalheiro, L. C. Duarte, F. Gírio, P. Moniz, in *Biomass Fractionation Technologies for a Lignocellulosic Feedstock Based Biorefinery*, Amsterdam, The Netherlands, **2016**, 315–347.
98. R. D. Rogers, K. R. Seddon, *Science*, **2003**, 302, 792–793.
99. S. Varanasi, C. A. Schall, A. P. Dadi, J. Anderson, K. Rao, P. Paripati, *Biomass Pretreatment*, **2008**, WO 2008/112291 A2.
100. N. Zhou, Y. Zhang, X. Gong, Q. Wang, Y. Ma, *Bioresour. Technol.* **2012**, 118, 512–517.
101. M. E. Lienqueo, M. C. Ravanal, R. Pezoa-Conte, V. Cortínez, L. Martínez, T. Niklitschek, O. Salazar, R. Carmona, A. García, S. Hyvärinen, P. Mäki-Arvela, J.-P. Mikkola, *Ind. Crops Prod.* **2016**, 80, 148–155.
102. N. Trivedi, C. R. K. Reddy, R. Radulovich, B. Jha, *Algal Res.* **2015**, 9, 48–54.
103. V. P. Soudham, Ph.D. Thesis, Umeå University, Umeå, **2015**.
104. S. M. Hyvärinen, Åbo Akademi University, Turku, **2014**.
105. L. Ge, P. Wang, H. Mou, *Renew. Energy* **2011**, 36, 84–89.
106. D.-H. Kim, S.-B. Lee, G.-T. Jeong, *Bioresour. Technol.* **2014**, 161, 348–353.
107. A. M. Da Costa Lopes, R. Bogel-Lukasik, *ChemSusChem* **2015**, 8, 947–965.
108. M. H. Abraham, P. L. Grellier, M. J. Kamlet, R. M. Doherty, R. W. Taft, J.-L. M. Abboud, *Rev. Port. Química* **1989**, 31, 85–92.
109. D. Xu, Q. Yang, B. Su, Z. Bao, Q. Ren, H. Xing, *J. Phys. Chem. B* **2014**, 118, 1071–1079.
110. G. D'Andola, L. Szarvas, K. Massonne, V. Stegmann, *Ionic Liquid for Solubilizing Polymers*, **2008**, WO 2008/043837 A1.
111. A. A. Rosatella, L. C. Branco, C. A. M. Afonso, *Green Chem.* **2009**, 11, 1406.
112. R. P. Swatloski, S. K. Spear, J. D. Holbrey, R. D. Rogers, *J. Am. Chem. Soc.* **2002**, 124, 4974–4975.
113. I. Anugwom, P. Mäki-Arvela, P. Virtanen, P. Damlin, R. Sjöholm, J.-P. Mikkola, *RSC Adv.* **2011**, 1, 452–457.
114. I. Anugwom, P. Mäki-Arvela, P. Virtanen, S. Willför, R. Sjöholm, J.-P. Mikkola, *Carbohydr. Polym.* **2012**, 87, 2005–2011.
115. V. Eta, I. Anugwom, P. Virtanen, K. Eränen, P. Mäki-Arvela, J.-P. Mikkola, *Chem. Eng. J.* **2014**, 238, 242–248.
116. I. Anugwom, V. Eta, P. Virtanen, P. Mäki-Arvela, M. Hedenström, M. Hummel, H. Sixta, J.-P. Mikkola, *ChemSusChem* **2014**, 7, 1170–1176.
117. I. Anugwom, P. Mäki-Arvela, P. Virtanen, S. Willför, P. Damlin, M. Hedenström, J.-P. Mikkola, *Holzforschung* **2012**, 66, 809–815.
118. I. Anugwom, V. Eta, P. Virtanen, P. Mäki-Arvela, M. Hedenström, M. Yibo, M. Hummel, H. Sixta, J.-P. Mikkola, *Biomass Bioenerg.* **2014**, 70, 373–381.
119. P. G. Jessop, D. J. Heldebrandt, X. Li, C. A. Eckert, C. L. Liotta, *Nature* **2005**, 436, 1102.
120. B. Yang, Z. Dai, S.-Y. Ding, C. E. Wyman, *Biofuels* **2014**, 2, 421–449.
121. Glycogenomics Group, Architecture et Fonction des Macromolécules Biologiques (AFMB) Laboratory, AIX-Marseille University, "CAZy - Carbohydrate Active Enzymes database," **2017**, (last accessed on 2017-08-15), can be found under http://www.cazy.org/
122. I. J. Migashi, *Physiology and Biochemistry of Plant-Pathogen Interactions*, Plenum Press, London, UK, UK, **1982**.
123. C. P. Kubicek, T. L. Starr, N. L. Glass, *Annu. Rev. Phytopathol.* **2014**, 1–25.
124. G. de Gonzalo, D. I. Colpa, M. H. M. Habib, M. W. Fraaije, *J. Biotechnol.* **2016**, 236, 110–119.
125. L. Pollegioni, F. Tonin, E. Rosini, *FEBS J.* **2015**, 282, 1190–1213.
126. S. M. Cragg, G. T. Beckham, N. C. Bruce, T. D. H. Bugg, D. L. Distel, P. Dupree, A. G. Etxabe, B. S. Goodell, J. Jellison, J. E. McGeehan, S. J. McQueen-Mason, K. Schnorr, P. H. Walton, J. E. M. Watts, M. Zimmer, *Curr. Opin. Chem. Biol.* **2015**, 29, 108–119.
127. M. Coca, G. González-Benito, M. T. García-Cubero, in *Biomass Fractionation Technologies for a Lignocellulosic Feedstock Based Biorefinery*, (Ed.: S.I. Mussatto), Amsterdam, The Netherlands, **2016**, 409–429.
128. R. Harun, J. W. S. Yip, S. Thiruvenkadam, W. A. W. A. K. Ghani, T. Cherrington, M. K. Danquah, *Biotechnol. J.* **2014**, 9, 73–86.
129. M. G. Borines, R. L. de Leon, J. L. Cuello, *Bioresour. Technol.* **2013**, 138, 22–29.
130. W. Y. Choi, J. G. Han, C. G. Lee, C. H. Song, J. S. Kim, Y. C. Seo, S. E. Lee, *Chem. Biochem. Eng. Q.* **2012**, 26, 15–21.
131. J. Y. Lee, Y. S. Kim, B. H. Um, K. Oh, *Renew. Energy* **2013**, 54, 196–200.

132. J. ye Lee, P. Li, J. Lee, H. J. Ryu, K. K. Oh, *Bioresour. Technol.* **2013**, 127, 119–125.
133. S. Kumar, R. Gupta, G. Kumar, D. Sahoo, R. C. Kuhad, *Bioresour. Technol.* **2013**, 135, 150–156.
134. P. Yazdani, K. Karimi, M. Taherzadeh, *World Renew. Energy Congress* **2011**, 186–191.
135. D. J. Lane, Ph.D. Thesis, University of Adelaide, Adelaide, **2015**.
136. P. Manara, M. Francavilla, M. Monteleone, A. Zabaniotou, in 2nd International Conference on Sustainable Solid Waste Management, Athens, **2014**, pp. 1–11.
137. W. Gao, K. Chen, J. Zeng, J. Xu, B. Wang, *Bioresour. Technol.* **2017**, 243, 212–217.
138. T. Kan, S. Grierson, R. De Nys, V. Strezov, *Energ. Fuels* **2014**, 28, 104–114.
139. L. M. Díaz-Vazquez, A. Rojas-Perez, M. Fuentes-Caraballo, I. V. Robles, U. Jena, K. C. Das, *Front. Energy Res.* **2015**, 3, 1–11.
140. S. U. Kadam, B. K. Tiwari, C. P. O'Donnell, *J. Agric. Food Chem.* **2013**, 61, 4667–4675.
141. A. Tanniou, S. Esteban Leon, L. Vandanjon, E. Ibanez, J. A. Mendiola, S. Cerantola, N. Kervarec, S. La Barre, L. Marchal, V. Stiger-Pouvreau, *Talanta* **2013**, 104, 44–52.
142. P. Mäki-Arvela, I. Hachemi, D. Y. Murzin, *J. Chem. Technol. Biotechnol.* **2014**, 89, 1607–1626.
143. D. J. McHugh, *A Guide to the Seaweed Industry*, FAO, Rome, **2003**, (last accessed on 2017-05-31), can be found under http://www.fao.org/docrep/006/y4765e/y4765e00.htm
144. D. J. Mchugh, G. Hernández-Carmona, D. Luz Arvizu-Higuera, Y. E. Rodríguez-Montesinos, *J. Appl. Phycol*. **2001**, 13, 471–479.
145. G. Hernández-Carmona, Rodríguez-Montesinos, Arvizu-Higuera, Reyes-Tisnado R, J. I. Murillo-Álvarez, M.- Ochoa, *Ing. Investig. y Tecnol.* **2012**, XIII, 155–168.
146. M. L. Garron, M. Cygler, *Curr. Opin. Struct. Biol.* **2014**, 28, 87–95.
147. J. H. Hehemann, A. B. Boraston, M. Czjzek, *Curr. Opin. Struct. Biol.* **2014**, 28, 77–86.
148. M. Kopel, W. Helbert, Y. Belnik, V. Buravenkov, A. Herman, E. Banin, *J. Biol. Chem.* **2016**, 291, 5871–5878.
149. AOAC, *Offical Methods of Analysis of AOAC International*, AOAC International, Gaithersburg, MD, United States, **2000**.
150. A. L. Merrill, B. K. Watt, *Energy Values of Food: Basis and Derivation*, Washington, DC, **1973**.
151. V. L. Singleton, J. A. Rossi, *Am. J. Enol. Vitic.* **1965**, 16, 144–158.
152. A. Von Gadow, E. Joubert, C. F. Hansmann, *J. Agric. Food Chem.* **1997**, 45, 632–638.
153. F. Ferreres, G. Lopes, A. Gil-Izquierdo, P. B. Andrade, C. Sousa, T. Mouga, P. Valentão, *Mar. Drugs* **2012**, 10, 2766–2781.
154. R. Schumann, N. Häubner, S. Klausch, U. Karsten, *Int. Biodeterior. Biodegrad.* **2005**, 55, 213–222.
155. R. J. Porra, W. A. Thompson, P. E. Kriedemann, *Biochim. Biophys. Acta* **1989**, 975, 384–394.
156. B. Ray, M. Lahaye, *Carbohydr. Res.* **1995**, 274, 313–318.
157. A. Sundberg, V. Pranovich, B. Holmbom, *J. Pulp Pap. Sci.* **2003**, 29, 173–178.
158. A. Sundberg, K. Sundberg, L. Camilla, B. Holmbom, *Nord. Pulp Pap. Res. J.* **1996**, 11, 216–219.
159. S. Willför, A. Pranovich, T. Tamminen, J. Puls, C. Laine, A. Suurnäkki, B. Saake, K. Uotila, H. Simolin, J. Hemming, B. Holmbom, *Ind. Crops Prod.* **2009**, 29, 571–580.
160. A. Robic, C. Gaillard, J. F. Sassi, Y. Leral, M. Lahaye, *Biopolymers* **2009**, 91, 652–664.
161. A. Robic, J. F. Sassi, M. Lahaye, *Carbohydr. Polym.* **2008**, 74, 344–352.
162. R. Koivikko, J. Loponen, K. Pihlaja, V. Jormalainen, *Phytochem. Anal.* **2007**, 18, 326–332.
163. J. Ortiz Viedma, *Composición nutricional y funcional de algas pardas chilenas : Macrocystis pyrifira y Durvillaea antarctica*, University of Chile, Santiago, **2011**, (last accessed on 2017-05-31), can be found under http://repositorio.uchile.cl/handle/2250/121459.
164. M. S. Tierney, T. J. Smyth, D. K. Rai, A. Soler-Vila, A. K. Croft, N. Brunton, Food Chem. **2013**, 139, 753–761.
165. S. Kindleysides, S. Y. Quek, M. R. Miller, *Food Chem.* **2012**, 133, 1624–1631.
166. A. López, M. Rico, A. Rivero, M. Suárez de Tangil, *Food Chem.* **2011**, 125, 1104–1109.
167. B. B. Li, B. Smith, M. M. Hossain, *Sep. Purif. Technol.* **2006**, 48, 182–188.
168. G. Taguchi, *Introduction to quality engineering*, McGraw-Hill, New York, US, **1990**.
169. A. W. T. King, J. Asikkala, I. Mutikainen, P. Järvi, I. Kilpeläinen, *Angew. Chemie - Int. Ed.* **2011**, 50, 6301–6305.
170. A. Parviainen, A. W. T. King, I. Mutikainen, M. Hummel, C. Selg, L. K. J. Hauru, H. Sixta, I. Kilpeläinen, *ChemSusChem* **2013**, 6, 2161–2169.
171. T. K. Ghose, *Pure Appl. Chem.* **1987**, 59, 257–268.
172. T. C. McIlvaine, *J. Biol. Chem.* **1921**, 49, 183–186.
173. Y. Milner, G. Avigad, *Carbohydr. Res.* **1967**, 4, 359–361.
174. N. Nelson, *J. Biol. Chem.* **1944**, 153, 375–380.
175. F. Tala, M. Velásquez, A. Mansilla, E. C. Macaya, M. Thiel, *J. Exp. Mar. Bio. Ecol.* **2016**, 483, 31–41.
176. R. Borras-Chavez, M. S. Edwards, D. L. Arvizu-Higuera, Y. E. Rodríguez-Montesinos, G. Hernández-Carmona, D. Briceño-Domínguez, *Bot. Mar.* **2016**, 59, 63–71.
177. R. Westermeier, P. Murúa, D. J. Patiño, L. Muñoz, A. Ruiz, D. G. Müller, *J. Appl. Phycol.* **2012**, 24, 1191–1201.
178. C. Costa, A. Alves, P. R. Pinto, R. A. Sousa, E. A. Borges Da Silva, R. L. Reis, A. E. Rodrigues, *Carbohydr. Polym.* **2012**, 88, 537–546.
179. M. Lahaye, *Carbohydr. Res.* **1998**, 314, 1–12.
180. B. Ray, M. Lahaye, *Carbohydr. Res.* **1995**, 274, 251–261.
181. M. Ikawa, T. D. Schaper, C. A. Dollard, J. J. Sasner, *J. Agric. Food Chem*. **2003**, 51, 1811–1815
182. T. Kuda, M. Tsunekawa, H. Goto, Y. Araki, *J. Food Compos. Anal.* **2005**, 18, 625–633.
183. E. Bergelin, S. von Schoultz, J. Hemming, B. Holmbom, *Nord. Pulp Pap. Res. J.* **2003**, 18, 129–133.
184. S. Willför, J. Hemming, A.-S. Leppänen, *Analysis of extractives in different pulps – Method development, evaluation, and recommendations*, Åbo Akademi University, Turku, **2006**, (last accessed on 2017-05-31), can be found under https://www.researchgate.net/publication/266605057_Analysis_of_extractives_in_different_pulps_-_Method_development_evaluation_and_recommendations.
185. M. Lahaye, B. Ray, *Carbohydr. Res.* **1996**, 283, 161–173.

186. O. Coste, E. jan Malta, J. C. López, C. Fernández-Díaz, *Algal Res.* **2015**, 10, 224–231.
187. G. Paradossi, F. Cavalieri, E. Chiessi, *Macromolecules* **2002**, 35, 6404–6411.
188. G. Paradossi, F. Cavalieri, L. Pizzoferrato, A. M. Liquori, *Int. J. Biol. Macromol.* **1999**, 25, 309–315.
189. A. Alves, S. G. Caridade, J. F. Mano, R. A. Sousa, R. L. Reis, *Carbohydr. Res.* **2010**, 345, 2194–2200.
190. H. Yaich, H. Garna, S. Besbes, M. Paquot, C. Blecker, H. Attia, *Food Hydrocoll.* **2013**, 31, 375–382.
191. B. Quemener, M. Lahaye, C. Bobin-Dubigeon, *J. Appl. Phycol.* **1997**, 9, 179–188.
192. E. Hernández-Garibay, J. A. Zertuche-González, I. Pacheco-Ruíz, *J. Appl. Phycol.* **2011**, 23, 537–542.
193. A. K. Siddhanta, A. M. Goswami, B. K. Ramavat, K. H. Mody, O. P. Mairh, *Indian J. Mar. Sci.* **2001**, 30, 166–172.
194. M. J. Selig, N. Weiss, Y. Ji, *Enzymatic Saccharification of Lignocellulosic Biomass*, National Renewable Energy Laboratory, US Department of Energy, **2008**.
195. R. Harun, M. K. Danquah, *Chem. Eng. J.* **2011**, 168, 1079–1084.
196. A. Ostonen, J. Bervas, P. Uusi-Kyyny, V. Alopaeus, D. H. Zaitsau, V. N. Emel'Yanenko, C. Schick, A. W. T. King, J. Helminen, I. Kilpeläinen, A. A. Khachatrian, M. A. Varfolomeev, S. P. Verevkin, *Ind. Eng. Chem. Res.* **2016**, 55, 10445–10454.
197. S. Jang, Y. SHhirai, M. Uchida, M. Wakisaka, *Food Sci. Technol. Res.* **2011**, 17, 155–160.
198. T. M. Aida, T. Yamagata, C. Abe, H. Kawanami, M. Watanabe, R. L. Smith, *J. Supercrit. Fluids* **2012**, 65, 39–44.
199. C. A. Marsh, in *Glucuronic acid Free and Combined*, (Ed.: G.J. Dutton), Academic Press, New York, US, **1966**, 3–136.
200. R. Wang, T. Neoh, T. Kobayashi, Y. Miyake, *Biosci. Biotechnol. Biochem.* **2010**, 74, 601–605.
201. J. V. Rissanen, D. Y. Murzin, T. Salmi, H. Grénman, *Bioresour. Technol.* **2016**, 199, 279–282.
202. M. E. Vallejos, F. E. Felissia, J. Kruyeniski, M. C. Area, *Ind. Crops Prod.* **2015**, 67, 1–6.
203. D. Nabarlatz, X. Farriol, D. Montané, *Ind. Eng. Chem. Res.* **2004**, 43, 4124–4131.
204. A. Mittal, S. G. Chatterjee, G. M. Scott, T. E. Amidon, *Chem. Eng. Sci.* **2009**, 64, 3031–3041.
205. A. Mittal, S. G. Chatterjee, G. M. Scott, T. E. Amidon, *Holzforschung* **2009**, 63, 307–314.
206. H. Grénman, K. Eränen, J. Krogell, S. Willför, T. Salmi, D. Y. Murzin, *Ind. Eng. Chem. Res.* **2011**, 50, 3818–3828.
207. T. Salmi, D. Y. Murzin, P. Mäki-Arvela, B. Kusema, B. Holmbom, S. Willför, *Am. Inst. Chem. Eng.* **2014**, 60, 1066–1077

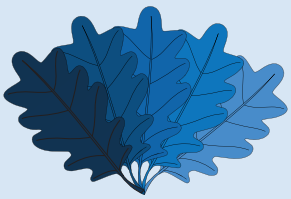

Johan Gadolin
Process Chemistry Centre

SUOMEN AKATEMIA
FINLANDS AKADEMI
ACADEMY OF FINLAND

Painosalama Oy
Turku, Finland 2017